Universitat de Girona

BIOELECTROCHEMICAL SYSTEMS FOR AMMONIUM REMOVAL IN CONTAMINATED WATER

Miguel Osset Álvarez

DOCTORAL THESIS

BIOELECTROCHEMICAL SYSTEMS FOR AMMONIUM REMOVAL IN CONTAMINATED WATER

MIGUEL OSSET ÁLVAREZ

2022

Universitat de Girona

DOCTORAL THESIS

Bioelectrochemical systems for ammonium removal in contaminated water

Miguel Osset Álvarez

2022

Doctoral Programme in Water Science and Technology

Supervisors: Dra. Maria Dolors Balaguer Condom, Dr. Sebastià Puig Broch and Dr. Narcís Pous Rodríguez

Tutor: Dr. Sebastià Puig Broch

Doctoral thesis submitted to the University of Girona for the degree of Doctor

CERTIFICADO DE DIRECCIÓN DE TESIS

La Dra. Maria Dolors Balaguer Condom, el Dr. Sebastià Puig Broch y el Dr. Narcís Pous Rodríguez, del Laboratori d'Enginyeria Química i Ambiental (LEQUIA) de la Universitat de Girona,

DECLARAMOS:

Que el trabajo titulado "*Bioelectrochemical systems for ammonium removal*", que presenta Miguel Osset Álvarez para la obtención del título de doctor, se ha realizado bajo nuestra dirección y que cumple los requisitos para poder optar a Mención Internacional.

Y para que así conste y tenga los efectos oportunos, firmamos el presente documento.

Dra. Maria Dolors Balaguer Condom Dr. Sebastià Puig Broch Dr. Narcís Pous Rodríguez

Girona, 14 de julio de 2022

Acknowledgments

Tras cuatro años de tesis tengo mucho que agradecer a mucha gente. En primer lugar, quiero dar las gracias a mis supervisores Sebastià, Marilós y Narcís, por haberme dado la oportunidad de trabajar en un campo en el que no tenía experiencia y especialmente por no haberse rendido conmigo. Gracias a Sebas por su apoyo constante en lo profesional y en lo personal, por su entusiasmo para debatir mil y una ideas y por involucrarme en tantos proyectos ilusionantes. Ya le he dicho varias veces que es el mejor jefe que he tenido, pero aprovecho estas líneas para repetírselo. A Marilós le quiero agradecer su energía, su pasión por la ciencia y sus infinitas aportaciones a mi trabajo, pero sobre todo la paciencia que ha tenido conmigo, porque no es fácil. Y en el caso de Narcís, creo que la palabra gratitud se queda muy corta. Haberme ayudado y aguantado tanto todos estos años, y además animarme todos los días a creer que las cosas suelen ir mejor de lo que parece tiene un mérito enorme. Si esta tesis ha salido adelante ha sido porque ellos se han empeñado.

A mis compañeros del grupo LEQUIA les quiero dar las gracias por lo bien que me han integrado en el equipo. Gracias a Laura, Alba Ceballos, Meritxell, Silvia, Giulia, Ramiro, Luca, Albert Rovira (Tico), Albert Magrí, Gaetan, Raquel, Alba Anfruns y Gemma por hacer del Parc Científic un lugar de trabajo ideal, tanto humanamente como a nivel profesional. Quiero destacar la situación vivida en los primeros meses de la pandemia del COVID-19, en la cual todos nos dedicamos a cuidar el trabajo de los demás, como ejemplo del compañerismo del Parc. Asimismo, me gustaría subrayar la importancia de los seminarios del grupo, que me permitieron entender mejor el trabajo de mis compañeros, incorporar nuevas ideas a mi propio trabajo y sentirme más cerca de Girona y del LEQUIA, especialmente durante mi estancia en Suiza y ahora desde Oviedo.

También quiero agradecer la labor de Marta, Bernat y Daniel, que como estudiantes me ayudaron a llevar a cabo esta tesis, y la de Teresa y Adela, que me ayudaron con todos los

trámites que acarrea hacer un doctorado, que no son pocos. Asimismo, le doy las gracias a Paola y Lluís (Cacho) del grupo gEMM – UdG por su trabajo en la identificación de los microorganismos presentes en mis reactores, and I would like to thank Dr. Benjamin Korth and Dr. Falk Harnisch from Helmholtz - Centre for Environmental Research - UFZ for their contributions in the frame of the WAFRA Project. No quiero olvidarme de Jesús, Héctor, Eli, Jan, Jordi, Manel y Albert Galizia, que también me ayudaron en este camino.

During this PhD project, I had the opportunity to make a research stay at the FHNW (Switzerland). I am very grateful to Prof. Dr. Phillip Corvini for allowing me to work with him at the Institute of Ecopreneurship. I would like to acknowledge Prof. Corvini and also Dr. Boris Kolvenvach for all their guidance and support during my stage, and I would like to thank Sabrina, Osagie, Riccardo, Lara, Zhuang, Alba, Ayaovi and the rest of the group for helping me in the laboratory and also outside (even though social activities were very limited at the time due to COVID-19 restrictions).

Fuera del mundo académico, le quiero dar las gracias a María haberme apoyado tanto y a Fran, Moi, Manu, Oscar y en general a todos mis amigos de Oviedo por hacerme más llevadero todo esto. También me quiero acordar de Montes. Te tenemos muy presente, amigo.

Por último, quiero agradecerle a mi familia todo lo que ha hecho por mí. A mi padre, por estar siempre ahí para mí. A mi tía, Dolores y a mi prima, Ana. A mi abuela, que espero que hoy se sienta orgullosa. A mi abuelo, que le echo de menos. Y a mi madre. A ella le debo esto y todo.

This PhD thesis was financially supported by a PhD grant from University of Girona (IFUdG2018/50), the project “Wireless Aquaponic Farming in Remote Areas: A smart adaptive socio-economic solution” (WAFRA; PCI2018-09294) funded by the Spanish Ministry of Science and Innovation and the European Union's Horizon 2020 project ELECTRA [no. 826244]. LEQUIA has been recognized as a consolidated research group by the Catalan Government (2017-SGR-1552).

List of peer reviewed publications presented as chapters of Ph.D. thesis

- Pous, N., Korth, B., **Osset-Álvarez, M.**, Balaguer, M. D., Harnisch, F., & Puig, S. (2021). Electrifying biotrickling filters for the treatment of aquaponics wastewater. *Bioresource Technology*, *319*, 124221. https://doi.org/10.1016/j.biortech.2020.124221
- **Osset-Álvarez, M.**, Pous, N., Hasan, S. W., Naddeo, V., Balaguer, M. D., & Puig, S. (2021). Electrified biotrickling filters as tertiary urban wastewater treatment. *Case Studies in Chemical and Environmental Engineering*, *4*, 100143. https://doi.org/10.1016/j.cscee.2021.100143
- **Osset-Álvarez, M.**, Pous, N., Chiluiza-Ramos, P., Bañeras, L., Balaguer, M. D., & Puig, S. (2022). Unveiling microbial electricity driven anoxic ammonium removal. *Bioresource Technology Reports*, *17*, 100975. https://doi.org/10.1016/j.biteb.2022.100975

Other publications

- **Osset-Álvarez, M.**, Rovira-Alsina, L., Pous, N., Blasco-Gómez, R., Colprim, J., Balaguer, M. D., & Puig, S. (2019). Niches for bioelectrochemical systems on the recovery of water, carbon and nitrogen in wastewater treatment plants. *Biomass and Bioenergy*, *130*, 105380. https://doi.org/10.1016/j.biombioe.2019.105380
- **Osset-Álvarez, M.**, Alsina, L., Pous, N., Blasco-Gómez, R., Colprim, J., Balaguer, M. D., & Puig, S. (2020). Niches for Bioelectrochemical Systems in Wastewater Treatment Plants. In *Frontiers in Water-Energy-Nexus—Nature-Based Solutions, Advanced Technologies and Best Practices for Environmental Sustainability* (pp. 329–331). Springer. https://doi.org/10.1007/978-3-030-13068-8_82

List of abbreviations

Anammox	Anaerobic ammonium oxidation
APHA	American Public Health Association
ASV	Amplicon sequence variant
ATU	Allylthiourea
BES	Bioelectrochemical system
BLAST	Basic Local Alignment Search Tool
CC	Current collector
CE	Coulombic efficiency
COD	Chemical oxygen demand
DIET	Direct interspecies electron transfer
DO	Dissolved oxygen
FAO	Food and Agriculture Organization of the United Nations
HRT	Hydraulic retention time
LOD	limit of detection
MEC	Microbial electrolysis cell
MET	Microbial electrochemical technology
MFC	Microbial fuel cell
$N\text{-}NH_4^+{}_{LR}$	$N\text{-}NH_4^+$ loading rate (Chapter 5)
$N\text{-}NH_4^+{}_{RR}$	Ammonium removal rate (Chapter 5)
$N\text{-}TN_{RR}$	Total nitrogen removal rate (Chapter 5)
NCBI	National Centre for Biotechnology Information
NCC	Net cathode volume
NiBES	Nitrifying BES
OCP	Open cell potential

POD	Pyruvic oxime dioxygenase
PVC	Polyvinyl chloride
Q	Volumetric flow rate (Chapter 5)
SHE	Standard hydrogen electrode
Ti-MMO	Titanium-mixed metal oxide
TN	Total nitrogen
TSS	Total suspended solids
WL	Water level
WW	Wastewater
WWTP	Wastewater treatment plant

List of contents

List of tables

List of figures

Summary

The presence of nitrogen species in water, especially ammonium (NH_4^+), generates environmental and health problems worldwide. Nitrification-denitrification is the method most commonly used in wastewater treatment plants (WWTPs) for the removal of ammonium. This process requires intensive aeration for the oxidation of NH_4^+ and also the addition of organic matter for the reduction of nitrate (NO_3^-), increasing the operational cost. The anaerobic ammonium oxidation (anammox) process partially solves these problems, as it needs no organic matter addition and less aeration than nitrification-denitrification. Nevertheless, oxygen supply is still needed for the oxidation of ammonium to nitrite (NO_2^-).

Microbial electrochemical technologies (METs) can provide a solution to these organic matter and oxygen requirements, as the electrodes can act as electron acceptors and donors. The use of MET for nitrogen removal started with the development of bioelectrochemical denitrification, in which a biocathode serves as the electron donor for the oxidation of NO_3^-. This technology can also be combined with aerobic nitrification for the removal of ammonium. This combination of aerobic nitrification and bioelectrochemical denitrification has been applied using all kinds of reactor configurations, resulting in bioelectrochemical systems (BES) able to remove NH_4^+ from different kinds of wastewaters.

Nevertheless, this MET still requires oxygen for the oxidation of ammonium. On the other hand, bioanodes could replace oxygen for this process. In the last years, the study of bioelectrochemical nitrification has revealed that NH_4^+ can be bioelectrochemical oxidised to nitrate and even to nitrogen gas (N_2) in anoxic conditions. However, the metabolic pathways ruling this process are still unclear.

This Ph.D. thesis is focused on the study of these two METs. The goal of this Ph.D. thesis concerning bioelectrochemical nitrification is to provide new information about the bioelectrochemical reactions involved in this process, as a way to contribute to the improvement

of the performance of this technology. On the other hand, this thesis pursues to showcase the applicability of bioelectrochemical denitrification, by developing a new MET that integrates bioelectrochemical denitrification into a biotrickling filter.

Chapter 4 aims at unveiling the mechanisms behind bioelectrochemical nitrification. A nitrifying BES (niBES) was operated in batch mode, with a feed containing initially NH_4^+ and later nitrification intermediates (nitrite, nitrate and hydroxylamine (NH_2OH)). These experiments revealed that *Achromobacter* sp., a nitrifying bacterium, was the most abundant microorganism in the niBES, and that NH_2OH and NO_2^- are electroactive compounds. The results obtained suggested that the conversion of NH_4^+ into N_2 was achieved by bioelectrochemical ammonium oxidation followed by denitrification and, to a lesser extent, by anammox.

Bioelectrochemical denitrification was combined in Chapters 5 with the nitrifying capacity of a biotrickling filter, creating electrified biotrickling filters or e-biofilters. E-biofilters showed higher ammonium removal capability than conventional biotrickling filters or denitrifying BES. On top of that, e-biofilters were able to transform the NH_4^+ present in synthetic aquaculture wastewater (50 mg $N\text{-}NH_4^+$ L^{-1}) into NO_3^- (10 mg $N\text{-}NO_3^-$ L^{-1}) and N_2, meeting the requirements for hydroponic culture, enabling, therefore, the establishment of an aquaponic system.

Finally, the e-biofilters were used in Chapter 6 to treat the secondary effluent of an urban WWTP, which contained ammonium (45 mg $N\text{-}NH_4^+$ L^{-1}) and low concentrations of organic matter (102 mg of chemical oxygen demand (COD) L^{-1}). The treatment removed most of the ammonium (reaching an ammonium concentration of 2 mg $N\text{-}NH_4^+$ L^{-1} and a total nitrogen concentration of 16 mg N L^{-1}), organic matter (63 % COD removal) and total suspended solids (TSS) (82 % TSS removal) present in the water, proving the capability of e-biofilters for holistic wastewater treatment.

In conclusion, this Ph.D. thesis expanded the current knowledge of the different processes involved in NH_4^+ removal in nitrifying BES. On top of that, e-biofilters were built (by integrating bioelectrochemical denitrification into a biotrickling filter) and evaluated during this Ph.D. thesis. The results obtained proved the suitability of e-biofilters for the removal of ammonium from wastewaters with low C/N ratios.

Resumen

La presencia en el agua de especies nitrogenadas, especialmente de amonio (NH_4^+), genera problemas medioambientales y de salud a nivel mundial. El proceso de nitrificación-desnitrificación es el método de eliminación de amonio más habitual en las estaciones de depuradora de aguas residuales (EDAR). Este proceso requiere de una intensa aireación para la oxidación del NH_4^+, así como de la adición de materia orgánica para la reducción del nitrato (NO_3^-), aumentando el costo operacional. El proceso de oxidación anaerobia del amonio (anammox) soluciona parcialmente estos problemas, al no requerir de la adición de materia orgánica y precisar de menor aireación que la nitrificación-desnitrificación. No obstante, aún precisa de oxígeno para la oxidación del amonio a nitrito (NO_2^-).

Las tecnologías microbianas electroquímicas (METs; siglas en inglés) pueden aportar una solución a esta demanda de materia orgánica y oxígeno, ya que los electrodos pueden actuar como aceptores y como fuentes de electrones. El uso de MET para la eliminación de nitrógeno comenzó con el desarrollo de la desnitrificación bioelectroquímica, en la cual un biocátodo actúa como aceptor de electrones para la oxidación de NO_3^-. Esta tecnología también se puede combinar con la nitrificación aerobia para eliminar amonio. Esta combinación de nitrificación aerobia y desnitrificación bioelectroquímica ha sido implementada utilizando todo tipo de configuraciones de reactor, dando lugar a sistemas bioelectroquímicos (BES; siglas en inglés) capaces de eliminar amonio de distintos tipos de aguas residuales.

Sin embargo, esta MET aún requiere oxígeno para la oxidación del amonio. Por otro lado, los bioánodos podrían reemplazar al oxígeno en este proceso. En los últimos años, el estudio de la nitrificación bioelectroquímica ha revelado que el NH_4^+ puede ser oxidado bioelectroquímicamente a nitrato e incluso a nitrógeno gas (N_2) en condiciones anóxicas. No obstante, aún no está claro qué rutas metabólicas rigen este proceso.

Esta tesis doctoral se centra en el estudio de estas dos METs. El objetivo de esta tesis doctoral respecto a la nitrificación bioelectroquímica es aportar nueva información acerca de las reacciones bioelectroquímicas involucradas en este proceso, como una forma de contribuir a la mejora del rendimiento de esta tecnología. Por otro lado, esta tesis busca mostrar la aplicabilidad de la desnitrificación bioelectroquímica mediante el desarrollo de una nueva MET que integra la desnitrificación bioelectroquímica dentro de un biofiltro percolador.

El Capítulo 4 aspira a desvelar los mecanismos que hay detrás de la nitrificación bioelectroquímica. Se hizo funcionar un BES nitrificante (niBES; siglas en inglés) alimentado en batch, conteniendo el alimento inicialmente NH_4^+ y posteriormente intermedios de nitrificación (nitrito, nitrato e hidroxilamina (NH_2OH)). Estos experimentos revelaron que, *Achromobacter* sp., una bacteria nitrificante, era el microorganismo más abundante en el niBES, y que la NH_2OH y el NO_2^- son compuestos electroactivos. Los resultados obtenidos sugirieron que la conversión del NH_4^+ en N_2 fue producida por la oxidación bioelectroquímica del amonio seguida de desnitrificación y, en menor medida, de anammox.

La desnitrificación bioelectroquímica fue combinada en el Capítulo 5 con la capacidad nitrificante de un biofiltro percolador para crear los biofiltros percoladores electrificados o e-biofioltros. Los e-biofiltros mostraron mayor capacidad de eliminación de amonio que los biofiltros percoladores tradicionales o que los BES desnitrificantes. Además, los e-biofiltros fueron capaces de transformar el amonio presente en agua sintética de acuicultura (50 mg N-NH_4^+ L^{-1}) en NO_3^- (10 mg N-NO_3^- L^{-1}) y N_2, cumpliendo con los requisitos necesarios para llevar a cabo cultivos hidropónicos, permitiendo así establecer un sistema acuapónico.

Finalmente, los e-biofiltros fueron usados en el Capítulo 6 para tratar el efluente secundario de una EDAR urbana, que contenía amonio (45 mg N-NH_4^+ L^{-1}) y bajas concentraciones de materia orgánica. (102 mg de demanda química de oxígeno (COD; siglas en inglés) L^{-1}) El tratamiento eliminó la mayoría del amonio (alcanzándose concentraciones de

amonio de 2 mg $N\text{-}NH_4^+$ L^{-1} y de 16 mg N L^{-1} de nitrógeno total), de la materia orgánica (eliminando el 63 % de la COD) y de los sólidos suspendidos totales (TSS; siglas en inglés) (eliminando el 82 % de los TSS), probando la capacidad de los e-biofiltros para el tratamiento holístico de aguas residuales.

Como conclusión, esta tesis doctoral expandió el conocimiento actual acerca de los diferentes procesos involucrados en la eliminación de NH_4^+ en BES nitrificantes. Además, los e-biofiltros fueron construidos (integrando la desnitrificación bioelectroquímica en un biofiltro percolador) y evaluados durante esta tesis doctoral. Los resultados obtenidos demostraron la idoneidad de los e-biofiltros para la eliminación de amonio en aguas residuales con bajo ratio C/N.

Resum

La presència d'espècies nitrogenades a l'aigua, especialment d'amoni (NH_4^+), genera problemes mediambientals i de salut a nivell mundial. El procés de nitrificació-desnitrificació és el mètode d'eliminació d'amoni més habitual a les estacions de depuradora d'aigües residuals (EDAR). Aquest procés requereix una ventilació intensa per a l'oxidació de l' NH_4^+, així com de l'addició de matèria orgànica per a la reducció del nitrat (NO_3^-), augmentant el cost operacional. El procés d'oxidació anaeròbia de l'amoni (anammox) soluciona parcialment aquests problemes, ja que no requereix l'addició de matèria orgànica i precisa de menor ventilació que la nitrificació-desnitrificació. No obstant això, encara necessita oxigen per a l'oxidació de l'amoni a nitrit (NO_2^-).

Les tecnologies microbianes electroquímiques (METs; sigles en anglès) poden aportar una solució a aquesta demanda de matèria orgànica i oxigen, ja que els elèctrodes poden actuar com a acceptors i com a fonts d'electrons. L'ús de MET per a l'eliminació de nitrogen va començar amb el desenvolupament de la desnitrificació bioelectroquímica, en la qual un biocàtode actua com a acceptor d'electrons per a l'oxidació de NO_3^-. Aquesta tecnologia també es pot combinar amb la nitrificació aeròbia per eliminar amoni. Aquesta combinació de nitrificació aeròbia i desnitrificació bioelectroquímica ha estat implementada utilitzant tot tipus de configuracions de reactor, donant lloc a sistemes bioelectroquímics (BES; sigles en anglès) capaços d'eliminar amoni de diferents tipus d'aigües residuals.

Tot i això, aquesta MET encara requereix oxigen per a l'oxidació de l'amoni. D'altra banda, els bioànodes podrien reemplaçar l'oxigen en aquest procés. En els darrers anys, l'estudi de la nitrificació bioelectroquímica ha revelat que l' NH_4^+ pot ser oxidat bioelectroquímicament a nitrat i fins i tot a nitrogen gas (N_2) en condicions anòxiques. No obstant, encara no és clar quines rutes metabòliques regeixen aquest procés.

Aquesta tesi doctoral se centra en l'estudi d'aquestes dues METs. L'objectiu d'aquesta tesi doctoral respecte a la nitrificació bioelectroquímica és aportar informació nova sobre les reaccions bioelectroquímiques involucrades en aquest procés, com una forma de contribuir a la millora del rendiment d'aquesta tecnologia. D'altra banda, aquesta tesi cerca mostrar l'aplicabilitat de la desnitrificació bioelectroquímica mitjançant el desenvolupament d'una nova MET que integra la desnitrificació bioelectroquímica dins un biofiltre percolador.

El Capítol 4 aspira a desvetllar els mecanismes que hi ha darrere de la nitrificació bioelectroquímica. Es va fer funcionar un BES nitrificant (niBES; sigles en anglès) alimentat en batch, contenint l'aliment inicialment NH_4^+ i posteriorment intermedis de nitrificació (nitrit, nitrat i hidroxilamina (NH_2OH)). Aquests experiments van revelar que *Achromobacter* sp., un bacteri nitrificant, era el microorganisme més abundant al niBES, i que la NH_2OH i el NO_2^- són compostos electroactius. Els resultats obtinguts van suggerir que la conversió de l' NH_4^+ a N_2 va ser produïda per l'oxidació bioelectroquímica de l'amoni seguida de desnitrificació i, en menor mesura, d'anammox.

La desnitrificació bioelectroquímica va ser combinada al Capítol 5 amb la capacitat nitrificant d'un biofiltre percolador per crear els biofiltres percoladors electrificats o e-biofioltres. Els e-biofiltres van mostrar més capacitat d'eliminació d'amoni que els biofiltres percoladors tradicionals o que els BES desnitrificants. A més, els e-biofiltres van ser capaços de transformar l'amoni present en aigua sintètica d'aqüicultura (50 mg $N\text{-}NH_4^+$ L^{-1}) a NO_3^- (10 mg $N\text{-}NO_3^-$ L^{-1}) i N_2, complint els requisits necessaris per dur a terme cultius hidropònics, permetent així establir un sistema aquapònic.

Finalment, els e-biofiltres van ser usats al Capítol 6 per tractar l'efluent secundari d'una EDAR urbana, que contenia amoni (45 mg $N\text{-}NH_4^+$ L^{-1}) i baixes concentracions de matèria orgànica (102 mg de demanda química d'oxigen (COD; sigles en anglès) L^{-1}). El tractament va eliminar la majoria de l'amoni (aconseguint concentracions d'amoni de 2 mg $N\text{-}NH_4^+$ L^{-1} i de 16

mg N L^{-1} de nitrogen total), de la matèria orgànica (eliminant el 63% de la COD) i dels sòlids suspesos totals (TSS; sigles en anglès) (eliminant el 82% dels TSS), provant la capacitat dels e-biofiltres per al tractament holístic d'aigües residuals.

Com a conclusió, aquesta tesi doctoral va expandir el coneixement actual sobre els diferents processos involucrats en l'eliminació de NH_4^+ a BES nitrificants. A més, els e-biofiltres van ser construïts (integrant la desnitrificació bioelectroquímica en un biofiltre percolador) i avaluats durant aquesta tesi doctoral. Els resultats obtinguts van demostrar la idoneïtat dels e-biofiltres per a l'eliminació d'amoni en aigües residuals amb baixa ràtio C/N.

Chapter 1. Introduction

1.1 Background

Anthropogenic emissions of reactive nitrogen (i.e., nitrogen pollution associated to human activity) are currently more than 10-fold higher than at the beginning of the 20th century (Penuelas et al., 2020). During this period, nitrogen pollution due to industrial fertilizers experimented a 100-fold increase, and now these industrial nitrogen fertilizers are responsible for half of the anthropogenic nitrogen pollution (Penuelas et al., 2020), as crops are unable to uptake more than half of the nitrogen present in them (Hakeem et al., 2017). These anthropogenic nitrogen emissions have also reached all sorts of water bodies (Zhao et al., 2021). Nitrogen pollution in water is a major concern as it has been consistently related to toxicity and eutrophication threads (Holmes et al., 2019).

Alternative configurations for wastewater (WW) treatment are a new challenge in terms of sustainability, efficiency, recovery and innovation (Garrido-Baserba et al., 2018). Despite the increasing interest in decentralised systems (Leigh & Lee, 2019; Lu et al., 2019; Torre et al., 2021; Vegas Niño et al., 2021), water infrastructures usually operate as centralised systems, collecting water from a wide area to a central wastewater treatment plant (WWTP) (Lu et al., 2019; Torre et al., 2021).

When WW enters a WWTP, it contains nitrogen, mainly in the form of ammonium (NH_4^+), at a concentration of around 60 mg N L^{-1} (Puig et al., 2010). The removal of ammonium is usually achieved by conventional nitrification-denitrification (Farazaki & Gikas, 2019). This process consists of aerobic oxidation of NH_4^+ to nitrate (NO_3^-) followed by the heterotrophic reduction of the NO_3^- produced to dinitrogen gas (N_2) (Table 1), which is carried out in anoxic conditions (Khin & Annachhatre, 2004). Conventional nitrification-denitrification has several drawbacks, such as the costs derived from the oxygen and organic carbon supply or the need for different environmental conditions to perform the process (Khin & Annachhatre, 2004). Most

of the energy consumed for nitrification-denitrification (2.65 kWh kg^{-1} N from a total of 3.54 kWh kg^{-1} N) is spent on aeration (Nutrient Reduction Technology Cost Task Force, 2002).

The increased aeration costs can be partially overcome using the anaerobic ammonium oxidation (anammox) process, which is carried out by bacteria that use nitrite (NO_2^-) as an electron acceptor for the autotrophic oxidation of ammonium, yielding N_2 and a small amount of NO_3^- (Jetten et al., 2002) (Table 1). The NO_2^- required for anammox reaction is obtained from partial aerobic oxidation of NH_4^+ (partial nitritation), so oxygen supply is still needed (Hu et al., 2013). The energy consumption of the anammox process is 1.44 kWh kg^{-1} N (Vineyard et al., 2020), significantly lower compared to a nitrification-denitrification conventional process. Moreover, this process does not require the addition of organic matter, reducing the operation cost (Kartal et al., 2013)

Table 1. List of possible reactions involved in nitrification, denitrification and anammox, and their Gibbs free energy.

Substrate	Product	Reaction	$\Delta G^{0'}$ (kJ $reaction^{-1}$)	Eq.	Ref.
Ammonium	Nitrite	$NH_4^+ + 2H_2O \rightarrow NO_2^- + 2H^+ + 3H_2$	436.4	(1)	(Thauer et al., 1977)
Nitrite	Nitrate	$NO_2^- + H_2O \rightarrow NO_3^- + H_2$	163.2	(2)	(Thauer et al., 1977)
Nitrite	Nitric oxide	$NO_2^- + ½\ H_2 + H^+ \rightarrow NO + H_2O$	-73.2	(3)	(Thauer et al., 1977)
Nitric oxide	Nitrous oxide	$2NO + H_2 \rightarrow N_2O + H_2O$	-306.3	(4)	(Thauer et al., 1977)
Nitrous oxide	Nitrogen	$2NO + H_2 \rightarrow N_2O + H_2O$	-341.4	(5)	(Thauer et al., 1977)
Ammonium & nitrite	Nitrogen	$NH_4^+ + NO_2^- \rightarrow N_2 + 2H_2O$	-357 kJ	(6)	(Kartal et al., 2011)

Microbial electrochemical technologies (METs) have been proposed as a promising alternative to conventional nitrogen removal processes, as they can solve the dependency on the aforementioned electron acceptors and donors (oxygen and organic matter, respectively) (Schröder et al., 2015). METs are based on the use of electron donors/acceptors, electrodes, biocatalysts enabling countless redox processes that can be applied to achieve very diverse goals. These applications go from the production of energy to the production of different valuable compounds or the removal of a plethora of different pollutants (Tiquia-Arashiro & Pant, 2020). Although METs were conceived over one century ago (Potter, 1911), and the first models of bioelectrochemical systems (BES) were assembled in 1931 (Cohen, 1931) and 1962 (Davis & Yarbrough, 1962), the real development of this technology has only recently started (Arends & Verstraete, 2012; Schröder, 2011). BES can be divided in two categories: microbial electrolysis cells (MECs), which require an energy input to be operated, and microbial fuel cells (MFCs), which generate an energy output.

1.2 Nitrogen removal by aerobic nitrification and bioelectrochemical denitrification

The first application of bioelectrochemical systems for nitrogen removal was the use of biocathodes as electron donors for the reduction of NO_3^- first to NO_2^- (Gregory et al., 2004) and later to N_2 (i.e. **bioelectrochemical denitrification**, (Clauwaert et al., 2007)). Bioelectrochemical denitrification was first used for nitrate removal alone and it was later coupled with aerobic nitrification (Table 2).

Table 2. Summary of the main characteristics of different studies targeting bioelectrochemical NO_3^- reduction

Main feature	Influent	Nitrogen removal rate (g N m^{-3} d^{-1})	Nitrogen end products	Reference

First bioelectrochemical denitrification, reduction of NO_3^- to NO_2^- in a MEC	193 mg N-NO_3^- L^{-1}	20 (to NO_2^-)	NO_2^-	(Gregory et al., 2004)
NO_3^- complete bioelectrochemical reduction to N_2 + organic carbon bioelectrochemical oxidation + energy production (MFC)	160 g N-NO_3^- m^{-3} d^{-1}	146	N_2	(Clauwaert et al., 2007)
First combination of aerobic nitrification + bioelectrochemical denitrification	88 mg N-NH_4^+ L^{-1}	410	N_2	(Virdis et al., 2008)
First simultaneous aerobic nitrification + bioelectrochemical denitrification in one reactor (SND)	53 mg N-NH_4^+ L^{-1}	104	N_2	(Virdis et al., 2010)
Double three-chamber MFC (one anode + two cathodes): one aerated-cathodes MFC + one anoxic-cathodes MFC	32 mg N-NH_4^+ L^{-1}	69	N_2	(Xie et al., 2011)
Single three-chamber MFC: anode + aerated cathode + anoxic cathode.	20 mg N-NH_4^+ L^{-1}	97 %*	N_2	(Zhang & He, 2012)
Bioelectrochemical system + microalgae (photo microbial fuel cell). Nitrification-denitrification + nitrogen uptake for algae growth	56 mg N-NH_4^+ L^{-1}	88 %*	N_2 Algae biomass	(Zhang et al., 2011a)
Bioelectrochemical denitrification integrated into a WWTP activated sludge rector configuration	37 mg N-NH_4^+ L^{-1}	19	N_2	(Tejedor-Sanz et al., 2016)
Groundwater desalination + nitrate removal by ion migration of NO_3^- and Na^+ from the groundwater into an MFC + bioelectrochemical denitrification	10 mg N-NO_3^- L^{-1}	483	N_2	(Zhang & Angelidaki, 2013)

Improvement of denitrification rate by reducing the hydraulic retention time (HRT)	33 mg N-NO_3^- L^{-1}	483	N_2	(Pous et al., 2017)

* Nitrogen removal efficiency is indicated when nitrogen removal rate was not specified.

The first successful attempt at bioelectrochemical nitrate reduction was carried out by Gregory et al. (2004), who proved that a culture of *Geobacter metallireducens* (a bacterium that had already been reported for its capacity to transfer electrons to an electrode) was able to use a graphite cathode poised at −0.5 V vs Ag/AgCl (sat. KCl, +0.197 V vs standard hydrogen electrode (SHE)) as the electron donor for the reduction of 20 g N-NO_3^- m^{-3} d^{-1} into NO_2^-. Then, Clauwaert et al. (2007) used an MFC to combine anodic organic carbon removal and cathodic complete denitrification and at the same time produce electricity, achieving a nitrate removal rate of 146 g N-NO_3^- m^{-3} d^{-1}. The anodic compartment was inoculated using the effluent from different high-performance MFCs, while the cathode was inoculated with a mixture of anaerobic and aerobic sediments and sludge.

Soon after the discovery of bioelectrochemical denitrification, MFCs were used in combination with aerobic nitrification to transform NH_4^+ into NO_3^- and then convert the latter into N_2 bioelectrochemically. Virdis et al. (2008) performed the first successful proof of concept of this combined process. To do this, the authors operated a two-chambers MFC in which the influent entered the system through the anodic chamber and then passed through an aerobic reactor for aerobic nitrification, before reaching the cathodic compartment, where nitrate was transformed to N_2 at a denitrification rate of 410 g N-NO_3^- m^{-3} d^{-1}.

From that point in time, many new configurations of this technology were evaluated. Virdis et al. (2010) innovated by applying simultaneous nitrification and denitrification in the cathodic compartment. This goal was achieved by introducing air into the cathode, enabling

ammonium aerobic oxidation and nitrate bioelectrochemical reduction could take place in the same chamber. A nitrogen removal rate of 104 g N m^{-3} d^{-1} was achieved. The system worked as an MFC, with an anode performing bioelectrochemical oxidation of acetate to CO_2 and the influent circulating from the anode to the cathode.

A different approach was followed by Xie et al. (2011), who connected two three-chambers MFCs to build an ammonium removal system able to remove nitrogen at a rate of 69 g N m^{-3} d^{-1}. Each MFC had an anode and two cathodes (two anodes and four cathodes in total for the system), but the cathodes of the first one were kept under aeration and inoculated with nitrifying sludge, while the cathodes of the second MFC were operated under anoxic conditions and inoculated with denitrifying sludge. The influent entered the system through the anodes, where organic carbon bioelectrochemical oxidation took place, then passed to the cathodes of the aerobic MFC for nitrification and finally reached the cathodes of the anoxic MFC for bioelectrochemical denitrification. Then, this technology was simplified by Zhang & He, (2012), who operated a 3-chamber MFC with an anode, an aerated cathode and an anoxic cathode in batch mode. Acetate bioelectrochemical oxidation took place in the anode, aerobic nitrification in the aerobic cathode and bioelectrochemical denitrification in the anaerobic cathode, achieving a nitrogen removal efficiency of 97 %. Similarly, to the previously mentioned works, part of the oxygen introduced to the system could also be reduced by the cathode, fuelling anodic organic matter oxidation.

This combination of aerobic nitrification and bioelectrochemical denitrification can be complemented with other processes to improve nitrogen removal. Zhang et al. (2011a) combined microbial electrochemical technology with microalgae cultivation, producing a technology called photo-microbial fuel cell that could be used for the removal of various pollutants as well as for the generation of energy. The reactor consisted of a sealed 500 mL glass bottle, with the anode placed at the bottom and the cathode, consisting of a carbon paper piece,

hung 5 cm above the anode. The anode was inoculated using the sediment of a lake that was accumulated at the bottom of the bottle, while the algae *Chlorella vulgaris* was added later to the reactor. The bioanode catalysed the bioelectrochemical oxidation of acetate to CO_2. This CO_2, along with solar light, was used by the algae to perform photosynthesis, which also contributed to ammonium removal by assimilation. The oxygen produced by microalgae was used for nitrification and also as an electron acceptor for the cathode. The NO_3^- produced was reduced by electrochemical and biological denitrification. Altogether, 88 % of the total nitrogen present in the influent was removed.

The abovementioned applications understood METs as stand-alone technology able to replace current WW treatment facilities. However, implementing microbial electrochemical technology into currently existing wastewater treatment facilities could be a way to boost the development and the use of this technology for the removal broader public. For example, Tejedor-Sanz et al. (2016) introduced a MEC into a system with the configuration of a WWTP-activated sludge reactor, resulting in a nitrogen removal rate of 19 g N m^{-3} d^{-1}. The cathodic electrode was placed in the anoxic compartment, while the anodic electrode was located in the aerobic section. The cathodic potential was set at -0.6 V vs SHE, and it enabled bioelectrochemical denitrification, while aerobic nitrification took place in the anodic compartment. The oxygen needed for the latter reaction was a combination of the oxygen dissolved in the wastewater, the one diffusing from the air and also the O_2 generated from water electrochemical oxidation (the anodic potential ranged between +1.3 and +1.6 V vs SHE). The wastewater entered the reactor through the cathode and left by the anode, but due to an internal recirculation system, two-thirds of the flow leaving the anode was recirculated to the cathode, and the remaining one-third exited the reactor.

The presence of nitrate in water bodies like groundwater is also an environmental hazard, so bioelectrochemical denitrification has also been applied for the removal of this

pollutant. Zhang & Angelidaki (2013) introduced an MFC in a bigger glass reactor containing groundwater, submerging the MFC under the groundwater to remove the NO_3^- and also reduce its salinity. The cathode of the MFC was fed with wastewater, which passed to the anode and left the system. Due to the electric current in the MFC, the nitrate in the groundwater migrated to the anode of the MFC through an anion exchange membrane, while Na^+ passed from the groundwater to the MFC's cathode through a cation exchange membrane. The organic matter present in the wastewater was oxidised to CO_2 in the anode, while the bioelectrochemical denitrification of the NO_3^- proceeding from the groundwater took place at the cathode. The NO_3^- removal rate was 483 g $N\text{-}NO_3^-$ m^{-3} d^{-1}. Pous et al. (2017) used a MEC with a cathodic potential of -0.123 V vs SHE for the bioelectrochemical reduction of nitrate from the groundwater. The NO_3^- removal rate was improved by reducing the HRT of the groundwater in the reactor, from 73 g $N\text{-}NO_3^-$ m^{-3} d^{-1} at an HRT of 10.89 h to 849 g $N\text{-}NO_3^-$ m^{-3} d^{-1} at an HRT of 0.46 h.

Over time, many authors have studied different ways to implement bioelectrochemical denitrification, and new applications are constantly being developed to face specific environmental challenges related to nitrogen pollution of different waterbodies. However, another nitrogen-removing MET has gained attention recently, **bioelectrochemical nitrification**.

1.3 Bioelectrochemical nitrification

Considering that aeration accounts for most of the energetic cost in nitrification-denitrification, the development of bioanodes, that could replace oxygen as electron acceptor for NH_4^+ oxidation, has started to be investigated in the last decades. Table 3 summarizes the current state of the art of bioelectrochemical nitrification.

Table 3. Brief description of the different studies about bioelectrochemical NH_4^+ oxidation explained during this PhD thesis.

Main feature	Influent NH_4^+ (mg N L^{-1})	NH_4^+ removal rate (g N m^{-3} d^{-1})	TN removal rate (g N m^{-3} d^{-1})	Nitrogen end products	Reference
Use of feammox bacteria (iron-reducing ammonium oxidisers) for anodic bioelectrochemical nitrification	70	0.3	-	NO_2^-	(Ruiz-Urigüen et al., 2019)
Synergistic use of iron particles and anodic electrode as electron acceptors for NH_4^+ oxidation	500	81	78	N_2, NO_2^-	(Zhu et al., 2021)
First bioelectrochemical nitrification, oxidation of NH_4^+ to NO_3^- in a MEC	70	17	-	NO_3^-	(Qu et al., 2014)
Bioelectrochemical oxidation of NH_4^+ to NO_2^- + reduction to N_2 by anammox	100	4.6	-	NO_2^-	(Zhu et al., 2016)
Excessive organic carbon concentration inhibits bioelectrochemical nitrification	500	100 %*	-	NO_2^-, NO_3^-	(Zhou et al., 2021)
Complete bioelectrochemical nitrification: oxidation of NH_4^+ to N_2 in a batch-mode operated MEC	140	12	12	N_2	(Zhan et al., 2014)

First complete bioelectrochemical oxidation of NH_4^+ to N_2 in a continuous-operated MEC	100	35	35	N_2	(Vilajeliu-Pons et al., 2018)
Combination of bioelectrochemical nitrification and methane production. Long-term experiment (over 600 days)	70	10 %*	10 %*	N_2	(Siegert & Tan, 2019)
Use of a MFC as power supply of a nitrifying MEC. NO_2^- reduction by denitrification and anammox	45	151	95	N_2, NO_3^-	(Koffi & Okabe, 2021)
Increasing anodic electrode surface enhances bioelectrochemical nitrification	52	42	38	N_2, NO_2^-, NO_3^-	(Oksuz & Beyenal, 2021)
Electroanammox: direct bioelectrochemical oxidation of NH_4^+ to N_2 (through NH_2OH) by anammox bacteria	56	N.R.**	N.R.**	N_2	(Shaw et al., 2020)

* Nitrogen or ammonium removal efficiencies are indicated when nitrogen or ammonium removal rate were not specified ** N.R. not registered.

The ability of different microorganisms to oxidise NH_4^+ using an electrode as an electron acceptor has been analysed to develop nitrifying bioanodes. Kim et al. (2008) attempted NH_4^+ bioelectrochemical oxidation using an MFC that had been inoculated with swine manure. Nevertheless, neither ammonium removal nor electricity generation were achieved (Kim et al.,

2008). Ammonium bioelectrochemical oxidation requires energy input to be carried out, as it is an endergonic reaction (Kuypers et al., 2018), so nitrifying BES (niBES) have to be operated as MECs instead of as MFCs.

Natural environments have been also researched to find microorganisms able to use electron acceptors alternative to oxygen for ammonium oxidation. For example, feammox bacteria can use iron oxide as an electron acceptor for the oxidation of NH_4^+ to NO_2^- and NO_3^- (Yang et al., 2012; Zhou et al., 2016), which makes them a good candidate for being able to perform bioelectrochemical nitrification since iron-reducing bacteria are usually able to use electrodes as electron acceptors (e.g. *Geobacter* sp.) (Lovley, 2008). On top of that, the feammox process is boosted by the presence of electron shuttles, suggesting that external electron transfer mechanisms could be involved in this process. Taking that into consideration, feammox bacteria were hypothesised as candidates for electricity-driven NH_4^+ oxidation. This was observed when a MEC colonised with a pure culture of the feammox bacteria *Acidimicrobiaceae* sp. strain A6 was able to produce an electric current by oxidising 0.3 g $N\text{-}NH_4^+$ m^{-3} d^{-1} into NO_2^- (Ruiz-Urigüen et al., 2019). Moreover, Zhu et al. (2021) showed the synergy between feammox and anodic NH_4^+ bioelectrochemical oxidation by operating an ammonium-oxidising MEC containing Fe_2O_3 particles. The NH_4^+ removal achieved (81 g $N\text{-}NH_4^+$ m^{-3} d^{-1}) was better than the one obtained with only the iron particles (but without electricity supply) (62 g $N\text{-}NH_4^+$ m^{-3} d^{-1}) or by the bioelectrochemical system on its own (with no Fe_2O_3 added) (33 g $N\text{-}NH_4^+$ m^{-3} d^{-1}). 96 % of the ammonium was converted to N_2 while the rest was converted into NO_2^-.

The first successful attempt to achieve anoxic ammonium bioelectrochemical oxidation was carried out by Qu et al. (2014). Ammonium was oxidised to nitrate under anoxic conditions at a rate of 17 g $N\text{-}NH_4^+$ m^{-3} d^{-1} using a discontinuous MEC inoculated with river sediments which had a cell voltage applied of 0.8 V.

Moreover, a continuous MEC was inoculated with anammox seed sludge by Zhu et al. (2016), who set an anodic potential of −0.5 V vs Ag/AgCl to carry out the bioelectrochemical oxidation of NH_4^+ to NO_2^- at a rate of 4.6 g N-NH_4^+ m^{-3} d^{-1}. Then, this NO_2^- was used by the anammox bacteria as the electron acceptor to oxidise more NH_4^+ into N_2. This approach reduced the electrons required to oxidise one molecule of ammonium, from the 8 electrons needed to produce nitrate to the 6 required for the generation of nitrite. Moreover, thanks to the anammox pathway, the NO_2^- generated could be used for the oxidation of more NH_4^+. On the other hand, Zhou et al. (2021) examined how the presence of organic matter affected bioelectrochemical nitrification in a MEC inoculated with nitrifying and denitrifying bacteria and operated in batch mode under an applied voltage of 0.6 V. Up to 76 % of the NH_4^+ present in the system was bioelectrochemically oxidised to NO_2^- and NO_3^- in the absence of organic matter, and all of it at C/N ratios of 1 and 1.5. However, no ammonium removal was observed when C/N was raised to 3, showing that an excess of organic matter can hinder bioelectrochemical nitrification.

There are other studies describing the bioelectrochemical oxidation of ammonium into N_2. Zhan et al. (2014) operated a discontinuous MEC at a potential of +0.8 V vs SHE. The microbiota of the anode of the reactor, proceeding from a WWTP mixed culture was able to catalyse the bioelectrochemical oxidation of ammonium to nitrogen gas at a rate of 12 g N-NH_4^+ m^{-3} d^{-1}. Moreover, the work of Vilajeliu-Pons et al. (2018) showed for the first time complete ammonium oxidation to N_2 in the anode of a MEC that worked in continuous mode and under anoxic conditions, achieving NH_4^+ oxidation to N_2 at a rate of 35 g N-NH_4^+ m^{-3} d^{-1}. The anode was inoculated with a mixture of different nitrifying reactors sludges, and the anodic potential was set at +0.8 V vs SHE. The nitrifying bacteria *Nitrosomonas* sp. were considered to have an important role in ammonium oxidation, while an intermediate nitrification compound known as hydroxylamine (NH_2OH) was proven to be the main target for bioelectrochemical oxidation. In a recent study, the anodic oxidation of NH_4^+ to N_2 was coupled with the production in the cathode

of hydrogen gas or methane (the latter only if some organic matter was present at the cathode) (Siegert & Tan, 2019). This experiment was performed in a discontinuous MEC, it took place for over 600 days and it yielded a total nitrogen removal efficiency of 10 %.

More recently, other authors have reported bioelectrochemical nitrification producing both N_2 and NO_3^- and/or NO_2^-. Koffi & Okabe (2021) used a single chamber MEC for the anoxic bioelectrochemical oxidation of the ammonium present in domestic wastewater. Domestic wastewater was also used to inoculate the MEC. The anodic potentials applied during this study ranged between 0 and +1.2 V (vs SHE), and the system was powered using a double chamber MFC or a potentiostat. The maximum ammonium removal rate (151 g $N\text{-}NH_4^+$ m^{-3} d^{-1}) was achieved at an anodic potential of +0.6 V vs SHE, being 63 % of it removed as N_2 and the rest as NO_3^-. Moreover, the ex-situ experiments performed by the authors revealed that the microorganisms present in the reactor could remove nitrite in two ways, denitrification (using organic matter present in WW) and anammox. Oksuz & Bernal (2021) evaluated the use of anodic electrodes with different surface areas for the bioelectrochemical oxidation of ammonium in a MEC with an anodic potential of +0.2 V vs SHE. The nitrogen removal rate obtained with an anode with a surface of 30.4 cm^2 (38 g N m^{-3} d^{-1}) was higher than the ones obtained with a 15.2 cm^2 anode (18 g N m^{-3} d^{-1}) and with a 3.8 cm^2 anode (7.2 g N m^{-3} d^{-1}). A small part of the ammonium (4 g $N\text{-}NH_4^+$ m^{-3} d^{-1}) was removed as NO_3^- and NO_2^-, resulting in a total ammonium removal rate of 42 g $N\text{-}NH_4^+$ m^{-3} d^{-1}.

Finally, Shaw et al. (2020) described a novel NH_4^+ bioelectrochemical oxidation mechanism called electro-anammox, performed by anammox microorganisms, in which ammonium is oxidised to hydroxylamine and then to nitrogen gas. This route, which took place under an anodic potential of +0.6 V vs SHE, would probably not occur in niBES with a microbiota mainly composed of nitrifiers and denitrifiers. Therefore, the NH_4^+ bioelectrochemical oxidation pathway for nitrifying microorganisms has not been elucidated yet.

In summary, there are currently two main METs suitable for nitrogen removal. Bioelectrochemical denitrification can be applied on its own for NO_3^- removal or in combination with aerobic nitrification for NH_4^+ removal. This process can be powered by a potentiostat or a power source in a MEC or it can be coupled with organic matter bioelectrochemical oxidation in an MFC. Due to its adaptability, this technology can be applied for water treatment in very diverse scenarios. On the other hand, bioelectrochemical nitrification (the oxidation of NH_4^+ using the bioanode of a MEC) has been developed as an oxygen-independent ammonium removal MET in recent years, and the mechanisms driving this process are still under research. The main processes involved in nitrogen-removing METs are represented in Figure 1.

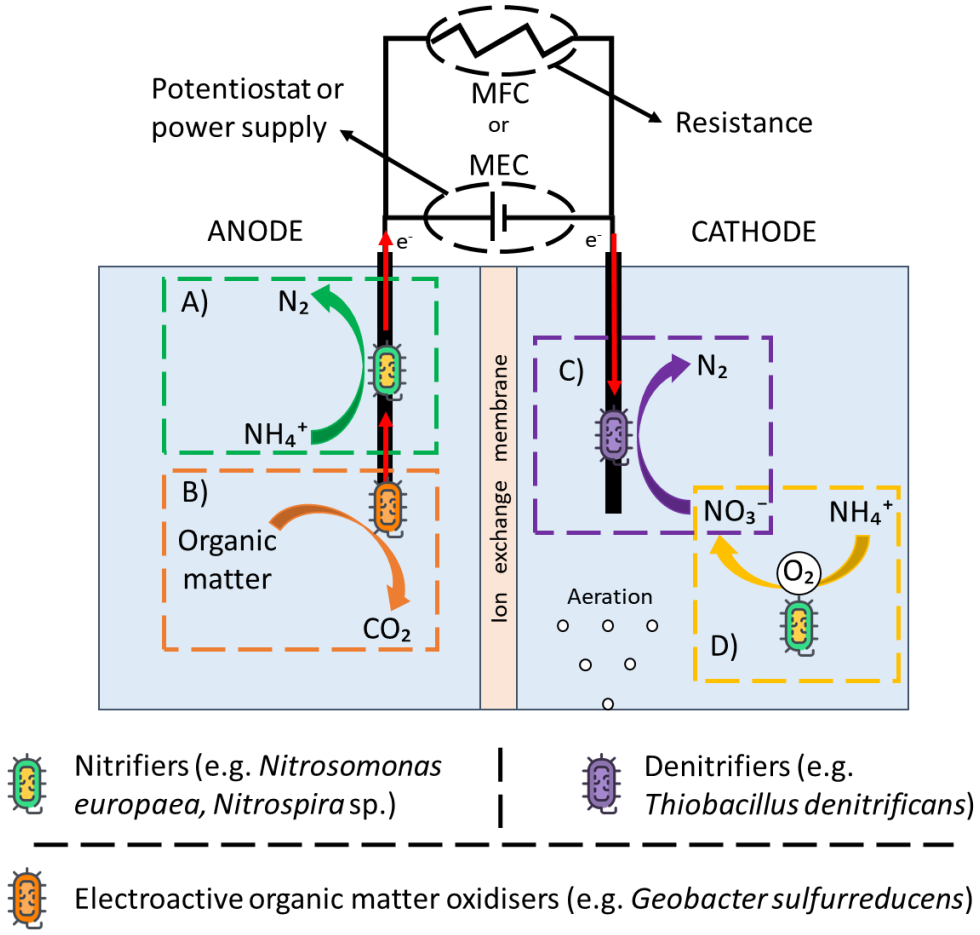

Figure 1. Main processes occurring in nitrogen removing BES: A) bioelectrochemical nitrification. B) organic matter bioelectrochemical oxidation. C) bioelectrochemical denitrification. D) aerobic nitrification.

Chapter 2. Objectives

The presence of ammonium in water poses an environmental hazard. Current NH_4^+ removal technologies are energy-intensive, while METs have been proposed as an alternative to them. **The objective of this Ph.D. thesis was to widen the current knowledge and applicability of METs for nitrogen removal**. Two different technologies, bioelectrochemical nitrification and bioelectrochemical denitrification, were studied to achieve the following sub-objectives:

- To increase the current knowledge on the fundamental mechanisms of bioelectrochemical nitrification. The specific pathway leading to the bioelectrochemical oxidation of NH_4^+ remains unknown. This PhD thesis contributed to investigating the nitrogen removal pathways in nitrifying BES dominated by nitrifying bacteria and with a low abundance of anammox culture.
- To develop a sustainable technology (named electrified biotrickling filters or e-biofilter) that integrates NO_3^- bioelectrochemical reduction into a conventional aerobic nitrifying reactor, biotrickling filters, as an innovative decentralized treatment for NH_4^+ removal. This work contributed to the development of e-biofilters and their validation on wastewaters with a low C/N ratio such as aquaculture and secondary treated wastewater.

Chapter 3. Methodology

3.1 Bioelectrochemical systems set-up

During this Ph.D. thesis, three main reactor configurations were used: rectangular reactor and glass-bottle reactor, both used in Chapter 4, and tubular reactor, used in Chapters 5 and 6.

3.1.1 Rectangular reactor

Duplicate BES systems used in Chapter 4 were built using two rectangular methacrylate frames that contained two 1 L chambers, an anode and a cathode (Vilajeliu-Pons et al., 2018) (Figure 2). These chambers were separated by an anion exchange membrane (AMI-7001, Membranes International Inc., USA), to prevent NH_4^+ migration from the anode to the cathode (Kim et al., 2008). A graphite rod (6 mm diameter x 130 mm length, Sofacel, Spain) was inserted in each chamber, acting as anodic and cathodic current collectors, and an Ag/AgCl reference electrode (+0.197 V vs SHE, model RE-5B, BASI, UK) was placed in the anodic chamber. Both the anodic and the cathodic compartments were filled with granular graphite (model 00541, 1.5 - 5 mm diameter, EnViro-cell, Germany), reducing the net liquid volume of each compartment to 0.4 L. This granular graphite acted as electron-conductive material and it had a specific electric resistivity of $1.2 \times 10^{-3} \pm 0.1 \times 10^{-4}$ Ohm m. The anodic and cathodic current collectors and the reference electrode were connected to a potentiostat (Model VSP, BioLogic, France), which was used to polarize the working electrode (anode) at +0.8 V vs SHE and was used to record the electric current data.

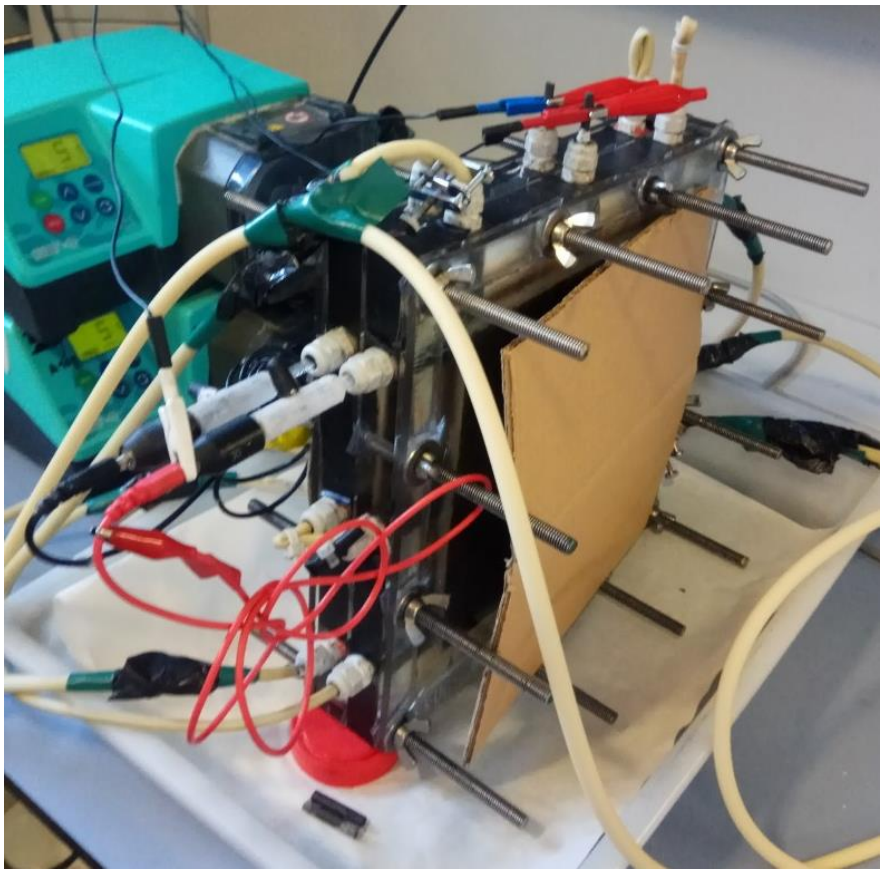

Figure 2. Image of a rectangular BES operated in Chapter 4.

Two buffer tanks (2 L) were connected to the anodic and the cathodic chambers, respectively. A peristaltic pump (model 205S, Watson Marlow, UK) was used to recirculate water between each compartment and the respective buffer tank as shown in Figure 3. The recirculation flow was initially adjusted to 7.5 L d^{-1} and subsequently incremented to 25 L d^{-1} (model 323 E/D, Watson Marlow, UK) to improve the flow distribution inside the reactor. The two buffer tanks were connected to 1 L gas-tight bags (Standard FlexFoil® Sample bag, SCK, UK) filled with dinitrogen gas, to prevent air intrusion during sampling and thus maintain the anoxic conditions during the experiment. The medium of the buffer tank was replaced when ammonium content was depleted. Immediately after medium replenishment, N_2 was flushed for 15 minutes, and the gas-tight bags were emptied and refilled with fresh N_2.

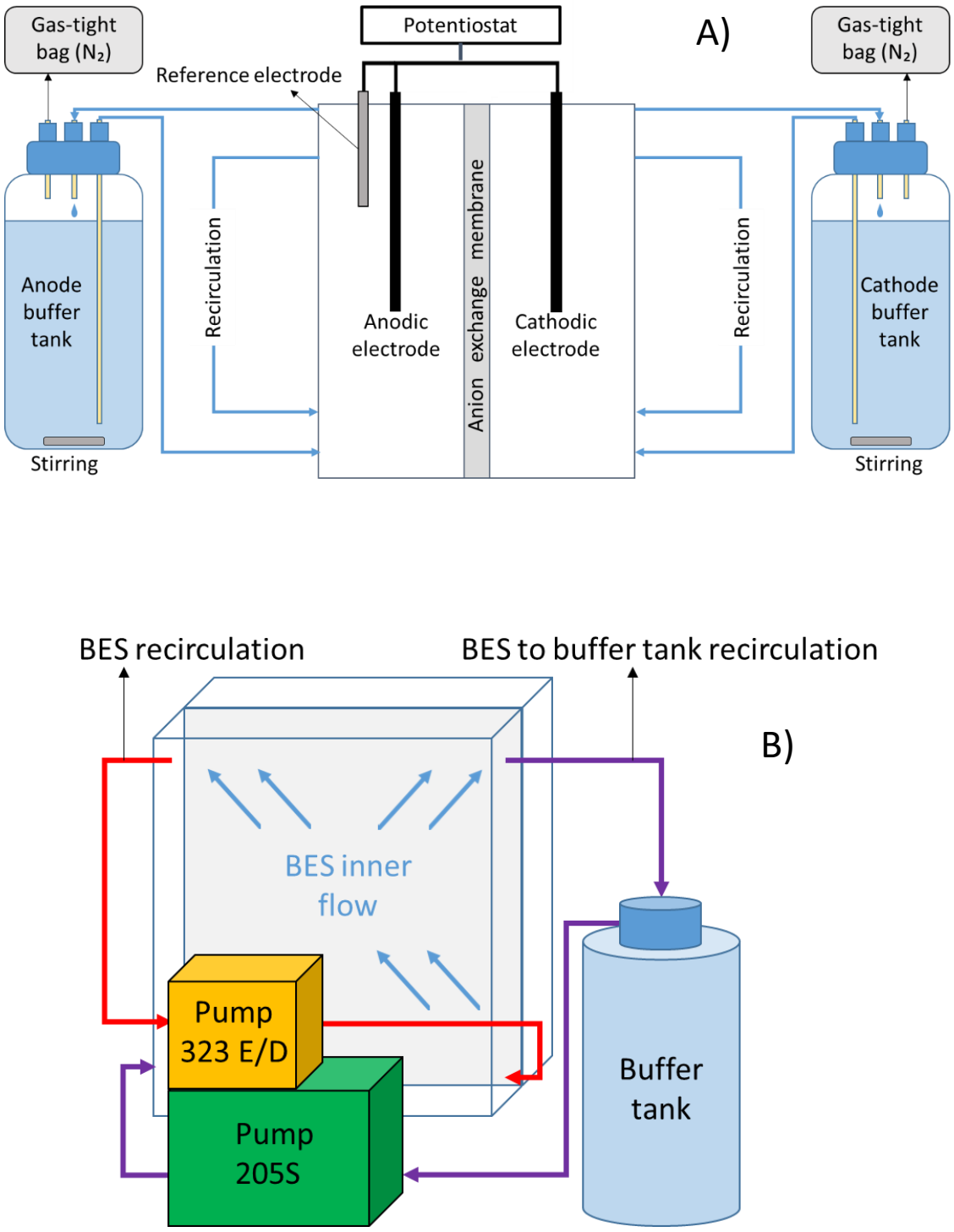

Figure 3. Schematic representation of the rectangular BES used in Chapter 4: A) general diagram of the system. B) scheme of the recirculation systems connected to the BES (representing the recirculation corresponding to only one of the two chambers of the reactor).

3.1.2 Set-up for abiotic tests

To perform the abiotic tests for Chapter 4, a 400 mL glass flask was used as shown in Figure 4. The glass flask contained 100 mL of granular graphite (model 00541, 1.5 - 5 mm diameter, EnViro-cell, Germany), presenting a net liquid volume of 200 mL. A graphite rod (6 mm diameter x 130 mm length, Sofacel, Spain) was introduced into the reactor, in contact with the granular graphite, and the rod and the granular graphite acted as the anodic electrode. A titanium-mixed metal oxide (Ti-MMO) rod (6 mm diameter x 225 mm length, NMT electrodes, South Africa) and an Ag/AgCl reference electrode (+0.197 V vs SHE, model RE-5B, BASI, UK) were used as cathodic and reference electrode, respectively. The three electrodes (anodic, cathodic and reference) were connected to a potentiostat (Model VSP, BioLogic, France), used to set the anodic potential at +0.8 V vs SHE and to register the electric current data. A continuous N_2 flush was applied to keep the anoxic conditions by removing oxygen from the reactor.

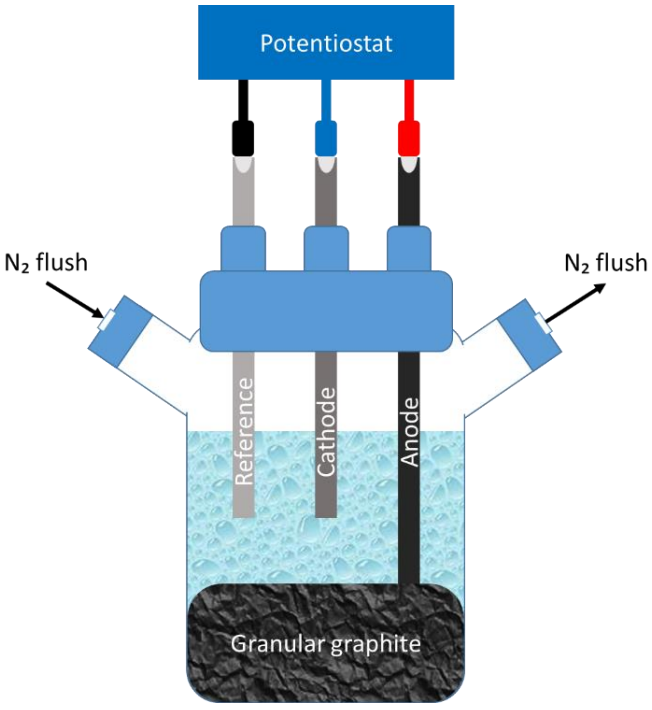

Figure 4. Schematic representation of the abiotic reactor used in Chapter 4.

3.1.3 Tubular reactors

The reactors used in Chapters 5 and 6 were all constructed using tubular polyvinyl chloride (PVC) reactors with an inner diameter of 4.2 cm and a height of 100 cm (resulting in an internal total volume of 1.39 L) (Figure 5). In total, four different configuration reactors were constructed. A conventional biotrickling filter (Reactor A) was built filling the reactor with PVC granules (diameter 2 - 8 mm), reducing its net liquid volume to 534 mL (Figure 6A). An Electroconductive (non-polarized) column reactor (Reactor B) was set using granular graphite (model 00514, diameter 1.5 - 5 mm, Enviro-cell, Germany) as filler instead (Figure 6B). These reactors had a net liquid volume of 633 mL.

Figure 5. Image of different tubular reactors used during this Ph.D. thesis.

The third tubular reactor configuration (Reactor C, Figure 6C) was filled with granular graphite, with the reactor net liquid volume being reduced to 655 mL. Nine graphite rods (6 mm diameter, Mersen Iberica, Spain) were placed vertically every 10 cm height, and eight of them were connected to a power source (IMHY3, Lendher, Spain), with four acting as cathodes (the ones placed at a height of 10, 20, 30 and 40 cm) and other four as anodes (those at 50, 60, 70 and 80 cm). An Ag/AgCl reference electrode (+0.197 V vs SHE, SE 11, Xylem Analytics Germany Sales GmbH & Co. KG Sensortechnik Meinsberg, Germany) was placed 20 cm high into the reactor, and a cathodic potential of -0.3 V vs Ag/AgCl was set and maintained throughout the experiment.

The fourth and final reactor configuration used (Reactor D) was an electrified biotrickling filter (or e-biofilter) (Figure 6D). The upper half of the e-biofilter was filled with PVC granules, and the lower half, with granular graphite. The e-biofilter net liquid volume was 777 mL. Two titanium rods (Grade 1, 8 mm diameter, Polymet Reine Metalle, Germany) served as the anodic and cathodic current collectors (CCs). The anodic CC was inserted into the reactor at 45 cm height, and the anodic CC, at 12 cm height, while an Ag/AgCl reference electrode was placed close to the anodic CC. A stainless-steel mesh (30 cm height, mesh path light 5 × 5 mm) was inserted around the inner wall at the bottom of the reactor to improve the cathode electrical distribution. The anodic and cathodic electrodes were connected to a power source to establish and keep the cathode potential at -0.3 V vs Ag/AgCl.

In all these reactors, the influent flowed from the top part of the reactor to the bottom. For the three first configurations, the water level (WL) in the reactor was kept at 100 cm. However, e-biofilters were operated under 50 cm and 75 cm WL configurations. All reactors except the conventional biotrickling filter were operated in duplicate.

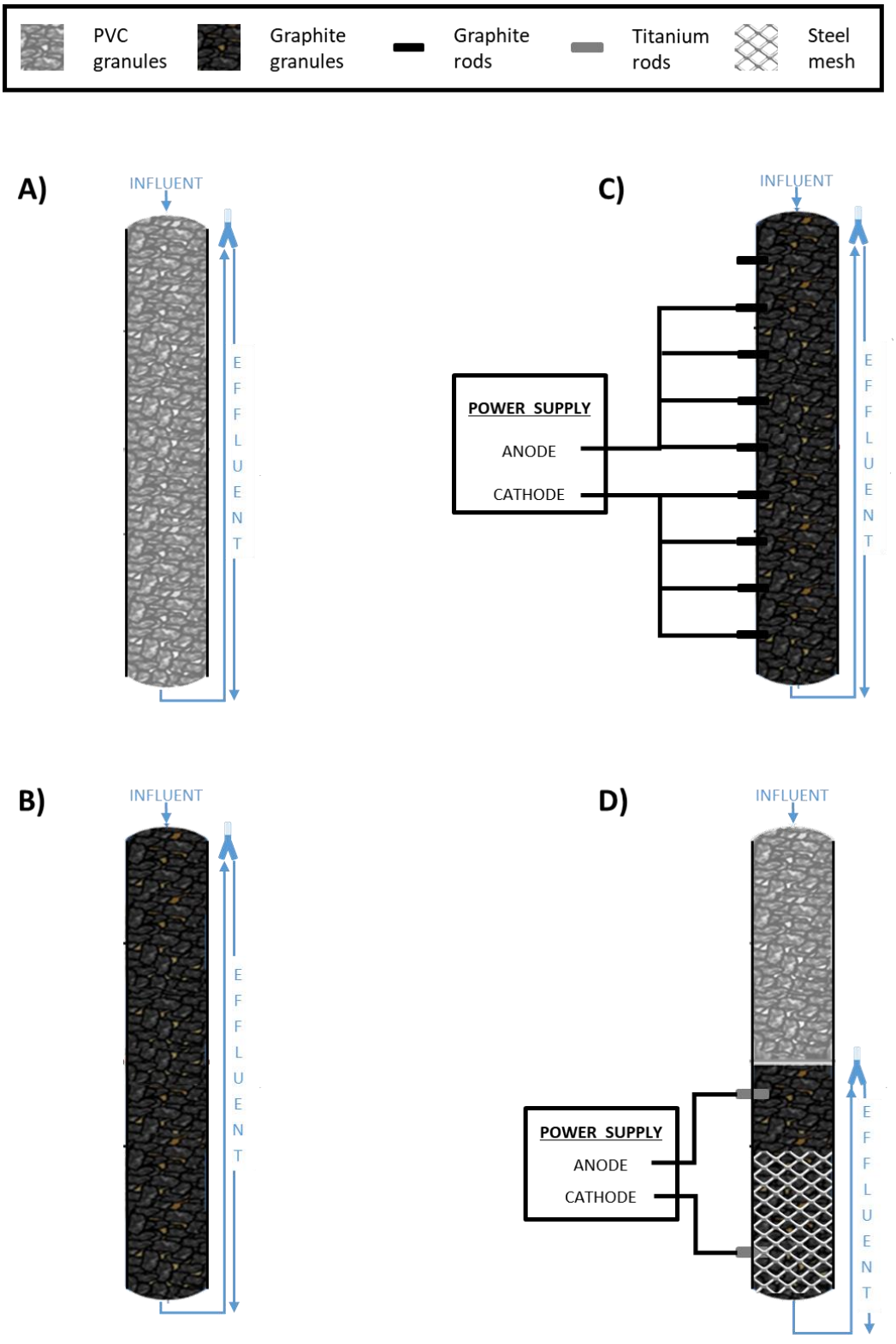

Figure 6. Diagram of the tubular reactors used during Chapters 5 and 6 of this thesis: A) Reactor A. B) Reactor B. C) Reactor C. D) Reactor D.

3.2 Medium and inoculum

Different natural and synthetic solutions were used during the inoculation and operation of the reactors used in this PhD thesis. A solution containing 1.072 g KH_2PO_4 L^{-1}, 1.05 g $NaHCO_3$ L^{-1}, 0.25 g NaCl L^{-1}, 0.162 g Na_2HPO_4 L^{-1}, 0.015 g $CaCl_2$ L^{-1}, 0.1 g $MgSO_4 \cdot 7\ H_2O$ L^{-1} and 0.1 mL L^{-1} of trace elements solution (Rabaey et al., 2005), hereafter referred as a minimal solution, was prepared alone or supplemented with different nitrogen species and used to feed the reactors in Chapters 4 and 5. In Chapter 6, the secondary effluent of an urban WWTP (Quart, Catalonia, Spain) was used as a feeding solution. This wastewater contained low chemical oxygen demand (COD) (101.7 ± 42.9 mg COD L^{-1}), a total suspended solids (TSS) content of 105.3 ± 95.1 mg TSS L^{-1}, an ammonium concentration of 44.9 ± 7.2 mg N-NH_4^+ L^{-1}, and small amounts of nitrate and nitrite (0.7 ± 1.0 mg N-NO_3^- and L^{-1} 0.9 ± 1.7 mg N-NO_2^- L^{-1}. respectively). Moreover, the inoculums used during this Ph.D. thesis were obtained from different wastewater treatment and nitrogen removal reactors.

3.3 Inoculation and start-up

3.3.1 Rectangular reactors – Nitrification tests

The rectangular BES were operated in batch mode. At the start of the inoculation phase, the anodic chamber and the buffer tank connected to it were initially fed with minimal solution supplemented with 0.2 g NH_4Cl L^{-1} (50 mg N-NH_4^+ L^{-1}) and also 50 % (V/V) of a mixed inoculum, half of it proceeding from an aerobic nitrification reactor of an urban WWTP (Girona, Spain) and the other 50 % coming from a partial nitrification reactor (Gabarró et al., 2012). The cathode was filled with a minimal solution with 0.2 g NH_4Cl L^{-1}. The solutions on both sides were renewed when ammonium was consumed for the first time. Then, once the anodic NH_4^+ removal was consistent (after 30 days of the experiment), the solution in the cathode was substituted by

minimal solution (without NH_4^+), concluding the inoculation phase. During inoculation and also operation phase, 6 mL samples were taken twice a week from the anode and the cathode of the BES, with the volume, sampled being replaced immediately with a fresh medium.

3.3.2 Tubular reactors – Biotrickling filter tests

The tubular reactors were inoculated in batch mode using an inoculation solution containing minimal solution supplemented with 50 mg $N\text{-}NH_4$ L^{-1} and a mixed inoculum. This inoculum contained the effluent of different reactors containing anammox (Akaboci et al., 2018), nitrification (Vilajeliu-Pons et al., 2018), denitrification (Pous et al., 2017) microorganisms, and also the effluent from the activated sludge of the urban WWTP of Quart. This solution, stored in a 10 L buffer tank, was replenished with fresh inoculation solution when ammonium was depleted. The inoculation took place for 23 days (21 in the case of Reactor D). During inoculation, the CCs in reactors C and D were not connected to the power source

Once inoculation finished, the reactors were changed to continuous-flow mode, and the feed was substituted by synthetic aquaculture wastewater (minimum solution supplemented with 50 mg $N\text{-}NH_4^+$ L^{-1}). This feed was stored in 10 L self-collapsible bags which were flushed with nitrogen gas prior to operation for 15 minutes. A start-up phase was initiated after the end of inoculation. During this stage, all the reactors were fed at a flow of 0.6 L d^{-1} (corresponding to a hydraulic retention time of 1.0 d), except Reactor D (0.7 L d^{-1}, HRT of 1.2 d). During this period, the performance of Reactor C was evaluated with 2, 4, 6 and 8 of the CCs connected to the power source (half as anodic and half as cathodic CCs). The 8 CCs configuration was chosen as the best one and maintained thereafter. The start-up phase was prolonged until the nitrogen removal and electric current data were stable, lasting 118 days for all reactors except Reactor D (30 days in this case). Reactor D was operated at WL 50 cm during the inoculation and start-up phase. Samples were taken twice a week from the influent and the effluent of the tubular reactors during inoculation, start-up and operation phases

3.4 Operational conditions

3.4.1 Rectangular reactor – Nitrification tests

In Chapter 4, after the completion of the inoculation phase, the rectangular BES were operated in batch mode to analyse the bioelectrochemical removal of ammonium and other nitrogen species. During 180 days, the ammonium concentration in the anode was replenished to 50 mg $N\text{-}NH_4^+$ L^{-1} periodically before depletion by spiking a concentrated NH_4^+:HCO_3^- (1:2) solution. After those 180 days, other nitrification intermediates (NO_2^-, NO_3^- and NH_2OH) were spiked into the reactor (with and without NH_4^+) in different experiments to analyse the effect of the transient accumulation of these compounds in the NH_4^+ removal process (details reported in Chapter 4). Samples were taken as described in section 3.3.1

3.4.2 Abiotic tests

The abiotic reactor was batch-fed with 200 mL of minimal solution, initially supplemented with NO_2^- and later withNH_2OH (details in Chapter 4). 6 mL samples were extracted daily from the reactor

3.4.3 Tubular reactor – Biotrickling filter tests

In Chapter 5, the performance of the different tubular reactors was tested after the start-up phase by feeding them synthetic aquaculture wastewater (minimal solution with 50 mg $N\text{-}NH_4^+$ L^{-1}) in the continuous-flow mode under different HRTs (around 1.0 d, 0.6 d and 0.3 d), with and without flushing N_2 to the influent in the self-collapsible feeding bags. These conditions were applied to Reactors A, B and C. For Reactor D, the influent was always flushed with N_2 for 15 minutes, and the three HRTs (1.2 d, 0.7 d and 0.3 d) were slightly different. Moreover, two WLs were evaluated (50 cm and 75 cm). The effect of electrode polarization was tested by operating reactor D under Open Circuit conditions for seven days.

Once the experiments in Chapter 5 were finished, a short set-up for Chapter 6 was carried out by operating Reactor D at HRT 1.4 d, WL 50 cm and NH_4^+ supplemented minimal solution used as influent. After 10 days of operation, the reactors were connected to a 240 L refrigerated tank (4ºC) containing Quart urban WWTP secondary effluent. This influent was fed to Reactor D at HRTs of around 1.4 d, 0.7 d and 0.3 d and WL of 50 cm and 75 cm. Samples were taken as explained in section 3.3.2

3.5 Analysis and calculations

3.5.1 Chemical analysis

For all the samples taken, the NH_4^+, NO_2^- and NO_3^- concentrations were measured using ion chromatography (Dionex IC5000, Vertex Technics, Spain), while the pH was recorded with a pH-meter (pH-meter basic 20+, Crison, Spain) and the conductivity was measured with a conductivity meter (EC-meter basic 30+, Crison, Spain).

Other analyses were performed specifically to certain experiments or reactors. The hydrazine (N_2H_4) concentration was analysed using a colourimetric kit (Spectroquant® Hydrazine test 109,711, Merck, Germany). The concentration of NH_2OH was measured by colourimetry (Oshiki et al., 2016). The concentration of nitrous oxide (N_2O) was occasionally measured with an N_2O liquid-phase microsensor (Unisense, Denmark) in the anode and cathode of the rectangular BES and in the effluent of Reactor D. An oxygen sensor (model 6050, Mettler Toledo, USA) was used to monitor the dissolved oxygen (DO) concentration in the rectangular BES and also to occasionally measure the DO in the effluent of Reactor D during Chapter 5. COD and TSS concentrations were measured following the American Public Health Association (APHA) standards (APHA, 2005) in the influent and the effluent of Reactor D during Chapter 6.

3.5.2 Calculations

The NH_4^+, NO_2^- and NO_3^- removal rates in Chapter 4 were calculated taking into account the reduction of each compound during each experiment and the duration of the experiment. In the case of the experiments in which nitrite or nitrate were added to the rectangular BES, the removal rates were estimated using linear regression of the first data points (i.e. initial activities) instead.

The Coulombic efficiency (CE, %) of different reactions possibly occurring during Chapter 4 was calculated by Equation 7

$$CE\ (\%) = 100\ \% \times C_{measured}/C_{theoric} \quad \text{(Equation 7)}$$

Where $C_{measured}$ represents the coulombs measured by the potentiostat (C) and $C_{theoric}$ represents the coulombs theoretically required or generated by the reduction or the oxidation of a certain nitrogen species, as described in Equation 8

$$C_{theoric} = \frac{-\Delta a \times n \times F}{14\ g\ N/mol\ N} \quad \text{(Equation 8)}$$

Where *F* is the Faraday constant (96,485 C mol of electrons^{-1}), *a* is the mass of the nitrogen species being oxidised or reduced (g N) (N-NH_4^+, N-NH_2OH, N-NO_2^-, and N-NO_3^-), and *n* are the mols of electrons required to oxidise or reduce 1 mol of nitrogen of that compound (mol of electrons mol N^{-1}). Values of *n* for the reactions considered in this work were: a) 3 for the oxidation of NH_4^+ to N_2; b) 3 for the oxidation of NH_2OH to nitric oxide (NO); c) 1 for the oxidation of NH_2OH to N_2; d) 2 for the oxidation of NO_2^- to NO_3^-; and e) 5 for the reduction of NO_3^- to N_2.

To estimate the current density in the rectangular BES (mA m^{-2}), the area of the anodic electrode ($A_{electrode}$, m^2) was calculated according to Equation 9

$$A_{electrode} = A_{GG} \times V_{TotalGG}/V_{GG} \quad \text{(Equation 9)}$$

Where A_{GG} is the area of a granule of graphite (m^2), considering the granules as perfect spheres with a mean diameter (according to the manufacturer) of 0.004 m, $V_{TotalGG}$ is the aggregated volume of all the graphite granules in the anodic chamber (0.0006 m^3) and V_{GG} is the volume of a single granule of graphite (m^3).

Regarding Chapters 5 and 6, the HRTs were calculated by dividing the net liquid volume of each tubular reactor by the flow rate applied. The NH_4^+ and total nitrogen (NH_4^+, NO_2^- and NO_3^-) removal rates were calculated as the difference between influent and effluent concentrations divided by the HRT. The electric consumption of Reactors C and D (kWh g N^{-1}) was calculated by dividing the energy provided by the power source (the product of the intensity and the voltage applied) by the amount of nitrogen removed in the reactor.

3.5.3 Microbial analyses

The microbiota present in the rectangular BES was analysed in Chapter 4. DNA was extracted from the granular graphite as explained by Vilajeliu-Pons et al. (2016). The partial sequences of the archaeal and bacterial 16S rRNA genes were obtained with the Illumina MiSEq PE250 sequencing platform, using primers 515F-806R targeting the V4 region (Kozich et al., 2013). Sequencing was carried out by the RTSF Core facilities (Michigan State University, USA, https://rtsf.atsci. msu.edu/).

Sequence quality filtering, trimming, dereplicating, and merging were carried out with the DADA2 based pipeline implemented in R (Callahan et al., 2016). Basic filtering methods were set to 230 and 180 bp for forward and reverse reads, with no ambiguous bases allowed and maximum expected error rates of 2. To avoid spurious diversity, singletons were removed from the final set of sequences. Bimeras were detected and removed (172 of 1395 input sequences) with the consensus method implemented in DADA2 package in R. Sequences were clustered into amplicon sequence variants (ASVs) (100 % similarity index).

The taxonomic assignments were carried out at the maximum taxonomic rank when possible using the Silva v132 train set to release as a reference, unless in case of poor taxonomical assignment. in that case, ASVs were assigned using nucleotide Basic Local Alignment Search Tool (BLAST) searches at the National Centre for Biotechnology Information (NCBI). The graphical representation of the relative abundances of specific taxons and microbiomes was executed with the Phyloseq package (McMurdie & Holmes, 2012) implemented in R.

Chapter 4. Unveiling microbial electricity-driven anoxic ammonium removal

Redrafted from**: Osset-Álvarez, M.**, Pous, N., Chiluiza-Ramos, P., Bañeras, L., Balaguer, M. D., & Puig, S. (2022). Unveiling microbial electricity-driven anoxic ammonium removal. *Bioresource Technology Reports*, *17*, 100975. https://doi.org/10.1016/j.biteb.2022.100975

4.1 Introduction

Bioelectrochemical systems are an innovative approach to accelerating bioremediation processes by supplying an unlimited source of electron donors/acceptors to bacteria. Biologic nitrogen removal is one of the bioremediation processes that could take a profit from BES. The external supply of oxygen (O_2, electron acceptor) and organic matter (electron donor) is usually required to carry out nitrification/denitrification reactions. The usage of an anodic electrode as an electron acceptor for microbial ammonium oxidation could reduce the need for aeration and the important associated costs (Vilajeliu-Pons et al., 2018).

Recently, Shaw et al. (2020) demonstrated a new mechanism for ammonium bioelectrochemical oxidation to N_2 in a BES inoculated with anammox culture and a polarized anode electrode at different potentials from -0.1 to +0.6 V vs SHE. The ammonium oxidation mechanism started with the oxidation of NH_4^+ to NH_2OH, which reacted with an additional molecule of NH_4^+ to form N_2H_4, an anammox-specific intermediary metabolite (van Teeseling et al., 2013), and it ended up with the oxidation of N_2H_4 to N_2. This process hereafter referred to as electro-anammox, where neither nitrite nor nitrate were generated or consumed, has been only reported for anammox bacteria. anammox-like bacteria such as Feammox have been reported to present electroactive activity (Ruiz-Urigüen et al., 2019; Zhu et al., 2021). Ruiz-Urigüen et al. (2019) suggested that Feammox (*Acidimicrobiaceae* sp. A6) oxidised NH_4^+ to nitrite, which was later reduced to N_2 due to the presence of iron (Fe^{2+}) in the medium. Such a behaviour (NH_4^+ oxidation to NO_2^-/NO_3^-) is the one that would be expected for nitrifying bacteria. Indeed, in some works, the usage of nitrifying bacteria in presence of a polarized electrode has reported the conversion of NH_4^+ into NO_2^-/NO_3^-, which can be later converted into N_2 by promoting processes such as anammox or heterotrophic denitrification (Koffi & Okabe, 2021; Qu et al., 2014; Tutar Oksuz & Beyenal, 2021; Zhou et al., 2021; Zhu et al., 2016).

However, in other works where no organic matter was present and the anodic microbial community presented a high abundance of nitrifiers, almost undetectable amounts of anammox, the ammonium conversion into dinitrogen gas has been observed (Siegert & Tan, 2019; Vilajeliu-Pons et al., 2018; Zhan et al., 2014). Different interpretations have been elucidated. For example, Zhan et al. (2014), who used an inoculum from a WWTP and set an anodic potential of +0.6 V vs Ag/AgCl, attributed the absence of NO_2^- and NO_3^- accumulation to the presence of denitrifying bacteria in the anodic biofilm (*Comamonas* sp. and *Paracoccus* sp.), even though no organic matter was supplemented to the medium. Siegert & Tan (2019), who tested different anodic potentials from +0.15 to +0.55 V vs SHE, observed a similar behaviour and they considered that denitrification could have a role in the cathode compartment. In Vilajeliu-Pons et al. (2018), the anode of a BES reactor was inoculated with different nitrifying bacteria and poised at +0.8 V vs SHE. From the results obtained, it was estimated that *Nitrosomonas* was the main responsible for the bioelectrochemical oxidation of NH_4^+ and NH_2OH (a nitrification intermediate), while very low concentrations of NO_2^- and NO_3^- were detected due to a combination of anammox and denitrification processes.

Without a better understanding of the underlying processes, an optimization of the operational conditions and the reactor setup might be threatened. For this reason, this work aimed at elucidating how NH_4^+ could be bioelectrochemically oxidised with a low presence (or absence) of anammox bacteria. A series of experiments were set up in two parallel fed-batch BES to study the removal of ammonium and other nitrogen species (nitrate, nitrite and hydroxylamine) that could be possibly involved in the process.

4.2 Materials and methods

4.2.1 Experimental set-up

Two BES were constructed using two rectangular methacrylate structures containing two 1 L chambers (anode and cathode) separated by an anion exchange membrane (AMI-7001, Membranes International Inc., USA) (Vilajeliu-Pons et al., 2018). The anion exchange membrane was used to minimize the diffusion of ammonium to the cathodic compartment (Kim et al., 2008). Each chamber was filled with granular graphite (model 00541, 1.5 - 5 mm diameter, EnViro-cell, Germany). Laboratory tests indicated that the bed of granular graphite presented a specific electric resistivity of $1.2 \times 10^{-3} \pm 0.1 \times 10^{-4}$ Ohm m. The elemental composition is shown in Table S4.1. An Ag/AgCl reference electrode was inserted in the anode compartment (+0.197 V vs SHE, model RE-5B, BASI, UK), and two graphite rods (3 mm radius x 130 mm length, Sofacel, Spain) were placed as current collectors in each chamber. The net liquid volume of each chamber was 0.4 L. A potentiostat (Model VSP, BioLogic, France) connected the anode/cathode current collectors and the reference electrode to polarize the working electrode (anode) at +0.8 V vs SHE.

Each chamber was connected to a 2 L tank using a peristaltic pump (model 205S, Watson Marlow, UK), with a recirculation flow of 7.5 L day^{-1} and later increased to 25 L day^{-1} (model 323 E/D, Watson Marlow, UK) to ensure a better flow distribution inside the reactor.

4.2.2 Inoculation and experimental procedure

The anodic compartments and buffers tanks of the BES were inoculated with a solution containing 50 % (V/V) of an inoculum that consisted of a 1:1 mix of biomass obtained from a partial nitritation reactor (Gabarró et al., 2012) and an aerobic nitrification reactor of an urban WWTP (Girona, Spain). Solution media contained 0.195 g NH_4Cl L^{-1} (corresponding to 50 mg $N\text{-}NH_4$ L^{-1}), 1.05 g $NaHCO_3$ L^{-1}, 0.015 g $CaCl_2$ L^{-1}, 0.1 g $MgSO_4 \cdot 7\ H_2O$ L^{-1}, 0.162 g Na_2HPO_4 L^{-1}, 0.25 g

NaCl L^{-1}, 1.072 g KH_2PO_4 L^{-1} and 0.1 mL L^{-1} of trace elements solution (Rabaey et al., 2005). The same solution, but without inoculum, was used in the cathode.

The system was operated in batch mode during both inoculation and operation, with 6 mL samples being taken twice a week from both compartments (anode and cathodes) of the reactors. The volume sampled was immediately replaced with a fresh medium. Each 2L tank was flushed with N_2 for 15 min before each batch experiment to avoid air intrusion and hence ensure anoxic conditions. 1 L gas-tight bags (Standard FlexFoil® Sample bag, SCK, UK) were filled with N_2 and connected to the tanks, with the gas being regularly replaced. During the inoculation phase, once NH_4^+ was exhausted for the first time, the medium in the anode was replaced with fresh inoculum solution (containing 50 mg N-NH_4^+ L^{-1}), while a new abiotic ammonium-rich solution replaced the medium present in the cathode. When consistent NH_4^+ removal was observed at the anode (30 days after starting the experiment), the solution in the cathode was changed to a solution without ammonium, and the inoculation phase was finished.

During the operational period, before anodic NH_4^+ was depleted, the anode was spiked with an NH_4^+:HCO_3^- solution (1:2 molar ratio) to increase the anodic ammonium concentration to 50 mg N-NH_4^+ L^{-1} to study ammonium removal in the long-term. Different experiments were performed to study the effect of transient accumulation of intermediate metabolites (nitrate, nitrite and hydroxylamine) on ammonium removal. After 180 days of operation, known amounts of intermediates were added to the anode or the cathode compartments in separate experiments (Table 4). Moreover, control tests were performed in the buffer tanks of the anode and the cathode to check whether ammonium was removed or not inside those tanks. Buffer tanks were disconnected from the BES and 5-day control tests were carried out by adding fresh intermediary metabolites (nitrite, nitrate) and ammonium to the buffer tanks. Finally, abiotic electrochemical tests with granular graphite were also conducted to elucidate the possible catalyzing role of granular graphite (see SI3 for full description).

Table 4. Nitrogen species were fed to the BES at the different experiments performed in Chapter 4.

Experiment (no. of batches)	Nitrogen species added		Time	Initial concentration (mg N L^{-1})					
	Anode	Cathode		NH_4^+ anode	NO_3^- cathode	NO_3^- anode	NO_2^- cathode	NO_2^- anode	NH_2OH anode
Exp. 1 (8)	NH_4^+	-	265 d	14-52					
Exp. 2A (2)	NH_4^+	NO_2^-	9 d	42-41			61-75		
Exp. 2B (4)	NH_4^+ + NO_2^-	-	15 d	27-86				54-139	
Exp. 2C (2)	NO_2^-	-	14 d					40-46	
Exp. 3 (4)	NH_4^+ + NH_2OH	-	6 h	22-32					15
Exp. 4A (2)	NH_4^+	NO_3^-	12 d	29-39	39-42				
Exp. 4B (2)	NH_4^+ + NO_3^-	-	14 d	49-73		35-40			
Exp. 4C (2)	NO_3^-	-	33 d			46-68			

4.2.3 Analyses and calculations

The concentrations of NH_4^+, NO_2^- and NO_3^- were measured by ion chromatography (Dionex IC5000, Vertex Technics, Spain). pH was determined with a pH-meter (pH-meter basic 20+, Crison, Spain). The concentration of N_2H_4 was measured using a colourimetric kit (Spectroquant® Hydrazine test 109711, Merck, Germany) The concentration of NH_2OH was determined colourimetrically (Oshiki et al., 2016). N_2O was occasionally monitored in the recirculation loop of each compartment using an N_2O liquid-phase microsensor (Unisense, Denmark). Oxygen probes (model 6050, the limit of detection (LOD) 0.1 mg O_2 L^{-1}, Mettler Toledo, USA) were permanently installed in the anodic compartment to have a continuous measurement of the concentration of dissolved oxygen in the medium.

Linear regression of the first data points (i.e. initial activities) was used to estimate the removal rates of nitrogen species in the experiments involving nitrate or nitrite.

Electron balances for the different potential electron donors/acceptors using the anode/cathode as electron sink/supply were performed through the calculation of the Coulombic efficiency (%) for the different possible reactions (Equation 10).

$CE\ (\%) = 100\ \% \times C_{measured}/C_{theoric}$ (Equation 10)

Where $C_{measured}$ means the coulombs measured in the potentiostat (C) and $C_{theoric}$ means the coulombs theoretically generated/required from the oxidation/reduction of an electron donor/acceptor as described in Equation 11.

$$C_{theoric} = \frac{-\Delta a \times n \times F}{14\ g\ N/mol\ N}$$ (Equation 11)

Where *F* is the Faraday constant (96,485 C mol of electrons^{-1}), *a* equals to the mass of the nitrogen specie substrate targeted in the different tests (g N) (i.e. N-NH_4^+, N-NH_2OH, N-NO_2^-, and N-NO_3^-), and *n* is the mols of electrons required to oxidise/reduce 1 mol N of the different nitrogen species targeted in the different tests (mol of electrons mol N^{-1}). The possible reactions considered in the different tests and theirs corresponding *n* values were: a) NH_4^+ oxidation to N_2 (n = 3); NH_2OH oxidation to NO (n = 3); NH_2OH oxidation to N_2 (n = 1); NO_2^- oxidation to NO_3^- (n = 2); NO_3^- reduction to N_2 (n = 5). Following the following CEs were calculated in the different conditions tested: a) CE (NH_4^+/N_2) were calculated for Experiments 1; b) CE (NO_2^-/NO_3^-) were calculated for Experiments 2; c) CE (NH_2OH/NO) and CE (NH_2OH/N_2) were calculated for Experiments 3 and d) CE (NO_3^-/N_2) were calculated for Experiments 4.

The area of the electrode ($A_{electrode}$, m^2) to estimate the current density in the reactor (mA m^{-2}) was calculated according to Equation 12

$A_{electrode} = A_{GG} \times V_{TotalGG}/V_{GG}$ (Equation 12)

Where A_{GG} means the area of a graphite granule (m^2), considering each granule as a perfect sphere of 0.004 m diameter (mean diameter according to manufacturer specifications

as shown above), $V_{TotalGG}$ means the total volume of granular graphite in the anodic compartment (0.0006 m^3) and V_{GG} means the volume of one single graphite granule (m^3).

4.2.4 Microbial analyses

DNA was extracted from graphite granules as described previously (Vilajeliu-Pons et al., 2016). Briefly, granules were incubated in a water ultrasonic bath for 60 s, detached biofilm and cells were collected by centrifugation and cells pellets were used for extraction of nucleic acids cells using the Fast DNA SPIN Kit for Soil (MP Biomedicals, USA) following the recommended instructions. Partial sequences of the bacterial and archaeal 16S rRNA genes were obtained using the Illumina MiSEq PE250 sequencing platform with primers 515F-806R targeting the V4 region (Kozich et al., 2013). Sequencing was conducted by the RTSF Core facilities (Michigan State University, USA, https://rtsf.atsci.msu.edu/).

Sequence quality filtering, trimming, dereplicating, and merging were performed using the DADA2 based pipeline implemented in R as recommended (Callahan et al., 2016). Basic filtering methods were set to 230 bp and 180 bp for forward and reverse reads, no ambiguous bases allowed, and maximum expected error rates of 2. Singletons were removed from the final set of sequences to avoid spurious diversity. Sequences were clustered into ASVs (100 % similarity index). Bimeras were detected and removed (172 out of 1395 ASVs) using the consensus method implemented in DADA2 package. Finally, taxonomic assignments were performed at the maximum taxonomic rank when possible, using the Silva v132 train set to release as a reference. Relative abundances of selected taxons and microbiome graphical representations were performed using the Phyloseq package (McMurdie & Holmes, 2012) implemented in R. Whenever it was necessary due to poor taxonomical assignment with the used reference dataset, ASVs were assigned taxonomically using nucleotide Blast searches at NCBI.

4.3 Results and discussion

4.3.1 Performance of the BES under an ammonium-rich medium

Duplicate BES reactors were operated in batch mode for 550 days (Figure S4.2 and S4.3). A representative batch profile of ammonium removal was selected as a control test (Experiment 1) and depicted in Figure 7. Ammonium was removed at a constant rate (4.8 g N-NH_4^+ m^{-3} d^{-1} in the anode, Table 5), while the current density remained stable (0.44 mA m^{-2}). This rate was found to be lower than in previous studies where bioelectrochemical anoxic ammonium removal was tested without the presence of organic matter (Siegert & Tan, 2019; Vilajeliu-Pons et al., 2018; Zhan et al., 2014). For example, Vilajeliu-Pons et al. (2018) observed an ammonium removal rate of 35 ± 10 g N m^{-3} d^{-1} when operating the system under the continuous-flow mode, while Zhan et al. (2014) observed removal of 60 g N m^{-3} d^{-1} in batch experiments. Considering the possible biological ammonium removal processes (i.e. nitrification, denitrification), no nitrite, nitrous oxide nor nitrate accumulation were observed. Ammonium removal *via* free ammonia (NH_3) volatilization was not likely to occur to a high extent at the working pH (7.6). Under these conditions, NH_3 represented a maximum of 2 % of the ammonium present in the system (NH_3/NH_4^+ pK_a of 9.25). Moreover, the reactors were tightly closed during all the experimental periods to avoid any gas leakage. The small amounts of NH_3 possibly present in the system could diffuse from the anode to the cathode chamber, giving a reasonable explanation for the slight changes in the cathodic NH_4^+ concentration observed (Figure 7).

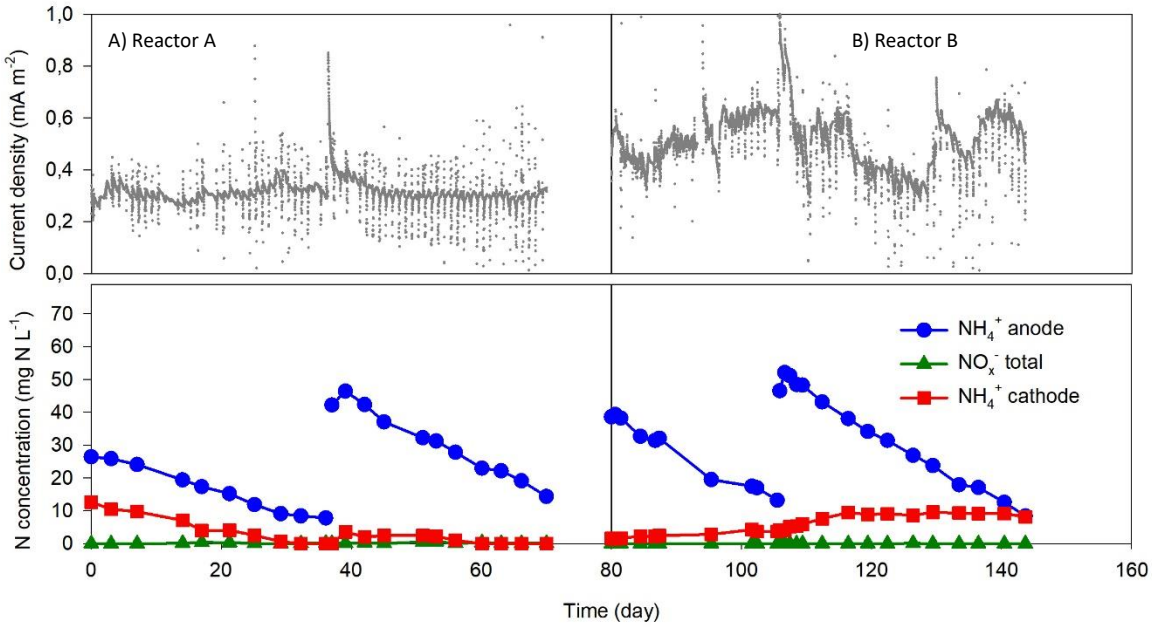

Figure 7. Representative batch tests for Experiment 1 in Chapter 4. Time evolution of nitrogen species content (NO_x^- total refers to NO_2^- + NO_3^-) and current density after adding NH_4^+ at the anode of reactors A (A, left) and B (B, right).

Conventional nitrification uses oxygen as an electron acceptor. However, ammonium oxidation in the reactors most likely occurred under anoxic conditions. The concentration of dissolved oxygen remained below the oxygen probe LOD of 0.1 mg O_2 L^{-1}, and abiotic batch tests previously performed in identical reactors and under the same anodic potential demonstrated that oxygen was not electrochemically produced in the system (Vilajeliu-Pons et al., 2018). On top of that, Lai et al. (2017) observed that graphite electrodes (the ones used in the current work) poised at high anodic potentials (+1.2 V vs SHE) did graphite oxidation to CO_2 instead of H_2O oxidation to O_2. Abiotic tests performed by Vilajeliu-Pons et al. (2018) also showed no ammonium removal, indicating that NH_4^+ oxidation in BES was a bioelectrochemical rather than a pure electrochemical process. Moreover, Vilajeliu-Pons et al. (2018) proved that the addition of allylthiourea (ATU), a selective inhibitor of ammonium oxidation to nitrite, ceased both electric current and ammonium removal, confirming the role of these microorganisms in electricity-driven NH_4^+ oxidation. In the experimental set-up used (Figure S4.1), one might

hypothesize that ammonium could be removed either in the BES reactor or in the buffer tanks used to support the recirculation loop. In addition to these previous tests, control tests were performed in the buffer tanks alone to elucidate the influence of the BES on ammonium removal. Negligible removals of ammonium or nitrate were observed, indicating that these reactions were only taking place in the BES. Thus, the tests performed assumed that ammonium was removed via an electricity-driven process in the absence of oxygen. Assuming oxidation of NH_4^+ to N_2, an average coulombic efficiency of 108 % could be estimated (Experiment 1, Table 5). This suggested that the current flow detected in the system corresponded to approximately 3 electrons per mole of NH_4^+ oxidised. Different tests with possible nitrogen species intermediates were performed to elucidate these possible reactions. The results obtained are presented in the following sections.

Table 5. Removal rates of nitrogen species concentration and coulombic efficiencies in the different experiments performed in Chapter 4.

Experiment (no. of batches)		Experiment 1 (8)	Experiment 2A (2)	Experiment 2B (4)*	Experiment 2C (2)	Experiment 4A (2)	Experiment 4B (2)	Experiment 4C (2)
Species involved		NH_4^+	NO_2^- + NH_4^+		NO_2^-	NO_3^- + NH_4^+		NO_3^-
Time (days)**		264.8	3.2	11.4	3.3	3.4	3.3	9.5
ΔNH_4^+ an. (g N $m^{-3}d^{-1}$)		-4.8 ± 2.5	-18.0 ± 1.3	-17.9 ±5.9	0.0 ± 0.0	-3.5 ±5.7	-11.9 ± 1.9	0.2 ± 0.4
ΔNO_2^- an. (g N $m^{-3}d^{-1}$)		0.0 ± 0.0	35.4 ± 11.7	-81.7 ± 25.7	-48.7 ± 6.5	1.5 ± 1.1	-0.5 ± 0.7	0.7 ±0.3
ΔNO_3^- an. (g N $m^{-3}d^{-1}$)		0.0 ± 0.0	5.7 ± 5.4	3.5 ± 3.9	9.5 ± 10.1	27.5 ± 12.2	-74.6 ± 2.5	-29.5 ± 4.4
ΔNH_4^+ ca. (g N $m^{-3}d^{-1}$)		-0.3 ± 1.0	4.8 ± 2.9	9.4 ± 11.4	6.8 ± 2.4	2.1 ± 3.0	3.5 ± 4.1	0.3 ± 1.2
ΔNO_2^- ca. (g N $m^{-3}d^{-1}$)		0.0 ± 0.0	-87.4 ± 35.7	4.1 ± 6.3	17.7 ± 8.5	4.2 ± 1.0	1.3 ± 0.3	1.7 ± 1.8
ΔNO_3^- ca. (g N $m^{-3}d^{-1}$)		0.0 ± 0.0	2.7 ± 2.3	2.0 ± 0.8	2.1 ± 0.5	-83.0 ± 5.7	16.1 ± 0.8	4.0 ± 5.8
Coulombic efficiency	Reaction	$NH_4^+ \rightarrow N_2$ (n = 3)	$NO_2^- \rightarrow NO_3^-$ (n = 2)			$NO_3^- \rightarrow N_2$ (n = 5)		
	(%)	108 ± 83	63 ± 20	65 ± 23	175 ± 5	2 ± 0	2 ± 0	2 ± 0

* The first batch from figure 8B was not used for the calculations of removal rates because ammonium was depleted before nitrite. **Time refers to the period used to determine the removal rates in each experiment, not to the complete duration of the experiments. The data from Experiment 3 were not included in this table because that experiment took place in a very short time (6 hours) and only the concentration of hydroxylamine changed during that experiment.

4.3.2 Performance of the BES under a nitrite-rich medium

In conventional nitrification processes, nitrite is the main intermediary metabolite. Its role in the overall BES process was investigated by performing different tests (Table 4, Figure 8), including: A) addition of nitrite to the cathode with ammonium present at the anode (Experiment 2A); B) addition of nitrite to the anode while NH_4^+ was present at the anode (Experiment 2B); and C) addition of NO_2^- at the anode with no ammonium present at the reactor (Experiment 2C).

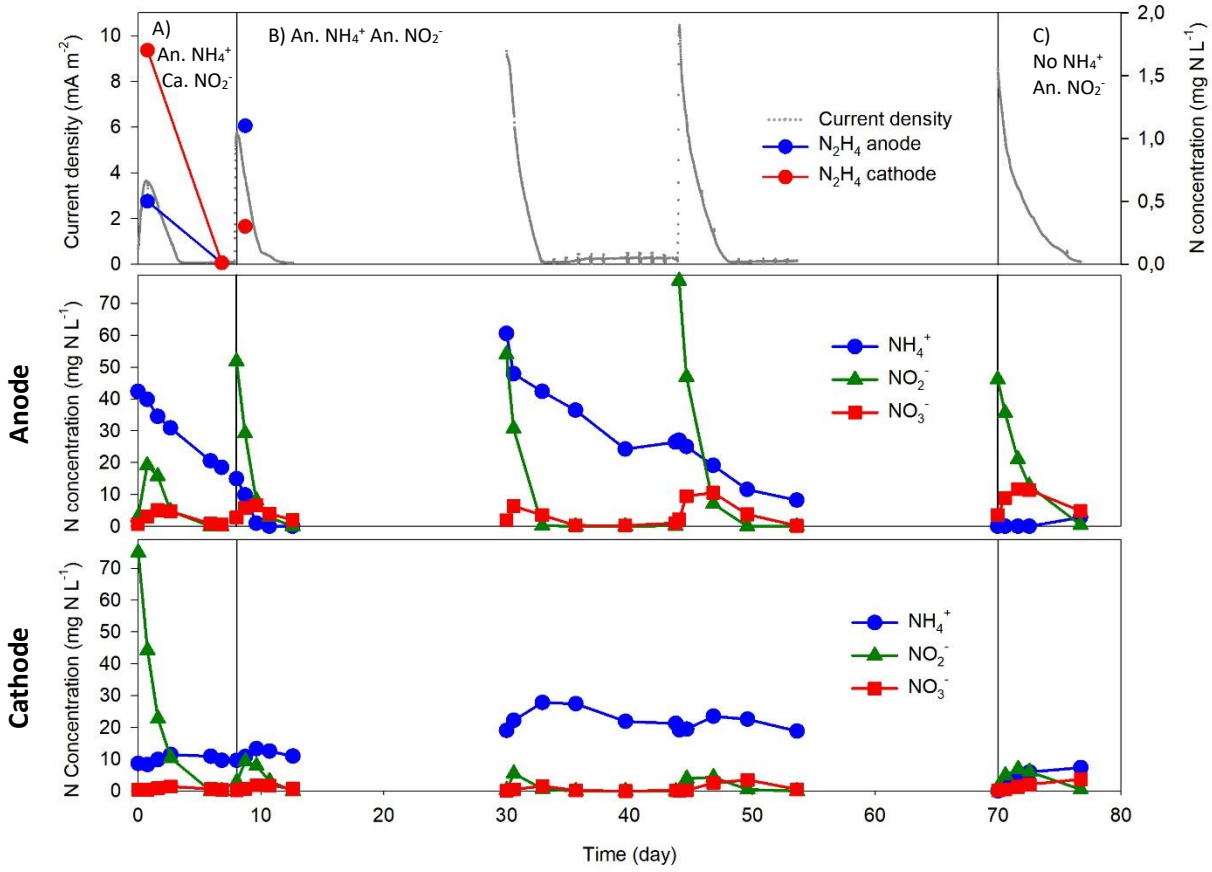

Figure 8. Representative batch tests for Experiment 2 in Reactor A (Chapter 4). Evolution of nitrogen species concentration and current density (top), nitrogen species concentration at the anode (middle) and nitrogen species at the cathode (bottom). A) Experiment 2A: addition of NO_2^- to the cathode with NH_4^+ present at the anode (left). B) Experiment 2B: addition of NO_2^- to the anode with NH_4^+ present at the anode (centre). C) Experiment 2C: addition of NO_2^- to the anode with no NH_4^+ present at the anode (right).

Nitrite was rapidly consumed in all tests. Focusing, first, on ammonium removal in Experiment 2, NH_4^+ removal rate was faster in the experiments where nitrite was present (Experiment 2A, 18.0 g N-NH_4^+ m^{-3} d^{-1} and Experiment 2B, 17.9 g N-NH_4^+ m^{-3} d^{-1}) than when NH_4^+ was alone (Experiment 1, 4.8 g N-NH_4^+ m^{-3} d^{-1}). It suggested that, somehow, ammonium promoted nitrite reduction, which could imply some anammox-like activity in the reactor (Kartal et al., 2011). However, the nitrite removal rates (48.7 - 87.4 g N-NO_2^- m^{-3} d^{-1}) were much higher

than the observed ammonium removal rates. This indicated that any nitrite generated from ammonium oxidation was rapidly removed from the reactor, avoiding any detectable nitrite accumulation. Interestingly, nitrite removal was faster in the tests where ammonium was present in the medium (Experiment 2A, 87.4 g $N\text{-}NO_2^-$ m^{-3} d^{-1} at the cathode and Experiment 2B, 81.7 g $N\text{-}NO_2^-$ m^{-3} d^{-1} at the anode) than in the tests where nitrite was spiked alone (Experiment 2C (48.7 g $N\text{-}NO_2^-$ m^{-3} d^{-1} at the anode) (Figure 8, Table 5). The increase in ammonium removal rate in presence of nitrite (13.2 - 13.1 g $N\text{-}NH_4^+$ m^{-3} d^{-1}) would require an increase in nitrite removal rate of 17.4 - 17.2 g $N\text{-}NO_2^-$ m^{-3} d^{-1} if the anammox process is considered (NH_4^+:NO_2^- 1:1.32). While the increase observed in nitrite removal rate in presence of ammonium was 45.7 - 40 g $N\text{-}NO_2^-$ m^{-3} d^{-1}. Therefore, an anammox-like process cannot fully explain the whole of the differences observed in nitrite removal rate in the presence/absence of ammonium. Putative anammox activity could be further elucidated by analysing the concentration of hydrazine, a metabolite only generated during anammox reaction (van Teeseling et al., 2013). Hydrazine was measured 24 hours after the start of Experiments 2A and 2B, as well as when nitrite was completely consumed in Experiment 2A (Figure 8). The concentration of N_2H_4 was 0.5 mg $N\text{-}N_2H_4$ L^{-1} at the anode and 1.7 mg $N\text{-}N_2H_4$ L^{-1} at the cathode for Experiment 2A and 1.1 mg $N\text{-}N_2H_4$ L^{-1} at the anode and 0.3 mg $N\text{-}N_2H_4$ L^{-1} at the cathode for Experiment 2B. When nitrite was fully depleted, hydrazine content was negligible (less than 0.01 mg $N\text{-}N_2H_4$ L^{-1} at each chamber at the end of Experiment 2A). Collectively, differences in the hydrazine concentrations confirmed that anammox-like processes could be taking place in the BES.

It is worth noting that current density increased steeply (reaching a maximum value of 10.5 mA m^{-2}) after nitrite addition and it subsequently plummeted to basal values together with the consumption of NO_2^- (Figure 8). In Experiments 2B and 2C, this current density trend appeared right after nitrite was added to the anode. However, it was not observed immediately after spiking NO_2^- to the cathode (Experiment 2A). Instead, the current density increased progressively, and it coincided with the migration of nitrite to the anode (Figure 8). The

maximum current and anodic NO_2^- concentration were reached at the same time, being both smaller than those observed when nitrite was directly added to the anode. This indicated that the current rise was generated by an anodic-specific process involving NO_2^-. One might hypothesize that the increase of current density could be attributed to a bioelectrochemical NO_2^- oxidation with the anode electrode serving as an electron acceptor. From the author's best knowledge, it would be the first time that bioelectrochemical nitrite oxidation to nitrate using an anode as an electron acceptor would be suggested. Transient anodic NO_3^- accumulation was observed in all three nitrite experiments, and then nitrate was removed (5.7 g $N\text{-}NO_3^-$ m^{-3} d^{-1} for Experiment 2A, 3.5 g $N\text{-}NO_3^-$ m^{-3} d^{-1} for Experiment 2B and 9.5 g $N\text{-}NO_3^-$ m^{-3} d^{-1} for Experiment 2C). Abiotic tests performed with nitrite and granular graphite as electrode also showed an increase in current density linked to nitrite removal (Figure S4.4), but in this case, all the NO_2^- removed was accumulated in the form of NO_3^-, without further processing. No abiotic nitrite oxidation had been observed previously when using graphite rods (Vilajeliu-Pons et al., 2018). Thus, the reason behind abiotic oxidation can be found in the higher level of impurities present on granular graphite compared to graphite rods (Table S4.1). Results observed in abiotic tests indicated that the oxidation of nitrite to nitrate in a BES was an anodic electrochemical and/or bioelectrochemical process. However, no NO_3^- accumulation was detected in BES reactors, instead, full conversion to N_2 was observed. Since it cannot be expected that pure electrochemical NO_2^- oxidation to NO_3^- was avoided in the BES, it must be hypothesized that a microbial-mediated process was in charge of the later conversion of NO_3^- to N_2. How this process occurred remains unknown (Figure 8).

Under the hypothesis that all the nitrite removed from the system was previously oxidised to nitrate, the coulombic efficiency of the oxidation of NO_2^- to NO_3^- in Experiment 2C (nitrite alone) was 175 %. Thus, nitrite oxidation to nitrate alone could not explain the whole increase of current observed, but the spike of nitrite could have initiated a cyclic process where nitrite was electrochemical/bioelectrochemically converted to nitrate, which, at the same time

was reduced into nitrite, explaining the over-current observed. However, the observation of nitrite and nitrate decreasing along the process indicated the existence of other parallel reactions involving nitrite, so the cyclic process would come to an end when all the NO_2^- and NO_3^- were removed (reduced to N_2). This could explain why the coulombic efficiency of the NO_2^- oxidation was lower in the experiments involving ammonium and nitrite, 2A and 2B (63% and 65 % respectively), which accounted for a faster NO_2^- removal than in absence of ammonium (Experiment 2C).

Hydroxylamine is an intermediate compound of nitrification previously elucidated as a probable electron donor in bioelectrochemical ammonium oxidation reactors (Vilajeliu-Pons et al., 2018). Experiment 3 evaluated the addition of NH_2OH at the anode (15 mg N-NH_2OH L^{-1} in the medium, Table 4). Hydroxylamine spike caused an increase in the current density that peaked at 90.6 mA m^{-2} (Figure 9), which was a value higher than the one observed after the addition of nitrite (10.5 mA m^{-2}). The concentration of hydroxylamine was measured at 1 and 2 hours after the spike, but NH_2OH was only detected (and at a low concentration, 2.1 mg N-NH_2OH L^{-1}) in the sample taken at the anode of reactor A after 1 hour. The hydroxylamine removal rate was estimated as 1082.7 g N-NH_2OH m^{-3} d^{-1}. Moreover, the concentration of NH_4^+, NO_2^- and NO_3^- did not change after the addition of NH_2OH (Figure 9). The abiotic tests performed with granular graphite (Figure S4.5) showed that, in the absence of bacteria, hydroxylamine was electrochemically oxidised to nitrite and subsequently to nitrate, reinforcing the hypothesis that microbial activity was needed to reduce intermediate oxidised species such as NH_2OH, NO_3^-, NO_2^- or NO to N_2.

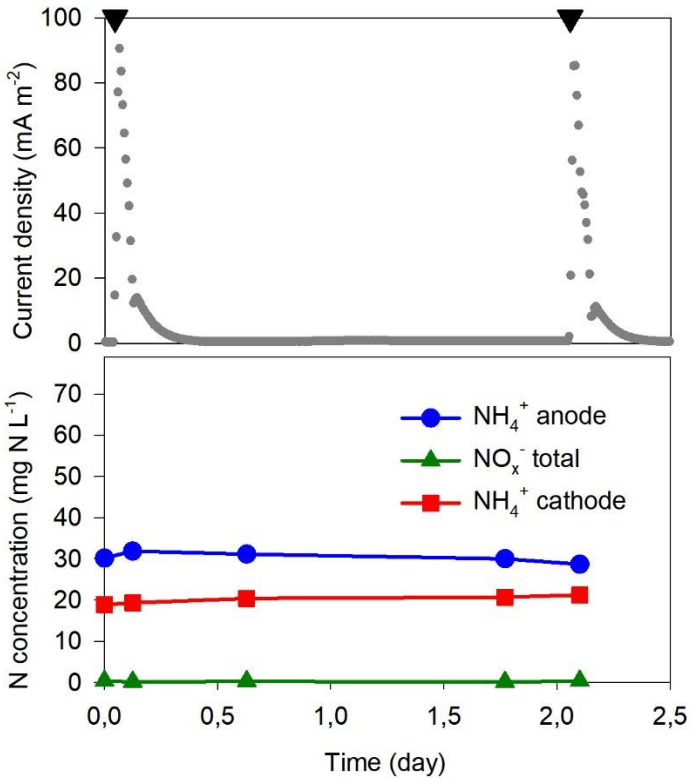

Figure 9. Representative batch test for Experiment 3 in Reactor A (Chapter 4). Evolution of nitrogen species concentration (NO_x^- represents the total concentration of NO_2^- and NO_3^- in both chambers) and current density after a pulse of NH_2OH at the anode in Reactor A. Black triangles in the top mark the times when hydroxylamine was added at the anode. Please, note changes in scale for comparison with Figures 7 and 8.

The current density peak observed in the BES tests was assumed to be generated by the anodic oxidation of NH_2OH, either electrochemically or bioelectrochemically (oxidation of hydroxylamine to nitric oxide, a reaction that is catalysed by (HAO), releasing 3 electrons (Caranto & Lancaster, 2017)). Considering the electric current and the NH_2OH removal observed in Experiment 3, the coulombic efficiency for the oxidation of NH_2OH to NO was 70 ± 13 % (i.e. for a 3-electrons reaction). The nitric oxide generated could be reduced to N_2 by denitrification instead of anammox. Although nitric oxide is used as an electron acceptor for NH_4^+ oxidation during anammox (Hu et al., 2019), no changes in the ammonium concentration were detected

during NH_2OH removal in the current study. For similar reasons, electro-anammox may not have been responsible for the removal of the hydroxylamine added in the Experiment 3, as NH_4^+ serves as an electron donor for the reduction of NH_2OH to N_2H_4 in electro-anammox (Shaw et al., 2020).

Finally, NH_2OH could also be directly oxidised to N_2 by a newly discovered hydroxylamine oxidase found in *Alcaligenes* sp. HO-1 (Wu et al., 2021). However, it is still unclear whether *Alcaligenes* sp. HO-1 can use an anode as an electron acceptor for this reaction. Recent experiments with this strain in the author's group pointed out an electrochemical potential of HO-1 strain for some oxidising steps (unpublished results). Nevertheless, if NH_2OH oxidation to N_2 reaction was considered (1-electron reaction), the coulombic efficiency for the bioelectrochemical oxidation of NH_2OH would be 210 ± 39 %, so even though this process could be occurring in the reactor, hydroxylamine should be first oxidised to other more-oxidised nitrogen species (such as NO or NO_2^-) to explain the whole of the current density observed.

4.3.3 Performance under a nitrate-rich medium

The removal of nitrate was also studied using different approaches: A) addition of NO_3^- to the cathode with NH_4^+ present at the anode (Experiment 4A Table 4), B) addition of NO_3^- to the anode with NH_4^+ present at the anode (Experiment 4B, Table 4) and, C) addition of NO_3^- to the anode with no NH_4^+ present at the anode (Experiment 4C, Table 4).

In the presence of nitrate, the current density declined (0.12 mA m^{-2} on average) compared to the values observed in presence of ammonium alone (0.44 mA m^{-2}). When nitrate was fully removed from the system, current density rose again to its previous levels (0.47 mA m^{-2}) (Figure 10). It suggested a plug-unplug mechanism, with current being interrupted by the presence of nitrate and restored after NO_3^- had been removed completely. Nitrate removal in Experiments 4A (83.0 g N-NO_3^- m^{-3} d^{-1} at the cathode), 4B (74.6 g N-NO_3^- m^{-3} d^{-1} at the anode), and 4C (29.5 g N-NO_3^- m^{-3} d^{-1} at the anode) (Table 5) occurred at a faster rate than the NH_4^+

removal observed under ammonium rich-medium (4.8 g N-NH_4^+ m^{-3} d^{-1} in the anode, Experiment 1 in section 4.3.1). According to the estimated rates, it was concluded that ammonium could not have ended up in any detectable nitrate accumulation in the reactor.

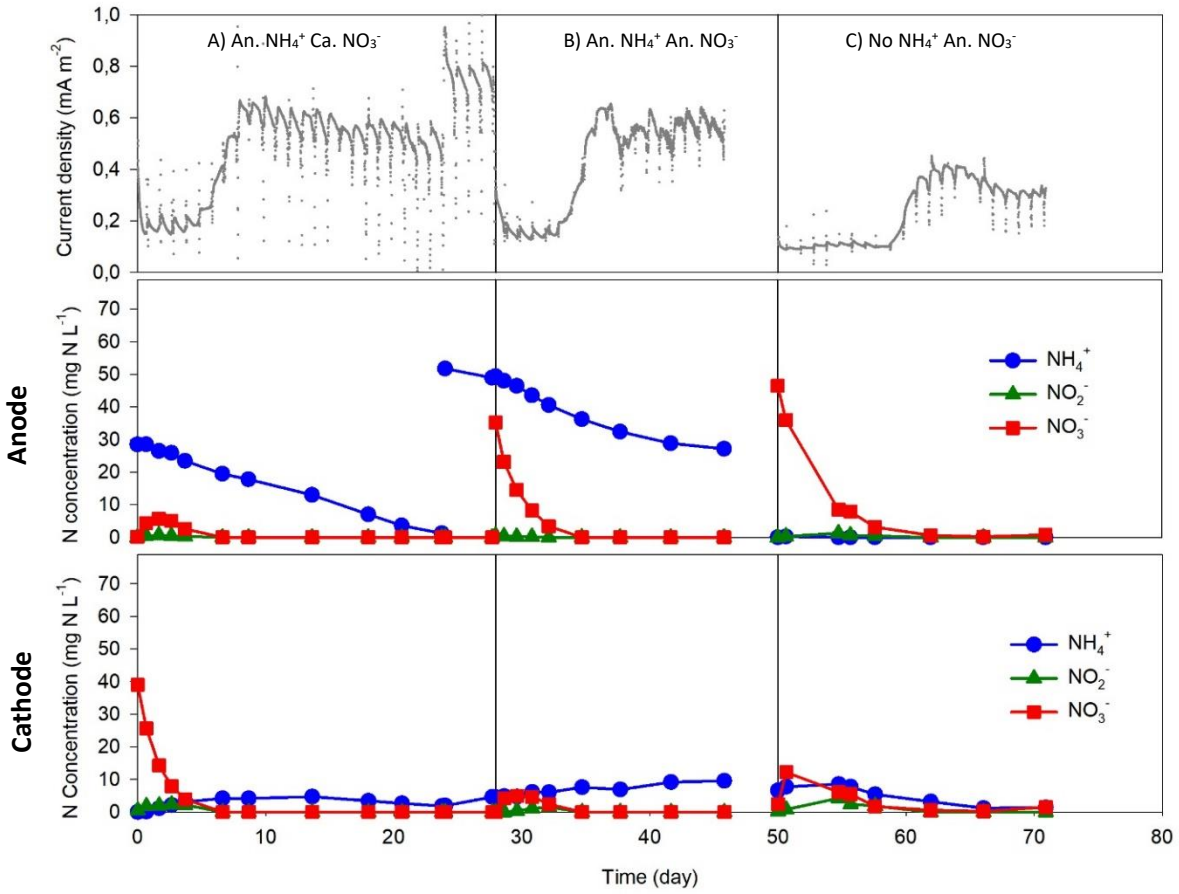

Figure 10. Representative batches for Experiments 4 in Reactor B (Chapter 4). Evolution of nitrogen species concentration and current density (top), nitrogen species concentration at the anode (middle) and nitrogen species at the cathode (bottom). A) Experiment 4A: addition of NO_3^- to the cathode with NH_4^+ present at the anode (left). B) Experiment 4B: addition of NO_3^- to the anode with NH_4^+ present at the anode (centre). C) Experiment 4C: addition of NO_3^- to the anode with no NH_4^+ present at the anode (right).

Nitrate removal rates were about three times faster in the presence of ammonium (83.0 and 74.6 g $N\text{-}NO_3^-$ m^{-3} d^{-1}) compared to 29.5 g $N\text{-}NO_3^-$ m^{-3} d^{-1} in the absence of ammonium. Similar behaviour was observed with nitrite (Section 4.3.2.) suggesting that NH_4^+ was accelerating the reduction of nitrogen oxides in the system. However, the effect of nitrate on the ammonium removal rate was unclear, as the anodic NH_4^+removal was faster in the presence of nitrate at the cathode (Experiment 4B - 11.9 g $N\text{-}NH_4^+$ m^{-3} d^{-1}) than in the presence of nitrate at the anode (Experiment 4A - 3.5 g $N\text{-}NH_4^+$ m^{-3} d^{-1}) or in the presence of ammonium alone (Experiment 1 - 4.8 g $N\text{-}NH_4^+$ m^{-3} d^{-1}). Electricity-driven nitrate removal was discarded since the number of electrons transferred from the anode to the cathode could only account for 2 % of the nitrate removal (considering 5 electrons are needed for the reduction of NO_3^- to N_2) in all the experiments performed with a nitrate-rich medium (4A, 4B and 4C), (Table 5).

4.3.4 Analysis of the BES microbiome

Samples from bulk and biofilm compartments of both anodes and cathodes were taken from the two duplicate reactors to determine the major microbial players contributing to the above set of reactions. Samples were taken after 450 days of operation (by that time, experiment 2B was being tested, Table 4). On average, 56,510 sequences were obtained per sample (ranging from 33,682 to 78,458). Sequences clustered in a total of 841 ASVs.

At the phylum level, no consistent differences were observed for anode and cathode compartments if the two BES reactors were considered together (Figure 11). More than half of the ASVs (488, accounting for 310,900 total reads) could be resolved at the genus level using a bootstrap level of 80. Archaeal signatures (mainly identified as *Methanobacterium* and *Methanobrevibacter*) were found at low abundances (< 1 %) and almost specifically in Reactor A, both in the anode and the cathode compartments. Most sequences belonged to the phylum *Proteobacteria*, *Actinobacteria*, *Bacteroidetes* and *Chloroflexi*. Differences according to the different compartments in the reactors (anode-cathode and bulk-biofilm) occurred at lower

taxonomic ranks and revealed interesting differences. For instance, *Achromobacter* spp. was found as the most dominant bacterium in the anodic biofilm of the two reactors (50 to 60 %). The relative abundance decreased to 13 and 26 % in the cathode of reactors A and B, respectively. A lower relative abundance of *Achromobacter* in the bulk liquid compared to biofilm samples was observed, which suggested an active role of these bacteria in biofilm formation and putative electrode-assisted nitrogen transformations. *Achromobacter* species have been related to heterotrophic simultaneous nitrification and denitrification (Padhi & Maiti, 2017) and heterotrophic nitrification (Basha et al., 2018). Heterotrophic nitrification has been more deeply studied with *Alcaligenes* sp. (Wu et al., 2021). According to the latest findings of Wu et al. (2021), the heterotrophic nitrifier *Alcaligenes* presents a novel oxidase that can oxidise hydroxylamine directly to N_2. Hence, it cannot be discarded a similar role of such a mechanism in *Achromobacter*. Another key enzyme in *Alcaligenes* heterotrophic nitrification, the pyruvic oxime dioxygenase (POD), has significant similarities to *Achromobacter* POD (Tsujino et al., 2017). Moreover, *Achromobacter* could use alternative electron donors, such as Mn^{2+}, for denitrification (Su et al., 2018) and it has been found in either anodic biofilm (Ceballos-Escalera et al., 2021) or cathodic biofilms (Zhang et al., 2011b) of different BES, suggesting that *Achromobacter* may be able to use electrodes as electron donor/acceptors for nitrification/denitrification processes.

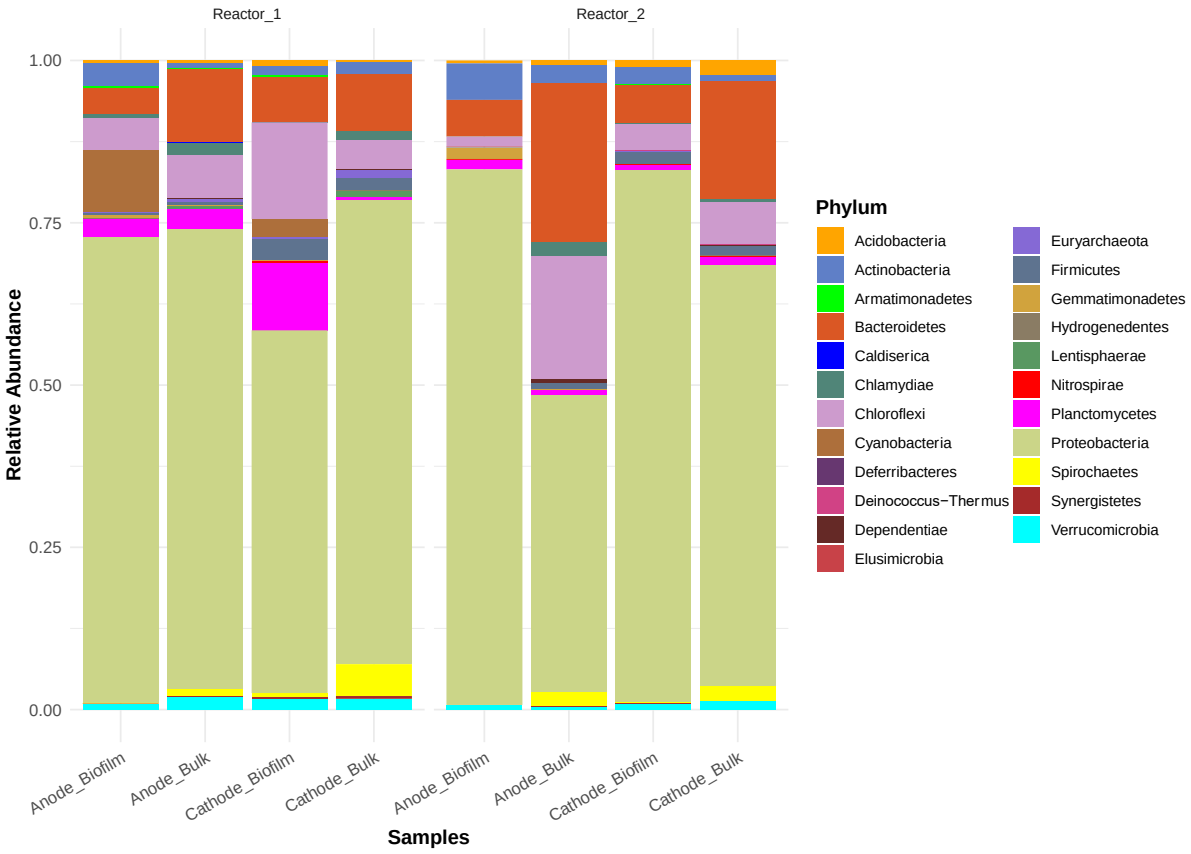

Figure 11. Relative abundance (number of sequences) of main Phyla in the reactors studied in Chapter 4. Samples are organized as per reactor and compartments (Anode-Cathode, bulk-biofilm) inside the reactor.

Denitratisoma, an autotrophic denitrifier (Deng et al., 2016), tended to accumulate in the cathode compartment of both reactors (10.0 ± 5.2 %) compared to the anode (4.1 ± 2.4 %). *Denitratisoma* sp. has previously been described as being dominant in the cathodic biofilm of a denitrifying BES (Ma et al., 2015), so it might have contributed to the removal of nitrogen-reduced species in our system. *Nitrosomonas* sp. and *Nitrospira* sp. were the only nitrifying bacteria that could be detected. In both cases, they showed a preference for growing on the biofilm. The relative abundance of *Nitrosomonas* was around 1 % of sequence reads in the anodic biofilm and it decreased to almost undetectable values in the bulk liquid of the two reactors. The maximum relative concentration (6.3 %) was found in the cathodic biofilm of

reactor A but not in reactor B (< 0.3 %). A similar distribution was detected for *Nitrospira* albeit much lower relative abundances were recovered (below 0.25 %).

Providing the kinetics observed in the two reactors were similar and the differences in the relative abundance of anammox bacteria, we hypothesised anammox was a secondary reaction in the reactors that could also have a role in the simultaneous reduction of nitrite in the presence of ammonium. "*Candidatus* Kuenenia" (*Brocadiales*) and "*Candidatus* Anammoximicrobium" (tentatively classified within *Pirellulales*) were the only predicted anammox bacteria (Kartal et al., 2013) found in the studied samples (Figure S4.6). "*Candidatus* Kuenenia" was more abundant, showing the highest relative abundances in the anodic biofilm of both reactors (1 to 2 % of sequences). Relative densities decreased below 0.3 % in the bulk samples and the cathode biofilm, suggesting a selective enrichment on the electrode surface.

4.3.5 Perspectives for anoxic ammonium removal using BES and the elucidation of the pathways for ammonium removal in BES

Recent advances on anammox and nitrifying bacteria behaviour on polarized anodes (Shaw et al., 2020; Vilajeliu-Pons et al., 2018) have allowed the scientific community to light up a near-future where the key components of wastewater (organic matter and nitrogen) can be fully removed with renewable electricity supply and without the need of external electron donors and acceptors. This opens the door to the implementation of BES-based technologies for removing different kinds of wastewater involving organic matter and nitrogen at low C/N ratios. For large-scale applications, such as the current operating wastewater treatment plants, the competence and lower operational cost of BES-based technologies might not be enough to replace them because the high capital outlays that have been invested still needs to be paid off. However, in the current transition from centralization to decentralization (Rabaey et al., 2020), BES-based technologies might be a reasonable alternative to current wastewater treatment technologies. In addition, the development of technologies able to carry out complex processes,

such as electricity-driven ammonium removal, with mixed cultures that do not require special care is a tool to implement sanitation solutions. For this reason, the work presented here can contribute to the implementation of BES-based sanitation solutions by providing a better understanding of the underlying processes behind anoxic ammonium removal in BES colonized by nitrifying bacteria.

Autotrophic ammonium removal in BES without accumulation of intermediary metabolites can be viewed as a complex process (Figure 12). Experiments performed with the sole presence of ammonium (Experiment 1) resulted in current densities corresponding to the use of 3 electrons per molecule of NH_4^+ oxidation to N_2 (theoretical value). Different nitrogen dynamics were revealed inside the reactor, which suggested the occurrence of different ammonium removal pathways. The preeminent one could be the first oxidation of ammonium to hydroxylamine, followed by second oxidation of this later. Hydroxylamine oxidation was found to be a highly electroactive reaction, following previous studies (Vilajeliu-Pons et al., 2018). Taking all results together, the final product of hydroxylamine oxidation was not clear, although an implication of the recently described hydroxylamine oxidase converting NH_2OH to N_2 has been speculated (Wu et al., 2021). This possibility was reinforced due to the large presence of *Achromobacter* spp. in the reactors, a microorganism with significant similarities to *Alcaligenes*. The electric current generated during NH_2OH removal indicates that an alternative, more oxidised, compound must be the major product of hydroxylamine oxidation, probably nitric oxide, which can be rapidly converted into nitrite (oxidation) or nitrous oxide (reduction) due to its instability. Although the most reasonable outcome for nitric oxide in an oxidative environment like the anode would be the production of nitrite, no accumulation of it was detected in the reactor after the addition of NH_2OH (Experiment 3), suggesting that nitric oxide oxidation may be a minor pathway. Moreover, no N_2O was detected in any of the experiments, and a complete reduction of NO to N_2 was considered.

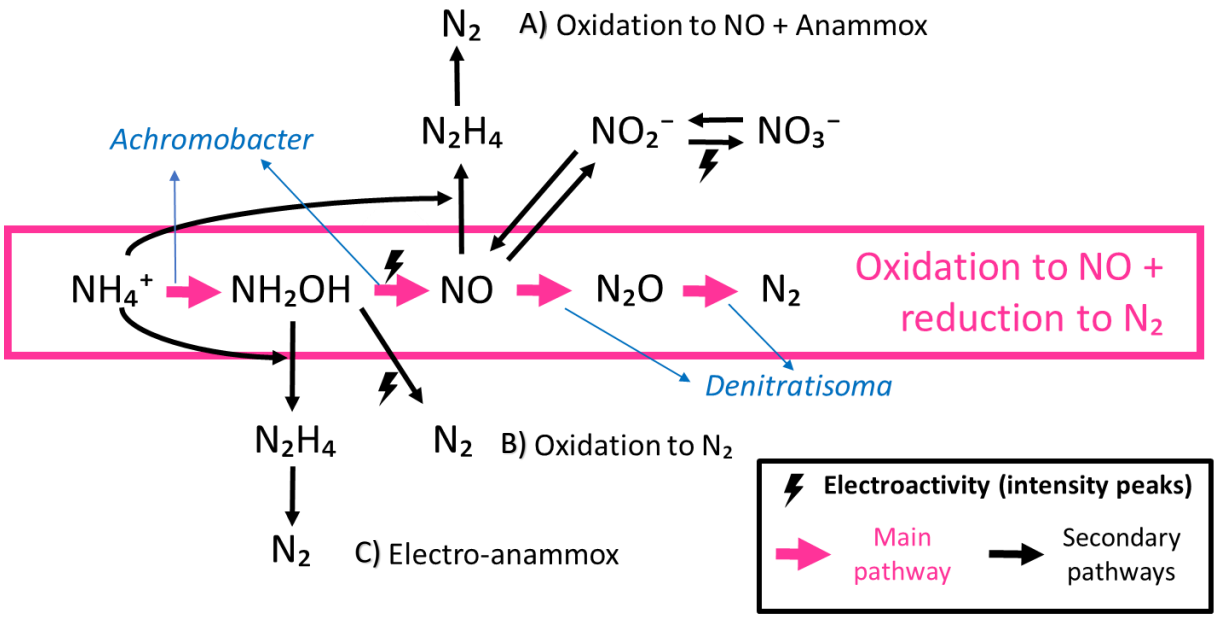

Figure 12. Summary of the reactions involving nitrogen compounds that could be occurring in the BES during Chapter 4. The main ammonium removal pathway proposed is the bioelectrochemical oxidation of NH_4^+ to NO, possibly performed by *Achromobacter*, followed by the reduction of NO to N_2, which could be carried out by *Denitratisoma* (all these routes are highlighted in pink), while the other 3 secondary routes are also considered: A) bioelectrochemical oxidation of NH_4^+ to NO followed by anammox, B) bioelectrochemical oxidation of NH_4^+ to N_2 and C) electro-anammox. The reactions of NH_2OH oxidation and NO_2^- oxidation are distinguished with an exclamation mark because they are the processes showing the most intense electrochemical response in this study.

Data from experiments where nitrate was added (Experiment 4) were analysed to elucidate the possible electron donors used for NO reduction. Results showed that different electron donor sources could be used for nitrate reduction. The cathodic electrode could be responsible for only a small part of the NO_3^- reduction, as the current could only explain 2 % of NO_3^- conversion into N_2 observed in experiments 4A, 4B and 4C. Heterotrophic denitrification had a minor role in this system because no organic matter was added. Thus, there was a deficiency of electrons to explain the whole nitrate reduction observed, which suggested the presence of other mechanisms. For example, an additional hypothesis could be linked to direct

interspecies electron transfer (DIET) by coupling oxidation of reduced nitrogen species, such as ammonium, with nitrate reduction. This hypothesis could be supported by the observation of current density suppression when nitrate was spiked in the system in presence of ammonium (Experiments 4A and 4B). However, DIET cannot explain the whole of the results observed, since nitrate was also removed in absence of ammonium or any other feasible electron donor (Experiment 4C).

Nitrite tests (Experiments 2) revealed that NO_2^- was electrochemically and bioelectrochemically oxidised to NO_3^- since nitrite removal could be linked to a significant spike in current density with and without ammonium presence in the reactor. A transient accumulation of nitrate in the system was observed, with a final complete conversion into N_2.

Finally, the presence of N_2H_4 was detected both in the cathodic and anodic chamber when both nitrite and ammonium were present in the system (Experiments 2A and 2B), while microbial analyses revealed the presence of anammox bacteria in the bulk a liquid and, particularly, on the anode surface ("*Candidatus* Kuenenia" and "*Candidatus* Anammoximicrobium"). It suggested that anammox reactions could also be having a role in the system. In this case, nitrite, nitric oxide, or the electrode may serve as electron acceptors for the oxidation of ammonium to nitrogen gas. However, anammox bacteria were found at a lower abundance than nitrifiers and denitrifiers. Anammox and electro-anammox could potentially be involved in NO and NH_2OH removal, respectively. Nevertheless, no NH_4^+ consumption was observed during NH_2OH (and subsequently, NO) removal, indicating that this could only be minority pathway (Figure 12).

Taking it all together, the system studied here presented a complex microbial community that was able to carry out a plethora of nitrogen removal mechanisms. From a black-box perspective, the system was able to handle different nitrogen compounds that are usually present in wastewater (i.e. ammonium, nitrite and nitrate) and convert them into dinitrogen gas

without the presence of organic matter. The gained know-how will be used to improve the reactor design and operation leading to an increase in the current ammonium removal rates and competing with anammox or other bioelectrochemically-induced ammonium oxidation.

4.4 Conclusions

Ammonium was converted into dinitrogen gas in an anoxic BES. A coulombic efficiency of 108 % was observed, suggesting that the anodic electrode acted as the electron acceptor for this process. Two highly electroactive reactions were identified (hydroxylamine and nitrite oxidation). Data obtained from nitrite and nitrate tests suggested that both denitrification and anammox-based reactions could take place in the BES to close the conversion of NH_4^+ into N_2. The dominant bacterium in the BES was a nitrifier (*Achromobacter* spp.), but the microbial community in the reactor included also anammox species ("*Candidatus* Kuenenia" and "*Candidatus* Anammoximicrobium") and denitrifying bacteria (*Denitratisoma* sp.).

Chapter 5. Electrifying biotrickling filters for the treatment of aquaponics wastewater

Redrafted from: Pous, N., Korth, B., **Osset-Álvarez, M.**, Balaguer, M. D., Harnisch, F., & Puig, S. (2021). Electrifying biotrickling filters for the treatment of aquaponics wastewater. *Bioresource Technology*, *319*, 124221. https://doi.org/10.1016/j.biortech.2020.124221

5.1 Introduction

The development of innovative and environmental-friendly food cultivation methods is required to face the near future (Godfray et al., 2010). One of the fastest growing food-producing sectors is aquaculture (FAO, 2018). World production has increased from 3 to 80 million tonnes of fish from 1970s to 2017. Thus, it accounts for about 50 % of the world's fish consumption. Aquaculture could decrease the pressure on the endangered aquatic wildlife, but its development needs a revision. Aquaculture impacts the environment by producing fish feed (usually produced from fish oils/flours) and nitrogen/antibiotics discharges (Read & Fernandes, 2003). At the same time, industrial agriculture is also being scrutinized. The expansion of agriculture causes increasing land use, higher fresh water consumption as well as nitrogen, phosphorus, and pesticides overloads (Tilman et al., 2001). In this perspective, hydroponics (soilless plant cultivation) is considered as an alternative to conventional agriculture as it decreases the demand for land, water, nutrients, and pesticide dosing (Gwynn-Jones et al., 2018). If nutrient-rich effluents coming from aquaculture are used in hydroponics and vice versa, a virtuous loop is generated, i.e., this is aquaponics. Aquaponics allows the production of both fish and edible plants while minimizing the environmental impact compared to conventional fishing and agriculture (FAO, 2014; Tyson et al., 2011), closing urban bio-cycles (Venkata Mohan et al., 2020).

From the conceptual point of view, aquaponics is a win-win situation, but its real-world implementation requires the correct management of the nitrogen cycle inside the system (Wongkiew et al., 2017). On the one hand, aquaculture effluents are usually characterized by high ammonium content, since about 60 - 70 % of the feed is excreted as ammonia (Kissil & Lupatsch, 2004). On the other hand, hydroponics requires almost ammonium-free water (< 0.8 mg $N\text{-}NH_4^+$ L^{-1}) but with a certain amount of nitrate (1 - 34 mg $N\text{-}NO_3^-$ L^{-1}) as the nitrogen source of cultured plants (FAO, 2014). In consequence, conventional nitrification-denitrification processes, usually focusing on full nitrogen removal, need to be adapted to the specific

requirements of aquaponics. Firstly, ammonium generated in the aquaculture pond should be converted into nitrate followed by controlled denitrification to avoid high nitrate accumulation (< 90 mg $N\text{-}NO_3^-$ L^{-1}) that could affect fish and plants growth (FAO, 2014; van Rijn et al., 2006), and to ensure no nitrite presence (< 0.3 mg $N\text{-}NO_2^-$ L^{-1}) due to its toxicity for plants and fish (Colt, 2006; FAO, 2014). Aquaculture recirculating systems can be easily adapted to aquaponics as they are already equipped with, e.g., biotrickling filters being characterized by a good nitrification performance. However, the denitrification performance of such systems is poor due to the lack of organic matter (C/N < 3) (Mook et al., 2012; van Rijn et al., 2006). Thus, an externally added electron donor is needed to control and adjust the nitrate content. The most common external electron donor is organic matter, but it introduces additional cost factors (i.e. chemical dosage and sludge disposal). By finding a solution for the treatment of aquaponics, a solution for the treatment of other wastewaters with low C/N ratio wastewaters (e.g. some urban wastewater) could be also found (Mook et al., 2012).

Primary microbial electrochemical technologies have emerged as a biotechnological alternative for directly supplying an electron donor/acceptor to electroactive microorganisms by means of an electron conductor termed electrode (Schröder et al., 2015). Integrating primary MET in aquaponics could result in a considerable improvement thereof, as they were demonstrated to drive both nitrification (Vilajeliu-Pons et al., 2018) and denitrification (Gregory et al., 2004). Still little is known about the recently discovered electricity-linked ammonium removal (Shaw et al., 2020), thus ammonium is usually oxidised into nitrate aerobically (He et al., 2016; Virdis et al., 2008). Microbial electrochemical denitrification has been widely tested in different waters such as wastewater (Virdis et al., 2008), groundwater (Pous et al., 2015a), or aquaculture effluents (Marx Sander et al., 2018). The microbial structure and activity of denitrifying MET rapidly changes with the mode of operation (Pous et al., 2015b) allowing better control of denitrification by fine-tuning different operational parameters, e.g., cathode potential

(Virdis et al., 2009), current density (Park et al., 2005), pH (Clauwaert et al., 2009), or the hydraulic retention time (Pous et al., 2017).

Besides MET implementation in aquaponics could be effective at low operational expenditures, the complexity and capital expenditures associated to its conventional configuration represents a matter of concern (for instance, usage of electrodes, membranes, potentiostats, etc.) (Sleutels et al., 2012). However, the development of MET-based treatment concepts such as snorkels (Cruz Viggi et al., 2015; Hoareau et al., 2019) or METlands (Aguirre-Sierra et al., 2020; Prado et al., 2020) highlights the importance of the microbial ecology function over reactor materials and engineering (Koch et al., 2018). In consequence, only two components might be needed to reach an improvement of bioremediation activities: the appropriate microbiome inhering electroactive microorganisms and a conductive support serving as electrode. Conventional technologies currently used in aquaculture and aquaponics (e.g., biofilters) are based on microbial degradation at non-conductive supports (Crab et al., 2007). Yet, it can be hypothesized that a conductive support integrated in the effluent treatment site will enhance nitrification and denitrification due to the activity of electroactive microorganisms. For this reason, this work explored the potential of biotrickling filters to be electrified for improving nitrification/denitrification rates and the efficient control of the nitrate content in the effluent. Consequently, a sustainable system was developed to improve aquaponics water recirculation by a controlled optimization of the nitrogen content in the aquaculture effluent according to actual requirements of hydroponics. This technology could be used for the treatment of other wastewaters containing ammonium at low C/N ratio.

5.2 Materials and methods

5.2.1 Influent characteristics

All reactors were fed with synthetic aquaculture effluent containing a representative amount of ammonium (0.2 g L^{-1} NH_4Cl ; 50 mg $N\text{-}NH_4^+$ L^{-1}) (Yin et al., 2018) and 0.1 g L^{-1} $MgSO_4$, 0.015 g L^{-1} $CaCl_2$, 0.162 g L^{-1} Na_2HPO_4, 1.072 g L^{-1} KH_2PO_4, 0.25 g L^{-1} NaCl, 1.05 g L^{-1} $NaHCO_3$, 0.1 mL L^{-1} micronutrients (Rabaey et al., 2005). All chemicals were of analytical or biochemical grade.

5.2.2 Study of the effect of material filling and electricity input (Reactor designs A, B, and C)

5.2.2.1 Reactor set-up and inoculation of reactor designs A, B, and C

Experiments were performed in PVC reactors of 100 cm height and 4.2 cm of internal diameter (5.0 cm external diameter – PVC 50 - 10 Atm), implying a total volume of 1385 mL (see supplementary information). In all reactors, the inlet was located at the upper side of the reactor. Influent water was dropped spread on a stainless steel mesh (mesh path light 5 x 5 mm) to get a better distribution along the whole reactor diameter and promote aeration. Water circulated downwards and the reactor water level was controlled by moving the outlet discharge point as shown in Figure 13. In a first round of tests, 3 different designs (A, B, and C) with different filling materials were used leading to different reactor net liquid volumes, A: One reactor filled with PVC granules (diameter 2 - 8 mm) representing a conventional biofilter (534 mL net liquid volume), B: Two non-polarized reactor replicates filled with granular graphite (model 00514, diameter 1.5 - 5 mm, Enviro-cell, Germany) (633 ± 38 mL net liquid volume), and C: Two polarized reactor replicates filled with granular graphite (model 00514, diameter 1.5 - 5 mm, Enviro-cell, Germany) (655 ± 21 mL net liquid volume). In reactor C, nine graphite rods (6 mm diameter, Mersen Iberica, Spain) located every 10 cm height and inserted ca. 3 cm in the tube serving as current collectors. CCs were connected to a power source (IMHY3, Lendher, Spain). All graphite electrodes (rods and granules) were washed with 1 M NaOH and 1 M HCl

prior to use. An Ag/AgCl reference electrode (+ 0.197 V vs SHE, SE 11, Xylem Analytics Germany Sales GmbH & Co. KG Sensortechnik Meinsberg, Germany) was introduced at height of 20 cm. If not stated otherwise, all potentials provided refer to Ag/AgCl sat. KCl reference electrodes (+0.197 V vs SHE).

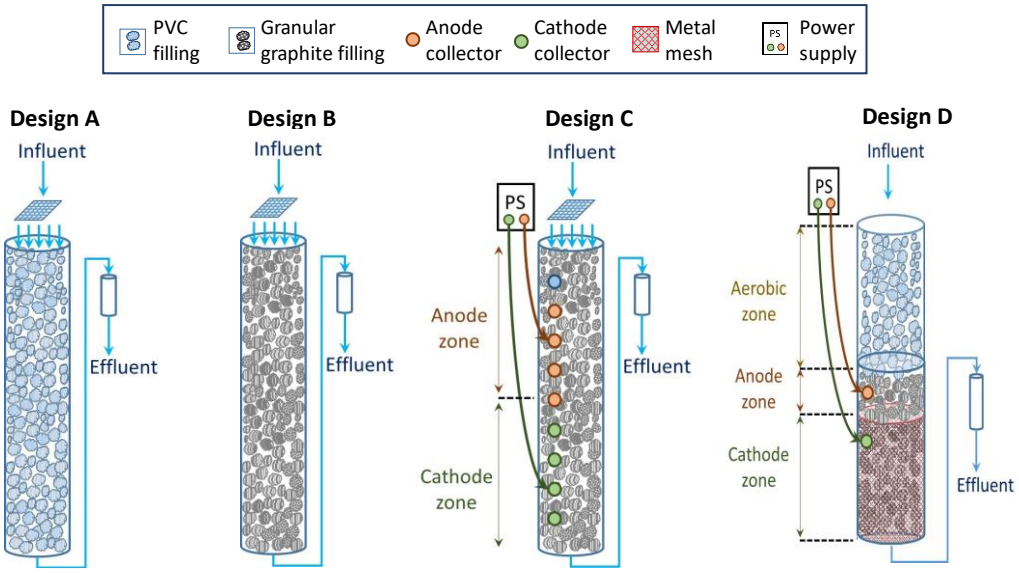

Figure 13. Reactor designs used in Chapter 5 (details see 5.2.2.1. Reactors set-up and inoculation).

All reactors were inoculated in batch mode for 23 days. Each reactor was connected to a 10 L buffer tank containing a solution with synthetic aquaculture medium (section 5.2.1) and a mixed inoculum. The inoculum contained effluent from different reactors performing nitrification (Vilajeliu-Pons et al., 2018), denitrification (Pous et al., 2017), anammox (Akaboci et al., 2018) and activated sludge from the urban wastewater treatment plant of Quart (N.E. Catalonia, Spain).

5.2.2.2 Operation and testing of reactor designs A, B and C

After 23 days of inoculation in batch mode, reactors were switched to continuous flow mode at 0.6 ± 0.1 L d^{-1} (around 1.0 d hydraulic retention time, HRT, depending on the reactor design).

The reactors were operated for 118 days with these flow conditions while testing the influence of electrically connecting different current collectors located at different heights of design C (see supplementary information). The configuration of 8 connected CCs (4 anodes and 4 cathodes) was finally used for the main experiments as it provided a better potential distribution. With this configuration, the CCs located at 50, 60, 70, and 80 cm height were used as anodes, while those at 10, 20, 30, and 40 cm height were used as cathodes. A cathode potential of -0.3 V (Pous et al., 2015a) ought to be applied by manual tuning of the power source.

When fairly stable performance in terms of nitrogen concentrations, current density and cathode potential under the applied condition (0.6 ± 0.1 L d^{-1}) was reached (see supplementary information), further operational reactor parameters were tested, each for two weeks, including: i) volumetric flow rate (Q) between 0.6 ± 0.1 and 2.6 ± 0.2 L d^{-1} corresponding to HRTs between 0.3 and 1.1 d, respectively, and ii) presence of oxygen at the influent (Influent reservoir stored in a 10 L self-collapsible bags and flushed, or not, with N_2 gas for 15 min). In total, the reactors were operated for 189 d.

5.2.3 Reactor for performance enhancement (Reactor design D)

5.2.3.1 Reactor set-up and inoculation of reactor design D

After taking into consideration the obtained results from the first reactor designs, a second set of experiments was performed using reactor design D (Figure 13 and supplementary information). Two reactor replicates were constructed with the lower half of the reactors filled with granular graphite. Two titanium rods (Grade 1, 8 mm diameter, Polymet Reine Metalle, Germany) were inserted ca. 3 cm in the tube serving as CCs for the anode and the cathode zone. Thereby, the cathodic and anodic CCs were located at 12 and 45 cm height, respectively. A stainless steel mesh (30 cm length, mesh path light 5 x 5 mm) was introduced at the inner wall of the PVC tube for improving potential distribution in the cathode zone. According to this set-up, the cathode zone had a height of 30 cm with 280 ± 6 mL of net cathode volume (NCC). The

upper half of the reactors was filled with PVC granules. In consequence, the net liquid volume of the whole reactors was 777 ± 10 mL. An Ag/AgCl reference electrode (+0.197 V vs SHE, SE 11, Xylem Analytics Germany Sales GmbH & Co. KG Sensortechnik Meinsberg, Germany) was introduced next to the cathode collector (height 12 cm) to measure the electrode potentials.

Reactors were inoculated following the same protocol and using effluent taken from the same reactors as it was performed for reactors A, B, and C (described in section 5.2.2.1).

5.2.3.2 Operation and testing of reactor design D

After 21 days of inoculation in batch mode, reactors were switched to continuous flow mode with 0.7 ± 0.1 L d^{-1} (1.2 ± 0.2 d HRT). This operation was followed for 44 d (days 30 - 44 constitute representative reactor operation reactors under this condition). Subsequently, different operational parameters were tested, each for 2 - 3 weeks: i) volumetric flow rates between 0.7 ± 0.1 and 2.3 ± 0.2 L d^{-1} corresponding to HRTs between 0.3 and 1.2 d, respectively, ii) WL of 50 % and 75 % of reactor height, and iii) not polarized graphite granule bed (i.e., open cell potential, OCP) for one week. In total, the reactors were operated for 142 d. All tests were performed with an influent flushed with N_2 for 15 min.

5.2.4 Chemical analyses and calculations

Influent and effluent samples were taken twice a week to measure pH, conductivity, nitrite (N-NO_2^-), nitrate (N-NO_3^-), and ammonium (N-NH_4^+) in accordance with the APHA standards (APHA, 2005). Nitrous oxide and dissolved oxygen were measured at the effluent of the reactor D using a N_2O liquid-phase microsensor (Unisense, Denmark) and an oxygen sensor (O.D. 6050, Crison - Hach Lange GmbH, Germany).

Ammonium removal was calculated as the difference between influent and effluent ammonium content. Total nitrogen (N-TN) removal was calculated as the total nitrogen (N-NH_4^+ + N-NO_2^- + N-NO_3^-) removal difference between influent and effluent. Ammonium and total

nitrogen removal rates ($N\text{-}NH_4^+{}_{RR}$ and $N\text{-}TN_{RR}$) were calculated taking into account the HRTs of reactors. HRT was calculated using the total net reactor volume of each reactor and the respective flow rates.

The electricity consumption of the systems C and D (kWh g N_{rem}^{-1}) were calculated using the voltage and current applied with the power source together the mass of nitrogen removed.

5.3 Results and discussion

5.3.1 Towards the electrification of biotrickling filter: Understanding the effect of material filling and electricity input over nitrogen removal (Reactor designs A, B, and C)

5.3.1.1 Influence of volumetric flow rates

Reactor designs A, B and C were designed with different configurations (Figure 13) to evaluate how the material filling and electricity input can influence biologic ammonium removal in a biotrickling filter. After a start-up process, the systems reached a steady-state (see supplementary information). As the last period of this first test phase (ca. 14 d) was fairly stable in terms of nitrogen concentrations, current density, and cathode potential at the applied condition (1.0 ± 0.1 d HRT), experimental test series started. In order to study the effect of different HRTs on the performance, tests with different volumetric flow rates were performed with an oxygen-deficient influent. Under these conditions, all oxygen available for aerobic nitrification would come from air dissolution at the upper layers of the reactors. Figure 14 shows the ammonium and total nitrogen removal performance at different HRTs.

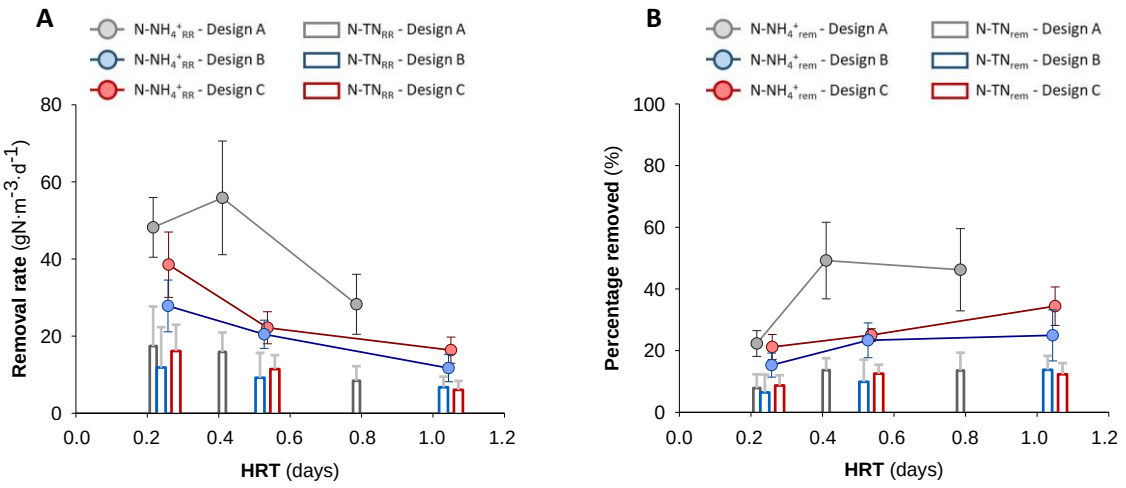

Figure 14. Removal rates of reactor designs A, B, and C operated at different HRTs treating an influent flushed with N_2 (Chapter 5). A) Evolution of N-NH_4^+ removal rates (Solid circles) and N-TN removal rates (Bar charts). B) Evolution of percentages of N-NH_4^+ removal (Solid circles) and percentages of N-TN removal (Bar charts). Error bars indicate standard deviation.

As a general trend, higher nitrification rates were observed at lower HRTs. Design A (PVC as filling material) exhibited the highest N-$NH_4^+{}_{RR}$, showing a maximum of 56 ± 15 g N m^{-3} d^{-1} at an HRT of 0.4 d (49 ± 12 % N-NH_4^+ removal). Assuming that aerobic nitrification was the major microbial process for ammonium removal, it can be deduced that the usage of PVC granules allowed a better oxygen distribution from the upper reactor layers to the inner parts of the reactor compared to graphite granules, which could be related to the bigger size of PVC granules (diameter 2 - 8 mm) compared to granular graphite. For the reactor designs with granular graphite, higher nitrification performance was observed for higher Q (low HRTs) and for a polarized granule bed (i.e., reactor design C). For example, the maximum ammonium removal rate of reactor design C (39 ± 8 g N m^{-3} d^{-1}) was ca. 1.4 times higher than of reactor design B (28 ± 7 g N m^{-3} d^{-1}) at an HRT of 0.3 d. This increase of performance could be related to the usage of a power supply in design C, which was daily adjusted for keeping the cathode CCs at -0.3 V for providing suitable conditions for bioelectrochemical denitrification (Pous et al., 2015a), resulting

in varying cell potential (1.3 ± 0.4 V) and anode potential (+0.5 ± 0.3 V). Consequently, a stratification of redox potential was observed along the different CCs between +0.7 ± 0.2 V (height 70 cm) and -0.3 ± 0.2 V (height 20 cm) (see supplementary information). Within this potential gradient, the higher ammonium removal rates observed in design C in comparison to design B can be explained by both current-driven ammonium oxidation (Shaw et al., 2020; Vilajeliu-Pons et al., 2018) as well as oxygen supply by electrochemical water splitting (> +0.6 V). However, the latter electrochemical reaction is not sustainable when using graphite due to exfoliation (Lai et al., 2017).

In terms of total nitrogen removal (Figure 14B), a similar rate was observed for all reactor designs. Operation at the lowest HRT (0.3 d) yielded the highest but still similar low N-TN_{RR} (mean values < 20 g N m^{-3} d^{-1}). Polarization of graphite granules in case of reactor design C did not provide additional denitrification activity. Due to the potential distribution, only a limited zone was at the desired potential for denitrification (-0.3 V) (Pous et al., 2015a). Nevertheless, a poor potential distribution could not have been the sole reason for the low denitrifying activity. The effluent nitrate concentrations were low (5 - 6 mg N-NO_3^- L^{-1}), suggesting that substrate was scarcely available for denitrifiers and identifying nitrification as the limiting step

5.3.1.2 Influence of dissolved oxygen in the influent

For analysing the effect of real-world aquaponics conditions on the performance of the developed reactor designs, reactors were fed with an influent not flushed with N_2 (aerobic). Reactor's influent in a real aquaponics application will have a DO concentration of around 4 - 8 mg O_2 L^{-1}, constituting a requirement for efficient fish respiration and growth (Wongkiew et al., 2017).

Although a general increase of the N-$NH_4^+{}_{RR}$ was expected for all reactor designs with this influent because of an increased oxygen availability for ammonium-oxidising bacteria, this was only observed for high HRTs (> 0.8 d). In reactor design B (i.e. unpolarised graphite granule

bed), the $N\text{-}NH_4^+{}_{RR}$ increased 187 % (34 ± 9 g N m^{-3} d^{-1}) at 1.0 d HRT, but decreased to only 21 % (34 ± 5 g N m^{-3} d^{-1}) at 0.2 d HRT. This improvement of $N\text{-}NH_4^+{}_{RR}$ for lower Q was higher in design B than in designs A and C either because of the better oxygen diffusion in PVC compared to graphite granules (in case of reactor design A) or because the presence of electricity-driven ammonium removal (in case of reactor design C) already brought these reactor designs close to their upper performance limits in terms of $N\text{-}NH_4^+{}_{RR}$. Still, the highest $N\text{-}NH_4^+{}_{RR}$ was exhibited by reactor design A, showing a maximum value of 68 ± 9 g N m^{-3} d^{-1} at 0.4 d HRT. This value represented an increase of 21 % in respect to the maximum observed $N\text{-}NH_4^+{}_{RR}$ with a N_2-flushed influent (Figure 14). In case of the N_2-flushed influent, the DO needed for nitrification was obtained only from air dissolving in the upper reactor layers. Influent flow rate affects the oxygen mass transfer from gas to liquid phase, and thus, at high Q (low HRT), the oxygen mass transfer increased, and aerobic nitrification improved. However, when oxygen was already available in the influent, the increase of nitrification activity related to additional oxygen was negligible, as DO was already saturated in the upper reactor layers.

As nitrification rates ought to increase, more nitrate was available for bioelectrochemical denitrification. As a consequence, a sharp increase of $N\text{-}TN_{RR}$ performance could be observed at high HRTs, but few differences at low HRTs (Figure 15).

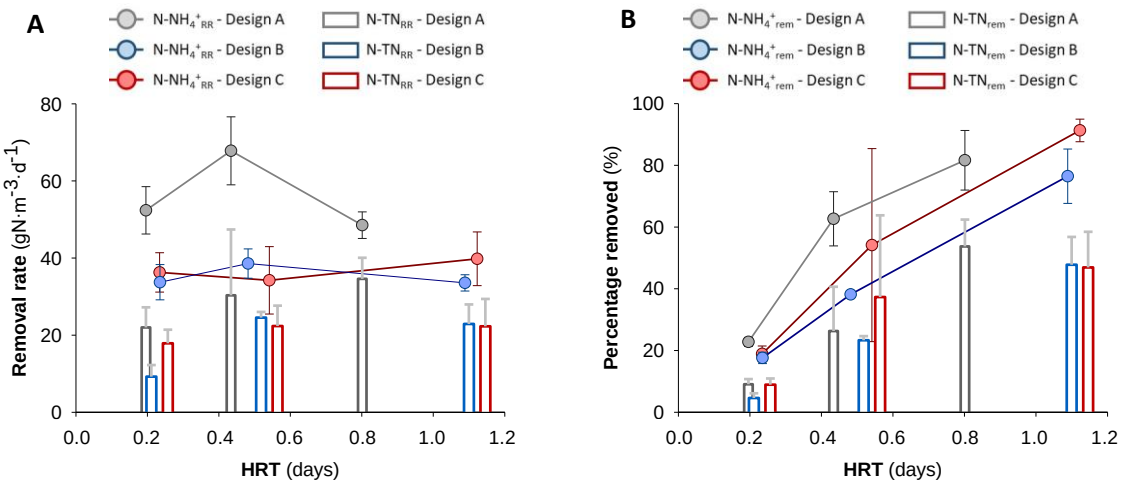

Figure 15. Removal rates of reactor designs A, B, and C at different HRTs treating an influent not flushed with N_2 (Chapter 5). A) Evolution of N-NH_4^+ removal rates (Solid circles) and N-TN removal rates (Bar charts). B) Evolution of percentages of N-NH_4^+ removal (Solid circles) and percentages of N-TN removal (Bar charts). Error bars indicate standard deviation.

This initial testing phase revealed that designs A, B, and C lacked a sufficient oxygen distribution in the reactor for nitrification. PVC was the filling material that provided better ammonium removal performances (Figures 14 and 15). The characteristics of PVC compared to granular graphite (lower porosity, larger size of granules) probably allowed a better oxygen penetration and distribution inside the reactor. In terms of total nitrogen removal using PVC provided some, but limited denitrification activity. This limitation is because no electron donor is present, therefore this process is enhanced and better controlled by polarizing the granular graphite bed and providing cathodic electrons (i.e. reactor design C). Granule polarization was required for total nitrogen removal, as the usage of non-polarized graphite granules (i.e. reactor design B) did not improve the results obtained with PVC (Figures 14 and 15). Nevertheless, in addition to the poor oxygen distribution, reactor design C was probably also affected by a poor potential distribution within the graphite granule bed. The redox potential control of the whole cathode zone at the desired potential was not achieved in the present reactor architecture and

thus bioelectrochemical denitrification was limited as the cathode could not deliver sufficient electrons at a sufficient redox potential. Therefore, the results suggested that a proper coupling of the different materials and conditions in a single reactor design could enhance the reactor performance even further.

5.3.2 Performance enhancement

A fourth reactor design was developed according to the knowledge obtained during the testing phase of the first reactor designs (see section 5.3.1). For this reactor configuration (i.e. reactor design D in Figure 13), an aerobic zone filled with PVC granules for promoting aerobic nitrification was coupled with an anoxic zone in the lower half of the reactors filled with a polarized granular graphite bed. Furthermore, a conductive stainless steel mesh was incorporated as CC in the granular graphite bed for setting a homogeneous potential distribution, and thus for improving and better controlling of denitrification rates (section 5.2.3).

As Figure 16 shows, the coupling of a polarized graphite granule bed with a PVC granule bed resulted in increased nitrification and denitrification rates. Initial testing was performed with the water level at 50 %, thus leaving the PVC granule bed fully exposed to air, while the graphite granule bed was completely covered with medium. At the initial HRT (1.2 ± 0.0 L d^{-1}, i.e. same initial flow rate than the other reactor designs but different HRT due to the different net volume), an $N\text{-}NH_4^+{}_{RR}$ of 39 ± 3 g N m^{-3} d^{-1} was achieved corresponding to 89 ± 9 % $N\text{-}NH_4^+$ removal and representing a higher removal rate than the previous reactor designs (Figures 14 and 15). However, the observed $N\text{-}TN_{RR}$ was still similar to reactor designs A, B, and C (11 ± 8 g N m^{-3} d^{-1}). The performance of reactor design D was further enhanced by lowering the HRT. The ammonium and total nitrogen removal rates increased to 94 ± 44 g N m^{-3} d^{-1} (72 ± 29 % $N\text{-}NH_4^+$ removal, Figure 16A) and 39 ± 6 g N m^{-3} d^{-1} (39 ± 13 % N-TN removal, Figure 16B), respectively, when an HRT of 0.3 d was applied. These values represented an increase of 39 % and 13 % of

the $N\text{-}NH_4^+{}_{RR}$ and $N\text{-}TN_{RR}$, respectively, compared to the maximum values achieved with the first reactor designs (Figures 14 and 15).

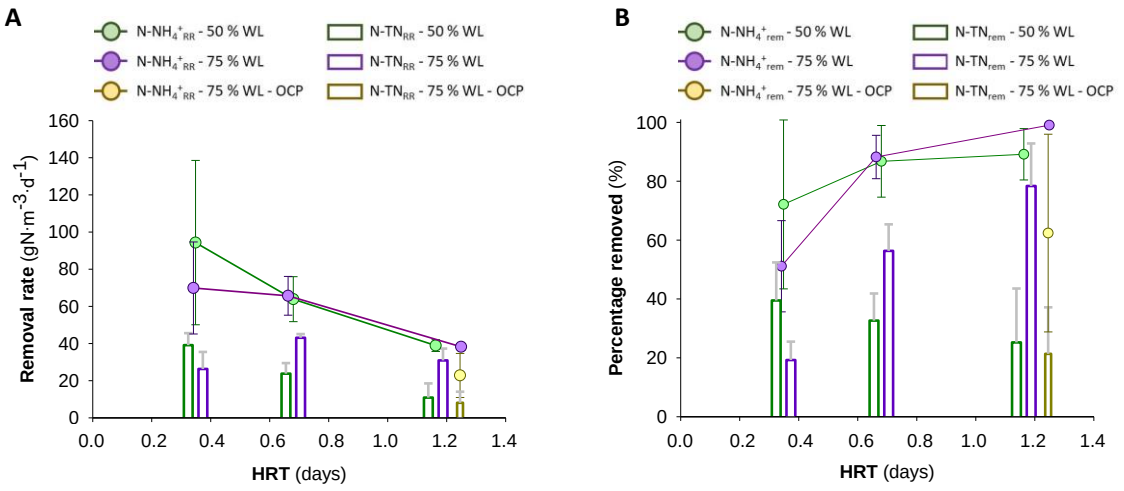

Figure 16. Removal rates of reactor design D at different HRTs treating an N_2-flushed influent at different WLs and without polarization of graphite granules (i.e., OCP) (Chapter 5). A) Evolution of $N\text{-}NH_4^+$ removal rates (Solid circles) and N-TN removal rates (Bar charts). B) Evolution of percentages of $N\text{-}NH_4^+$ removal (Solid circles) and percentages of N-TN removal (Bar charts). Error bars indicate standard deviation.

It is of note that the cathode potential was high (+0.1 ± 0.2 V; see supplementary information) even though higher cell potentials were applied to the reactors (3.3 ± 1.3 V) suggesting that a high concentration of DO occurred due to the low water level (WL, 50 %) limiting nitrate removal. Once the WL was increased to 75 %, the oxygen diffusion to the denitrifying zone was hindered leading to a depletion of oxygen already in the upper parts of the water column (i.e., PVC granule bed and anode zone of granular bed).

First, the increase of the WL to 75 % also resulted in an improved cathode potential of -0.2 ± 0.1 V (by applying a cell potential of 3.8 ± 0.5 V) indicating suitable conditions for bioelectrochemical denitrification (Pous et al., 2015a). Furthermore, a WL of 75 % ought to

decrease the aerobic zone further suggesting a negative effect on ammonium removal performed by ammonium-oxidising bacteria. However, this was not the case for high HRTs. The ammonium removal varied only slightly compared to a WL of 50 % and reached removal rates of 66 ± 10 and 38 ± 2 g N m^{-3} d^{-1} (88 ± 7 and 99 ± 1 % N-NH_4^+ removal) for HRT of 0.7 and 1.2 d, respectively (Figure 16). However, the N-$NH_4^+{}_{RR}$ stabilized to 70 ± 17 g N m^{-3} d^{-1} at HRT of 0.3 d, corresponding to 51 ± 15 % N-NH_4^+ removal.

The maximum N-TN_{RR} obtained in reactor design D operated at WL 75 % was 43 ± 2 g N m^{-3} d^{-1} (HRT of 0.7 d), representing the highest removal rates being observed during the experiments. Hence, the increase of the WL from 50 % to 75 % also improved the reactor performance in terms of total nitrogen removal. Total nitrogen removal performance was particularly enhanced at 1.2 d, HRT where a change of WL from 50 % of 75 % increased the total nitrogen removal from 25 ± 18 % to 78 ± 14 %.

The effect of the polarization of the graphite granule bed on nitrogen removal was tested by operating the system under open circuit potential while the water level and the HRT were 75 % and 1.2 d, respectively (Figure 17). By switching the reactors to OCP, a collapse on denitrification performance was observed. N-TN_{RR} declined from 31 ± 6 to 8 ± 6 g N m^{-3} d^{-1}, indicating that denitrification in the reactors was mainly based on activity of electroactive bacteria. The application of OCP conditions not only affected the N-TN_{RR} but also the N-$NH_4^+{}_{RR}$, which decreased from 39 ± 8 to 23 ± 12 g N m^{-3} d^{-1}. The decrease of N-$NH_4^+{}_{RR}$ by 25 % indicates that aerobic nitrification in the PVC bed was the dominating but not the sole process for ammonium removal. Apparently, the electricity-linked ammonium removal had a certain relevance in the reactor design D (Shaw et al., 2020; Vilajeliu-Pons et al., 2018). This was further supported by recovery of both N-$NH_4^+{}_{RR}$ and N-TN_{RR} to 36 ± 2 and 31 ± 4 g N m^{-3} d^{-1}, respectively, when reactors were polarized again (Figure 17).

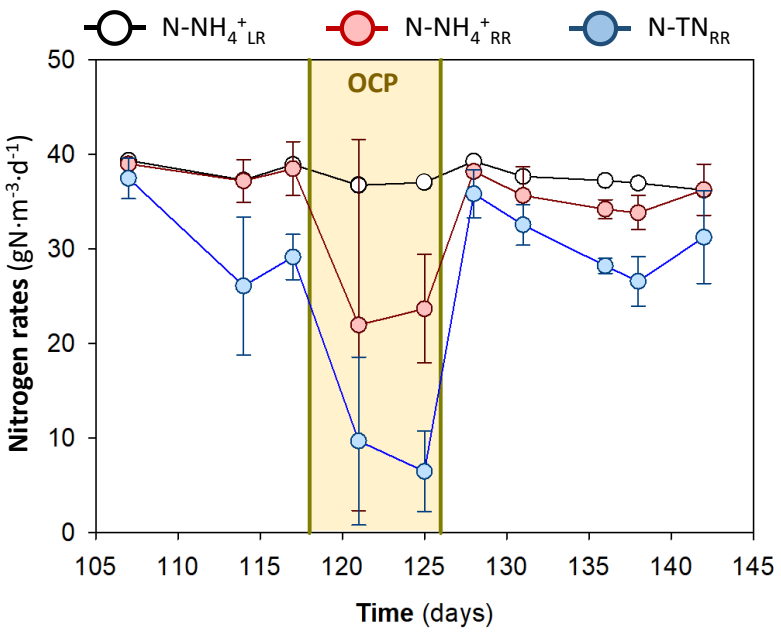

Figure 17. Removal rates of reactor design D during OCP conditions in Chapter 5. Evolution of N-NH_4^+ loading rate (N-$NH_4^+{}_{LR}$), N-$NH_4^+{}_{RR}$ and N-TN_{RR}.

5.3.3 Moving towards a sustainable aquaponics treatment: Effluent qualities and energetic requirements of the developed reactor designs

In this section, the performances of the developed reactor designs are discussed regarding their capabilities to treat a reasonable ammonium-rich influent (i.e., 50 mg N-NH_4^+ L^{-1} (Yin et al., 2018)) and to achieve nitrogen concentrations that the Food and Agriculture Organization of the United Nations (FAO) considers as ideal for aquaponics loop: < 0.8 mg N-NH_4^+ L^{-1}, < 0.3 mg N-NO_2^- L^{-1} and 1 - 34 mg N-NO_3^- L^{-1} (FAO, 2014). If these conditions are reached, aquaculture effluent could be used as hydroponics influent, closing the aquaponics loop. Table 6 summarizes the highest effluent qualities obtained with the different reactor configurations.

Table 6. Best effluent conditions reached with the different reactor designs in Chapter 5.

Reactor design	Condition	HRT (days)	N-NH_4^+ effluent (mg N-NH_4^+ L^{-1})	N-NO_2^- effluent (mg N-NO_2^- L^{-1})	N-NO_3^- effluent (mg N-NO_3^- L^{-1})	Electricity consumption (kWh g N_{rem}^{-1})
A	N_2-flushed influent	1.0	26.1 ± 7.2	2.4 ± 1.2	13.5 ± 4.9	-
	Aerobic influent	1.0	8.9 ± 4.9	3.0 ± 1.7	12.1 ± 5.1	-
B	N_2-flushed influent	1.0	37.0 ± 5.1	0.4 ± 0.2	5.4 ±3.7	-
	Aerobic influent	1.0	11.3 ± 4.4	0.5 ± 0.2	15.1 ± 4.0	-
C	N_2-flushed influent	1.0	32.4 ± 4.3	1.0 ± 1.0	10.1 ± 2.7	$1.1 \times 10^{-1} \pm 1.1 \times 10^{-1}$
	Aerobic influent	1.0	4.2 ± 1.8	0.6 ± 0.5	22.6 ± 5.5	$2.8 \times 10^{-2} \pm 2.7 \times 10^{-2}$
D	WL 50 % N_2-flushed influent	1.0	5.7 ± 4.7	1.0 ± 1.1	31.5 ± 8.5	$9.3 \times 10^{-2} \pm 10.2 \times 10^{-2}$
	WL 75 % N_2-flushed influent	1.0	0.5 ± 0.4	0.2 ± 0.2	9.8 ± 6.8	$8.3 \times 10^{-2} \pm 4.6 \times 10^{-2}$

Notably, the best effluent qualities for the different reactor designs were obtained with a similar HRT (around 1.0 d), representing the highest tested. All reactor designs achieved the required nitrate concentrations being sufficient for cultivating plants in hydroponics, allowing the establishment of the aquaponics loop. Thus, the difference between the reactor designs is mainly based on their capacity to degrade the most harmful compounds for fish and plants growth (i.e. ammonium and nitrite). Considering all different experimental conditions and reactor designs, only reactor design D (WL 75 %) provided a sufficient effluent quality to be used in aquaponics applications (0.5 ± 0.4 mg N-NH_4^+ L^{-1} and 0.2 ± 0.2 mg N-NO_2^- L^{-1}). With this configuration, a proper nitrification-denitrification process without intermediates accumulation was obtained (N_2O was rarely detected in the effluent when testing the different HRTs) and no main changes on pH was observed between influent (7.5 ± 0.3 pH) and effluent (7.4 ± 0.2 pH).

Nevertheless, for a real-world application, it is also needed to take into account the fish feed, the dynamic fish output rates, dynamic plant uptake rates, and the actual flow regime to understand how the here described system can be further adapted to different cultivated plants and fishes (Buzby & Lin, 2014; Endut et al., 2010; Hu et al., 2015). Therefore, a discussion of obtained results should also consider the maximum $N\text{-}NH_4^+{}_{RR}$ and $N\text{-}TN_{RR}$ because they normalize the reactor activity according to its reactor volume and HRT of operation. In this sense, the highest performances were also provided by reactor design D (94 g N m^{-3} d^{-1} and 43 g N m^{-3} d^{-1}, respectively).

The $NH_4^+{}_{RR}$ values obtained here are in the range of conventional biotrickling filters reported for the treatment of aquaculture in literature (about 90 g N m^{-3} d^{-1} – Losordo et al., 1999; Tyson et al., 2008) while being lower than those expressed for a commercial reactor (e.g. MAT-RAS company biofilters removes NH_4^+ at around 500 g N m^{-3} d^{-1} (MAT-RAS, 2020)). However, it should be noted that the aerobic zone in reactor design D (i.e., main nitrification zone) is comparable small as it occupies only 25 - 50 % of the total reactor volume. Further potential improvements of the reactor design D for increasing nitrification rate include optimization of the used filling material (e.g. higher surface area for bacterial growth, good drainage properties), increasing air flow distribution (e.g., by incorporating venting tubes), and obtaining a better knowledge on electricity-linked ammonium removal (Shaw et al., 2020; Vilajeliu-Pons et al., 2018). Remarkably, the electrified biotrickling filter provides not only ammonium but also nitrate removal without the need for adding chemicals, being current standard procedure in aquaculture recirculating systems (van Rijn et al., 2006), but by polarizing the graphite granule bed. The usage of autotrophic denitrifiers also decreases the risk filter blocking by heterotrophic denitrifiers growth. Although the anaerobic requirements for bioelectrochemical denitrification decreased the DO in the effluent of the reactor (< 0.2 mg O_2 L^{-1}), DO values required for the aquaponics loop (FAO, 2014) could be easily recovered by integrating cascade systems between electrified biotrickling filter and hydroponics tank.

The introduced reactor configuration moves METs one step closer to its application for the removal of nitrogen in wastewaters deficient in organic matter (C/N < 3), as it has no need of mechanical aeration, membranes or tailor-made structures as well as representing an approach with a low complexity. For comparing the here obtained total nitrogen removal rates with MET-based denitrification processes, the bioelectrochemical denitrification rates should be normalized to the NCC (Clauwaert et al., 2007). Considering that denitrification in reactor design D occurs only in the cathode zone (280 ± 6 mL), the maximum observed N-TN_{RR} (43 ± 2 g N m^{-3} d^{-1} at 0.7 d HRT and 75 % WL) corresponds to 120 ± 6 g N m^{-3}_{NCC} d^{-1} being comparable to values commonly found in literature (Marx Sander et al., 2018; Pous et al., 2015a; Virdis et al., 2009). However, the denitrification potential of reactor design D is underachieved, since reactors specifically optimized for bioelectrochemical denitrification have achieved rates higher than 500 g N m^{-3}_{NCC} d^{-1} (Clauwaert et al., 2009; Pous et al., 2017). Nevertheless, rates on total nitrogen removal obtained in the present study (43 ± 2 g N m^{-3} d^{-1}) are competitive when compared to already reported low-complex MET for the treatment of urban wastewater. Noteworthy, these wastewaters contained organic matter, while the system tested here was fully autotrophic. For instance, microbial electrochemical wetlands reached values below 15 g N m^{-3} d^{-1} (Aguirre-Sierra et al., 2020; Xu et al., 2017). When a constructed wetland was coupled with a denitrifying MET, a maximum total nitrogen removal rate of 76 g N m^{-3} d^{-1} was observed (He et al., 2016). It is worth noting that this process required two steps (Wetland + MET) and the influent wastewater was composed of a mixture of nitrate and ammonium (40 mg N-NO_3^- L^{-1} and 20 mg N-NH_4^+ L^{-1}) with a C/N ratio of 0.75. Thereby denitrification was not limited by nitrification, and the C/N ratio could explain an equal contribution of heterotrophic and autotrophic denitrification. Yet, total nitrogen removal rates achieved here with reactor design D need to be increased, if they should reach the performance of conventional alternatives pursuing full nitrogen removal in organic-carbon deficient waters. For example, partial-nitritation anammox processes can

provide removal rates of around 200 g N m^{-3} day^{-1} when treating wastewater containing 50 mg $N\text{-}NH_4^+$ L^{-1} (Chatterjee et al., 2016).

However, the low complexity of the presented approach should be considered when interpreting results. In order to improve the applicability of this technology into the aquaponics sector, the complexity and hence the capital expenditures of the reactors can be expected to be significantly lower than a conventional MET used for nitrogen removal (i.e. 2-chamber BES connected to a potentiostat (Virdis et al., 2009)). The electrified biotrickling has no need of a membrane, decreases the number of pumps (no recirculation is applied and influent water flows from the anode to the cathode by gravity), uses cheap materials (i.e. PVC tubes as reactor body and granular graphite bed as electrode), and only needs a DC power supply instead of a potentiostat. Furthermore, in this work and based on aquaponics characteristics, a redox-stratified food web was established. The influent water contained only ammonium that was aerobically and anodically degraded in the upper parts of the reactors. The therefrom produced nitrate was bioelectrochemically treated in the lower reactor parts by cathodic electron supply. Thus, denitrifying activity was dependent on nitrification performance. A poor ammonium oxidation rate implied low nitrate availability for denitrifiers, being its activity restricted by substrate limitation. By improving, e.g., flow conditions and potential distribution, the capability of redox-stratified food web is likely to be enhanced.

The electrification of the biotrickling filter implies extra costs related to the usage of a DC power supply, electrodes and few electrical components. However, as the cost of the conductive filling material is low (about 0.2 € L^{-1}) and as the components required for electrification were kept deliberately simple compared to previous researches, the envisaged reactor system would be comparable cheap. Moreover, an electrified biotrickling filter allows the suppression of organic matter dosing for denitrification and chemical dosing for maintaining appropriate aquaponics conditions representing two main operational costs. Due to the lower

biomass accumulation, the sludge management of the electroactive microbiome presumably also represents an economic advantage compared to conventional aquaponics systems (Brown et al., 2015; Delaide et al., 2019). Although the energy consumption for nitrogen removal is relatively high comparing MET literature, it should be considered that this work represents a proof-of-concept offering several opportunities for improvements (e.g., flow conditions, potential distribution, oxygen leakage). For instance, the electricity consumption related to the DC power supply of reactor design D (between 2.7×10^{-1} and 8.3×10^{-2} kWh g N^{-1}) was higher than those related to the usage of a potentiostat for bioelectrochemical anoxic ammonium removal (1.16×10^{-3} kWh g N^{-1} (Vilajeliu-Pons et al., 2018)) or denitrification (1.3×10^{-2} kWh g N^{-1} (Pous et al., 2015a)) but similar comparing literature also using conventional power supply for bioelectrochemical nitrate removal (7.0×10^{-2} kWh g N^{-1} (Sakakibara & Nakayama, 2001)). This electricity cost would not be the total operational cost related to the system, since pumps would probably be the most important contributor to electricity consumption. Actually, pumps are already present in aquaponics, and they could be used as well to feed the system. Thus, the savings provided by the electrified biotrickling filter in terms of less sludge production and less chemical demand (pH adjustment and organic matter) could overcome the costs related to the power source.

Finally, the recent Covid-19 lockdown allowed observing that reactor design D also inheres a certain resilience and robustness (see supplementary information). The results presented in this work were obtained before the lockdown and during this period, the volumetric flow rate was decreased to 0.3 L d^{-1} (4.6 d HRT) for 2 months. After the lockdown, HRTs of 1.2, 0.7, and 0.4 days were tested again (2 weeks each) and similar maximum $N\text{-}NH_4^+{}_{RR}$ and $N\text{-}TN_{RR}$ rates were observed (97 ± 18 g N m^{-3} d^{-1} and 55 ± 15 g N m^{-3} d^{-1}, respectively).

5.4 Conclusions

Sustainable electrification of biotrickling filters was achieved by combining an aerobic zone (filled with a non-conductive material) with an anoxic electrified zone (filled with a conductive material). Relevant ammonium and nitrate removal rates were obtained (94 g N m^{-3} d^{-1} and 43 g N m^{-3} d^{-1}, respectively) and the effluent quality criteria for an aquaponics application was reached. The reactor design developed in this study is a promising alternative for aquaponics but also for the treatment of organic carbon-deficient ammonium-contaminated water.

Chapter 6. Electrified biotrickling filters as tertiary urban wastewater treatment

Redrafted from: **Osset-Álvarez, M.**, Pous, N., Hasan, S. W., Naddeo, V., Balaguer, M. D., & Puig, S. (2021). Electrified biotrickling filters as tertiary urban wastewater treatment. *Case Studies in Chemical and Environmental Engineering*, *4*, 100143. https://doi.org/10.1016/j.cscee.2021.100143

6.1 Introduction

Nitrification-denitrification is a well-established method in WWTPs. Ammonium is oxidised to nitrate using oxygen as electron acceptor (nitrification) and NO_3^- is further reduced to dinitrogen gas under anoxic conditions using organic matter as an electron donor (denitrification) (Ahn, 2006). However, secondary effluents can occasionally contain excessive nitrogen content (Sander et al., 2017).

Biofilters can be a suitable technology to reach the nitrogen standards, but the lack of electron donors in urban wastewater might hinder the performance of denitrification (Jokela et al., 2002; Zhao et al., 2020). Microbial electrochemical technologies have been postulated as a promising alternative for nitrogen removal (Osset-Álvarez et al., 2019). Full ammonium removal was reported for the first time in 2008 (Virdis et al., 2008). Thereafter, different configurations have been studied. For example, simultaneous nitrification-denitrification was promoted in an aerated biocathode (Virdis et al., 2010) or the integration of bioelectrochemical nitrogen removal in a WWTP configuration (Tejedor-Sanz et al., 2016), among others. Following the principle of integrating METs into existing wastewater treatment technologies, electrified biotrickling filters (e-biofilters) aims at upgrading the current biotrickling filters by incorporating a denitrifying, electrified zone to promote bioelectrochemical denitrification (Pous et al., 2021). Consequently, e-biofilters maintain nitrification activity and promote denitrification processes in wastewaters with a low Carbon/Nitrogen ratio, such as secondary wastewaters. For this reason, this work assesses for the first time the application of an e-biofilter to treat the secondary effluent of an urban WWTP.

6.2 Materials and methods

6.2.1 Reactor set-up

The e-biofilter, originally constructed, inoculated and described in Pous et al. (Pous et al., 2021) consisted of a 1.39 PVC tubular reactor (100 cm height x 4.2 cm of internal diameter). The lower half of the reactor was filled with granular graphite (model 00514, diameter 1.5 - 5 mm, Enviro-cell, Germany), while the upper half was filled with PVC granules, (effective volume 0.77 L) (Figure 18). Two titanium rods (Grade 1, 8 mm diameter, Polymet Reine Metalle, Germany) connected to a power source (IMHY3, Lendher, Spain) were inserted in the reactor at 45 and 12 cm height, serving as anode and cathode current collectors, respectively. A stainless-steel mesh (30 cm height, mesh path light 5 × 5 mm) was placed around the reactor inner wall to improve the cathode electrical distribution. An Ag/AgCl reference electrode (+0.197 V vs SHE, SE 11, Xylem Analytics Germany Sales GmbH & Co. KG Sensortechnik Meinsberg, Germany) was placed next to the cathode collector to set a cathode potential of -0.3 V (vs Ag/AgCl) by routinely adjusting the power supply. The objective was to promote bioelectrochemical denitrification (Pous et al., 2015b). Influent wastewater was continuously supplied from the top of the reactor and it flowed down to the effluent. The upper section of the reactor was fully exposed to air (aerobic zone) to promote aerobic nitrification while the lower section was submerged to promote anoxic conditions. The height of the water level was initially set at 50 cm (50 % WL). In the second part of the study, the WL was raised to 75 cm (75 % WL) (Figures 18B and 18C, respectively).

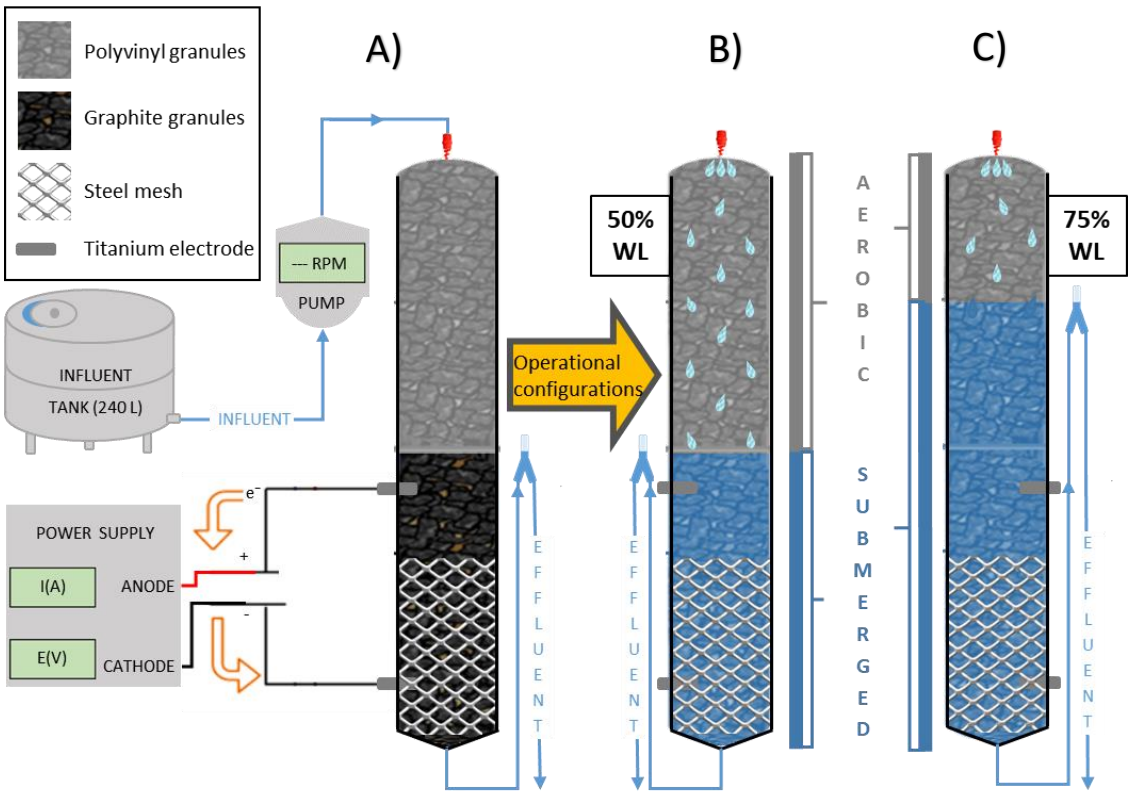

Figure 18. Schematic representation of the e-biofilter design used in Chapter 6 (A) and the WL configurations (WL 50 % (B) and WL 75 % (C)).

6.2.2 Experimental conditions

Synthetic wastewater, described by Pous et al. (Pous et al., 2021) was used as the influent for the first 10 days. Thereafter, the e-biofilter was fed with real secondary effluent of an urban WWTP (Quart, Catalonia, Spain). Secondary wastewater was stored in a 240 L refrigerated tank at 4 ◦C. It contained 44.9 ± 7.2 mg $N\text{-}NH_4^+$ L^{-1}, 0.9 ± 1.7 mg $N\text{-}NO_2^-$ L^{-1}, 0.7 ± 1.0 mg $N\text{-}NO_3^-$ L^{-1}, the chemical oxygen demand of 101.7 ± 42.9 mg COD L^{-1} and a total suspended solids content of 105.3 ± 95.1 mg TSS L^{-1}. Table 7 presents the operational configurations evaluated for the treatment of wastewater.

Table 7. Set of operational conditions tested during the experimental study in Chapter 6.

Operational condition	HRT 1.4 d (50 % WL)	HRT 0.4 d (50 % WL)	HRT 1.4 d (75 % WL)	HRT 0.7 d (75 % WL)	HRT 0.3 d (75 % WL)
Water level height (cm)	50	50	75	75	75
Flow rate ($L \cdot d^{-1}$)	0.6 ± 0.0	2.1 ± 0.3	6.0 ± 0.0	1.1 ± 0.0	2.3 ± 0.1
HRT (days)	1.4 ± 0.1	0.4 ± 0.0	1.4 ± 0.0	0.7 ± 0.0	0.3 ± 0.0
Experimental time duration (days)	40	10	7	7	7

6.2.3 Chemical analyses and calculations

NH_4^+, NO_2^-, NO_3^-, COD and TSS concentrations, pH and conductivity were routinely measured at the influent and the effluent of the reactor, following the American Public Health Association standards (APHA, 2005). Nitrous oxide was measured at the effluent using an N_2O liquid-phase microsensor (Unisense, Denmark). The hydraulic retention time of the reactor was determined by using the reactor net volume and the different influent flow rates applied. Ammonium and total nitrogen ($NH_4^+ + NO_2^- + NO_3^-$) removal rates were calculated as the difference between the influent and the effluent, divided by the HRT. The energy required to remove nitrogen content (kWh g N^{-1}) was calculated from the voltage and current applied together with the nitrogen removal observed.

6.3 Results and discussion

The performance of the e-biofilter was assessed at different operational conditions (WL 50 % and 75 %, HRT from 0.3 to 1.4 days). The system was initially operated at HRT 1.4 ± 0.1 days and WL 50 %. Almost all ammonium was oxidised (1.7 ± 1.5 mg $N\text{-}NH_4^+$ L^{-1} in the effluent, Figure 19A). However, most of the NO_x^- ($NO_2^- + NO_3^-$) produced by nitrification was not removed, yielding a

concentration of 27.3 ± 5.6 mg $N\text{-}NO_x^- \cdot L^{-1}$ in the effluent. No N_2O was detected during the experiment. When the HRT was reduced to 0.4 ± 0.0 days, both ammonium and nitrogen removal rates increased (43.4 ± 13.1 g $N\text{-}NH_4^+$ m^{-3} d^{-1} and 35.7 ± 14.6 g N m^{-3} d^{-1}, Figure 19B), but also the ammonium content at the effluent (40.8 ± 7.1 mg $N\text{-}NH_4^+$ L^{-1}, Figure 19A).

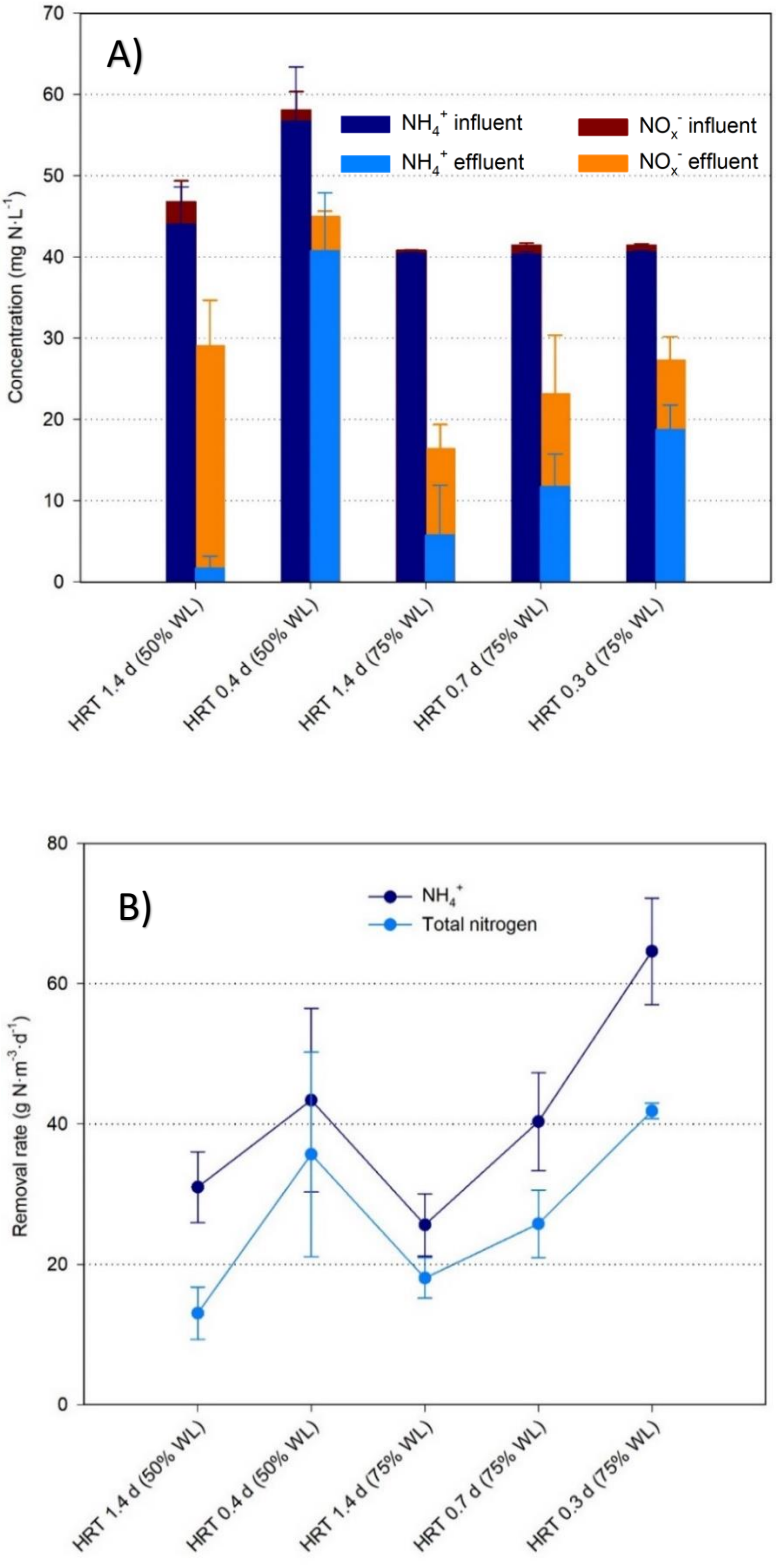

Figure 19. Influent and effluent NH_4^+ and NO_x^- (NO_2^- + NO_3^-) average concentrations (A) and ammonium and total nitrogen average removal rates (B) for each experimental condition in Chapter 6. Error bars represent standard deviation (n > 3).

In the second round of tests, the water level was lifted to 75 cm (WL 75 %) aiming to boost bioelectrochemical denitrification by reducing the potential presence of oxygen in the submerged zone. As a trade-off, halving the volume of the aerobic zone could hinder nitrification. At an HRT at 1.4 ± 0.0 days, the nitrogen content in the effluent decreased to 5.8 ± 6.2 mg $N\text{-}NH_4^+$ L^{-1} and 10.6 ± 3.0 mg $N\text{-}NO_x^-$ L^{-1} (Figure 19A). Subsequently, the decrease of the HRT to 0.7 ± 0.0 and 0.3 ± 0.0 days increased the NH_4^+ effluent concentration to 11.8 ± 4.0 mg $N\text{-}NH_4^+$ L^{-1} and 18.8 ± 3.0 mg $N\text{-}NH_4^+$ L^{-1}, respectively (Figure 19A). Nevertheless, the NO_x^- content slightly moved from the values observed at HRT 1.4 days. A further decrease of the HRT to 0.3 days improved the ammonium and total nitrogen removal rates to 64.6 ± 7.6 g $N\text{-}NH_4^+$ m^{-3} d^{-1} and 41.9 ± 1.1 g N m^{-3} d^{-1}, respectively (Figure 19B). These results implied a slight improvement in the performance compared to HRT 0.4 days WL 50 % (43.4 ± 13.1 g $N\text{-}NH_4^+$ m^{-3} d^{-1} and 35.7 ± 14.6 g N m^{-3} d^{-1}). This unexpected enhancement of the nitrification observed at WL 75 % could be linked to a difference in the influent COD (36.7 ± 8.2 mg COD L^{-1} at HRT 0.3 WL 75 % vs 102.5 ± 6.4 mg COD L^{-1} at HRT 0.4 WL 50 %, Figure 20). Organic matter competed with NH_4^+ for O_2, hampering nitrification. However, COD could also serve as the electron donor for heterotrophic denitrification, contributing alongside bioelectrochemical denitrification to overall nitrogen removal. On average, the e-biofilter removed 63.1 ± 19.3 % of the influent COD, yielding similar effluent COD concentrations for the different experimental conditions evaluated (between 43.9 ± 11.0 and 21.8 ± 4.0 mg COD·L^{-1}, Figure 20). Solids removal was also higher (82.4 ± 18.7 % mean TSS removal), with effluent concentrations ranging from 57.5 ± 24.7 to 1.1 ± 1.6 mg TSS L^{-1} (Table 8). These values upgrade e-biofilters to a holistic treatment with a high potential to produce an effluent water valuable for reuse (RD 1620/2007, 2007).

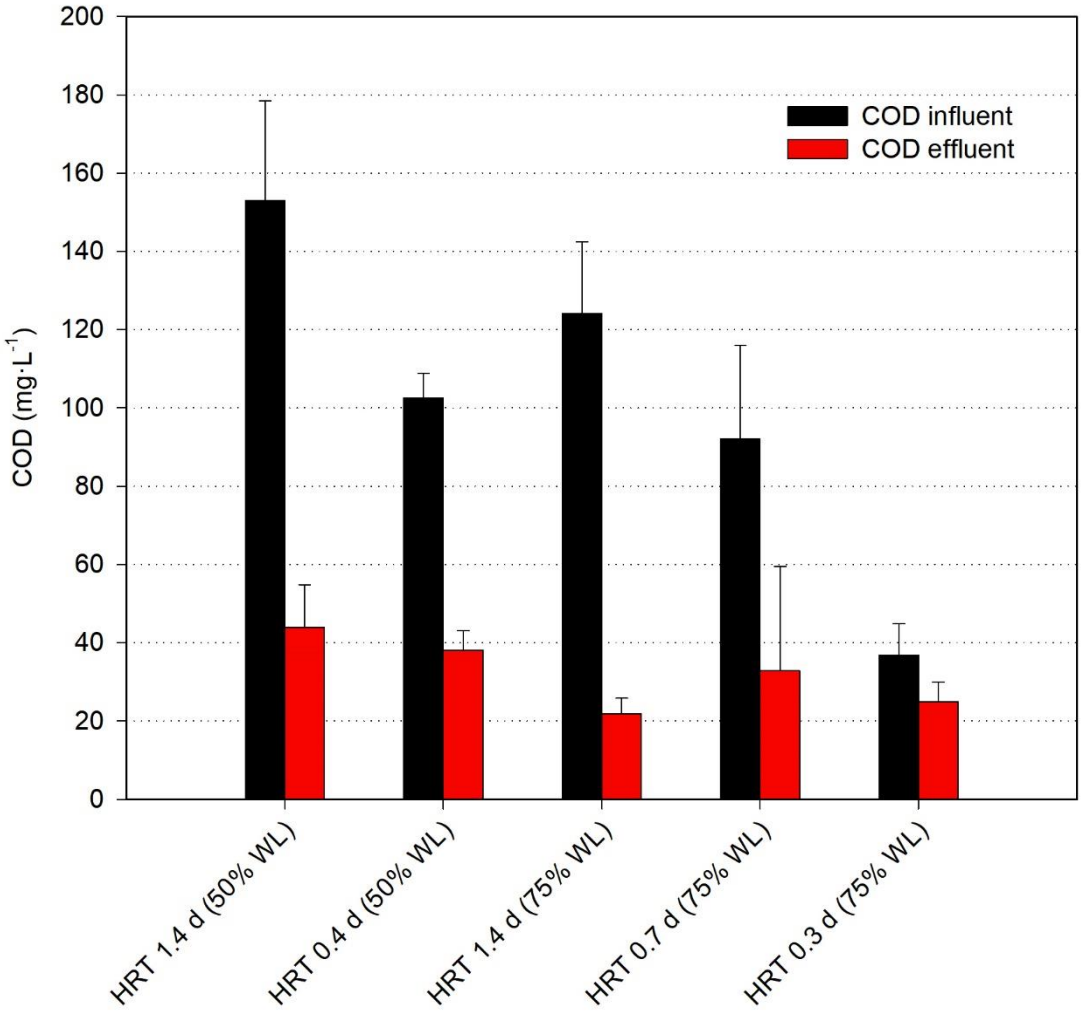

Figure 20. Influent and effluent average COD at each experimental condition in Chapter 6. Error bars represent standard deviation (n > 3).

The NH_4^+ and nitrogen removal rates registered at an HRT 0.3 days with a WL of 75 % (64.6 g $N\text{-}NH_4^+$ m^{-3} d^{-1} and 41.9 g N m^{-3} d^{-1}, Figure 19B) were higher than the ones observed in electroconductive biofilters treating urban wastewater (15.0 g $N\text{-}NH_4^+$ m^{-3} d^{-1} and 6.7 g N m^{-3} d^{-1} (Aguirre-Sierra et al., 2020)) and close to those achieved by soil trickling biofilters treating swine wastewater digested liquid (78.2 g $N\text{-}NH_4^+$ m^{-3} d^{-1} and 49.2 g N m^{-3} d^{-1} (Zhao et al., 2020)) or e-biofilters treating synthetic aquaponics wastewater (94 g $N\text{-}NH_4^+$ m^{-3} d^{-1} and 43 g N m^{-3} d^{-1} (Pous et al., 2021)). Nevertheless, the e-biofilter presented a nitrogen removal energetic efficiency

higher in real wastewater (consuming between 1.0 x 10^{-2} and 3.9 x 10^{-2} kWh g N^{-1}, Table 8) than in synthetic aquaponics wastewater (2.7 x 10^{-1} to 8.3 x 10^{-2} kWh g N^{-1} (Pous et al., 2021)).

Table 8. Dynamics of different parameters depending on the experimental condition applied in Chapter 6.

Experimental condition	HRT 1.4 d (50 % WL)	HRT 0.4 d (50 % WL)	HRT 1.4 d (75 % WL)	HRT 0.7 d (75 % WL)	HRT 0.3 d (75 % WL)
Influent TSS (mg L^{-1})	230.0 ± 141.4	97.5 ± 46.0	87.8 ± 5.4	93.0 ± 108.9	18.0 ± 2.8
Effluent TSS (mg L^{-1})	57.5 ± 24.7	25.0 ± 21.2	2.1 ± 3.0	10.0 ± 8.5	1.1 ± 1.6
Cathode potential (V)	-0.3 ± 0.1	-0.3 ± 0.3	-0.4 ± 0.2	-0.1 ± 0.1	-0.3 ± 0.3
Energy efficiency (kWh g N^{-1})	3.9 x 10^{-2}	1.0 x 10^{-2}	3.4 x 10^{-2}	3.9 x 10^{-2}	2.6 x 10^{-2}
Influent pH	8.2 ± 0.3	8.1 ± 0.1	7.9 ± 0.1	7.8 ± 0.2	7.9 ± 0.1
Effluent pH	7.9 ± 0.3	8.0 ± 0.1	7.4 ± 0.2	7.2 ± 0.3	7.4 ± 0.1
Influent conductivity (mS cm^{-1})	1.3 ± 0.1	1.5 ± 0.0	1.5 ± 0.2	1.3 ± 0.0	1.3 ± 0.0
Effluent conductivity (mS cm^{-1})	1.1 ± 0.1	1.4 ± 0.0	1.2 ± 0.1	1.1 ± 0.0	1.2 ± 0.0

6.4 Conclusions

E-biofilters were applied, for the first time, for the treatment of real secondary wastewater. The e-biofilter was shown as a promising technology for nitrogen polishing in secondary effluents. The operation at WL 50 % enhanced aerobic nitrification, which decreased the effluent ammonium concentration to 1.7 mg $N\text{-}NH_4^+$ L^{-1}. The operation at WL 75 % favoured bioelectrochemical denitrification, which reduced the effluent total nitrogen concentration to 16.4 mg N L^{-1}. The highest NH_4^+ and total nitrogen removal rates were achieved when applying low HRTs (0.3 days), yielding 64.6 g $N\text{-}NH_4^+ \cdot m^{-3} \cdot d^{-1}$ and 41.9 g $N \cdot m^{-3} \cdot d^{-1}$, respectively. Better effluent qualities were obtained when working at higher HRTs (e.g. 1.4 days). In addition, high

removal efficiencies in terms of organic matter (63.1 % COD) and solids (82.4 % TSS) were achieved, showcasing the ability of e-biofilters to polish a set of pollutants that are the key to generating an effluent suitable for water reuse.

Chapter 7. General discussion

This Ph.D. thesis was built around two different applications of microbial electrochemical technologies for NH_4^+ removal in low organic carbon content wastewater. The first of these applications was the recently developed ammonium bioelectrochemical oxidation (Vilajeliu-Pons et al., 2018), an application with important potential advantages over current NH_4^+ removal technologies. In this case, this Ph.D. thesis focused on unravelling the mechanisms for the anoxic transformation of NH_4^+ into dinitrogen gas in bioelectrochemical systems (Chapter 4).

The second METs application of this PhD thesis was the electrification of a well-established decentralised system such as biotrickling filters for reinforcing the removal of NH_4^+ from different kinds of carbon-deficient wastewaters, aquaculture water (Chapter 5) and urban wastewater (Chapter 6). The electrified biotrickling filter, or e-biofilter, integrates bioelectrochemical denitrification into a trickling biofilter, a traditional aerobic nitrification system. Therefore, the NH_4^+ oxidation ability of a currently used ammonium removal technology was complemented with an improvement in NO_3^- reduction, enhancing its overall nitrogen removal capability sustainably.

7.1 Unveiling anoxic bioelectrochemical ammonium removal

The interest in bioelectrochemical ammonium oxidation has grown in the last few years (Shaw et al., 2020; Siegert & Tan, 2019; Tutar Oksuz & Beyenal, 2021). Research carried out so far has highlighted the viability of MET as an oxygen-independent ammonium removal alternative, providing a promising solution to the high aeration costs associated with aerobic nitrification (4.6 kWh kg^{-1} N (Ekman et al., 2006)). Vilajeliu-Pons et al. (2018) established the proof of concept showing that niBES could remove significant concentrations of NH_4^+ (100 mg $N\text{-}NH_4^+$ L^{-1}) from synthetic wastewater at a removal rate (35 g $N\text{-}NH_4^+$ m^{-3} d^{-1}) comparable to nitrification-denitrification processes, but 35 times less energy consumption (0.13 kWh kg^{-1} N). However, the pathways leading to the removal of ammonium were not elucidated. This is a piece

of key information for paving the ground for future scaling up of the process. Shaw et al. (2020) reported a direct pathway for bioelectrochemical oxidation of NH_4^+ to N_2, called electro-anammox, performed by anammox microorganisms. Other studies have also reported the bioelectrochemical oxidation of ammonium N_2 was even though anammox was not dominant in the microbiota (Koffi & Okabe, 2021; Ruiz-Urigüen et al., 2019; Shaw et al., 2020; Siegert & Tan, 2019; Tutar Oksuz & Beyenal, 2021; Vilajeliu-Pons et al., 2018; Zhan et al., 2014; Zhou et al., 2021; Zhu et al., 2021). In all these cases, ammonium should be oxidised by a route different from electro-anammox, and two questions arose:

- Is NH_4^+ bioelectrochemically oxidised to NO_2^- or NO_3^- and then reduced to N_2, following a similar scheme to conventional nitrification-denitrification?
- Does ammonium follow another removal pathway, in which neither nitrite nor nitrate are involved?

Chapter 4 of this PhD thesis (Osset-Álvarez et al., 2022) analysed the removal of NH_4^+ and other nitrogen species, NO_2^-, NO_3^- (which are the main products of NH_4^+ oxidation during conventional nitrification) and NH_2OH (the first intermediate compound of nitrification) in niBES. Ammonium was removed by bioelectrochemical oxidation, without accumulation of any intermediate nitrogen compound (i.e. nitrite, nitrate, nitrous oxide…) at a removal rate of 4.8 g $N\text{-}NH_4^+$ m^{-3} d^{-1}. Once NO_2^- and NO_3^- were spiked to the niBES, both compounds were reduced to N_2 at higher removal rates (ranging between 29.5 and 87.4 g N m^{-3} d^{-1}), indicating that ammonium could have been oxidised to nitrite or nitrate and then reduced to N_2. Interestingly, bioelectrochemical denitrification played a minor role, since the cathode provided only 2 % of the electrons required for the nitrate reduction observed. As no organic matter was added to the reactor, and with the reactor being operated for over 550 days, a still unknown electron donor should be involved in denitrification. Future studies should be carried out to elucidate the electron donors responsible for nitrate reduction.

Nevertheless, NH_2OH (an intermediate of nitrification that was found as the main target for bioelectrochemical oxidation by Vilajeliu-Pons et al. (2018)) was removed from the reactor much faster than NO_2^- or NO_3^- (1083 g N-NH_2OH m^{-3} d^{-1}) without any intermediate accumulation, indicating that the oxidation of NH_2OH was probably truncated before reaching the production of NO_2^-. The bioelectrochemical oxidation of NH_2OH to NO, a reaction that releases 3 electrons and with a coulombic efficiency of 70 %, was considered the main hydroxylamine removal pathway, since the oxidation of NH_2OH to N_2, which would release 1 electron, would mean a CE of 210 %. According to abiotic tests performed outside of the reactor, granular graphite (was able to electrochemically oxidise NH_2OH to NO_2^- and NO_3^- (as final products). This suggested that the microbiota was responsible for the reduction of the NO produced in the niBES, which would have been further oxidised to nitrite. Denitrification was considered the main pathway for NO reduction, even though the electron donors used are still unknown. On the other hand, anammox reactions could only have played a minor role in NH_2OH and NO removal pathways, since NH_4^+ concentration remained stable in the niBES while NH_2OH was being consumed. It is noteworthy that, when both NH_4^+ and NO_2^- were added to the reactor, N_2H_4 was detected, indicating the occurrence of anammox (van Teeseling et al., 2013)

Taken all together, the results obtained in this PhD thesis suggested that the main ammonium removal pathway taking place in a niBES started with the bioelectrochemical oxidation of NH_4^+ to NH_2OH, which was subsequently electrochemically and/or bioelectrochemically oxidised to NO and then further reduced to N_2 by denitrification. This proposed ammonium removal mechanism, which resulted in the oxidation of NH_4^+ into N_2 with a CE of 108 % and energy consumption of 4.3 x 10^{-4} kWh g^{-1} N, is represented in Figure 21. The lack of intermediate accumulation revealed that each step of the pathway was faster than the one precedent, with NH_4^+ oxidation to NH_2OH being the rate-limiting step of the process. This route involves fewer steps than conventional nitrification-denitrification. Shaw et al. (2020) described a more direct NH_4^+ oxidation pathway, but this reaction was catalysed by anammox

bacteria, while the reactor operated during this PhD thesis was mainly colonised by nitrifying (*Achromobacter*) and denitrifying bacteria (*Denitratisoma*).

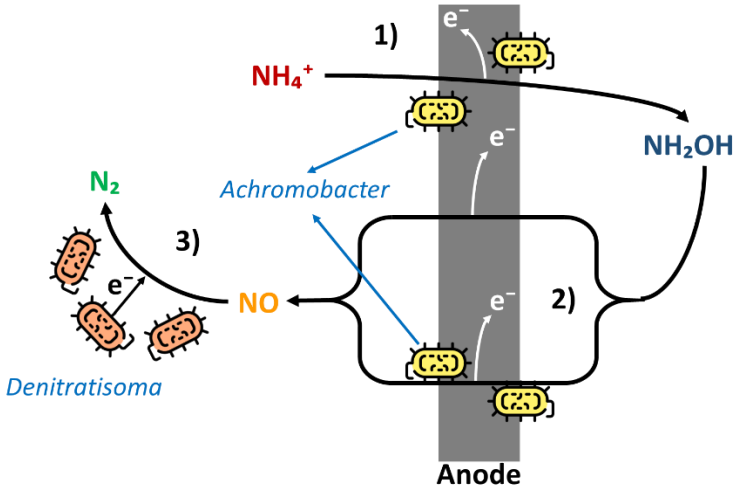

Figure 21. Schematic representation of the main ammonium removal pathway proposed for the niBES operated in this Ph.D. thesis, which is composed of 1) bioelectrochemical oxidation of ammonium to hydroxylamine, 2) electrochemical and/or bioelectrochemical oxidation of hydroxylamine to nitric oxide and 3) reduction of nitric oxide to dinitrogen gas by denitrification.

The ammonium removal rates reported by different studies targeting nitrifying bioelectrochemical systems ranged widely, from 4.6 g $N\text{-}NH_4^+$ m^{-3} d^{-1} (Zhu et al., 2016) to 151 g $N\text{-}NH_4^+$ m^{-3} d^{-1} (of which 95 g $N\text{-}NH_4^+$ m^{-3} d^{-1} were transformed in N_2, and the rest were oxidised to NO_3^-) (Koffi & Okabe, 2021) (Table 9). Koffi & Okabe (2021) achieved the highest ammonium (151 g $N\text{-}NH_4^+$ m^{-3} d^{-1}) and total nitrogen (95 g $N\text{-}NH_4^+$ m^{-3} d^{-1}) removal rates and it was the only one using real wastewater (with a COD of 65 g m^{-3} d^{-1}). The presence of organic matter promoted heterotrophic denitrification (Koffi & Okabe, 2021), suggesting that the nitrogen removal rate of this technology could be improved when it is applied for real wastewater treatment.

Regarding the NH_4^+ removal pathway, most of the studies reported N_2 as the final product of ammonium oxidation, but only Shaw et al. (2020) described a complete route from NH_4^+ to N_2. However, this mechanism, electro-anammox, is carried out by anammox bacteria, (Shaw et al., 2020), so other pathways should be involved in reactors where anammox is not abundant. These alternative pathways are likely more similar to nitrification-denitrification. For example, Qu et al. (2014) obtained NO_3^- from NH_4^+ bioelectrochemical oxidation, while the results in Chapter 4 of this thesis suggested that NO was also a possible outcome for ammonium bioelectrochemical oxidation. In this sense, Vilajeliu-Pons et al. (2018) found that the main bioelectrochemical step of the process is the oxidation of NH_2OH, and the results of this PhD thesis reinforced this hypothesis. The results in Chapter 4 suggested that NO was reduced to N_2 by denitrification, because the abiotic tests pointed out that in the absence of microorganisms, NH_2OH was electrochemically oxidised and accumulated as NO_3^-. Hence, the results presented here suggest a pathway that goes through hydroxylamine and nitric oxide towards dinitrogen gas.

Table 9. Key performance data from different studies targeting niBES.

Influent NH_4^+ (mg N L^{-1})	Operation mode	Waste-water	COD (g m^{-3} d^{-1})	NH_4^+ removal rate (g N m^{-3} d^{-1})	TN removal rate (g N m^{-3} d^{-1})	COD removal rate (g m^{-3} d^{-1})	Nitrogen end products	Anodic potential (V vs SHE)	Reaction & CE (%)	Key microorganisms	Reference
70	Batch	Synthetic	0	17	-	-	NO_3^-	+0.8	$NH_4^+ \rightarrow NO_3^-$ (n = 8) 33 %	*Nitrosomonas europaea, Empedobacter*	(Qu et al., 2014)
100	Continuous	Synthetic	0	4.6	-	-	NO_2^-	-0.3	$NH_4^+ \rightarrow NO_2^-$ (n = 8) 9 %	Anammox, ammonia-oxidising bacteria	(Zhu et al., 2016)
140	Batch	Synthetic	0	12	12	-	N_2	+0.8	$NH_4^+ \rightarrow N_2$ (n = 3) 80 %	*Nitrosomonas, Comamomas, Paracoccus*	(Zhan et al., 2014)
100	Continuous	Synthetic	0	35	35	-	N_2	+0.8	$NH_2OH \rightarrow NO_2^-$ (n = 4) 32 %	*Nitrosomonas*, denitrifiers, anammox	(Vilajeliu-Pons et al., 2018)
45	Continuous	Real	65	151	95	15	N_2 and NO_3^-	+0.6	$NH_4^+ \rightarrow N_2$ (n = 3) 30 %	Heterotrophic denitrifiers, anammox, nitrifiers	(Koffi & Okabe, 2021)
56	Batch	Synthetic	0	N.R.	N.R.	-	N_2	+0.6	$NH_4^+ \rightarrow N_2$ (n = 3) 88 %	*Ca*. Brocadia, *Ca*. Scalindua	(Shaw et al., 2020)
50	**Batch**	**Synthetic**	**0**	**4.8**	**4.8**	**-**	**N_2**	**+0.8**	**$NH_4^+ \rightarrow N_2$ (n = 3) 108 %**	***Achromobacter*, *Denitratisoma***	**Chapter 4**

7.2 Electrification of conventional ammonium removal technologies

Despite the potential advantages of bioelectrochemical nitrification over conventional aerobic ammonium oxidation, this technology is still in development. However, the knowledge gained on METs has been used to promote the proliferation of electroactive activity in conventional technologies such as constructed wetlands (Ramírez-Vargas et al., 2019) or anaerobic digesters (Park et al., 2018), providing an additional improvement in their performances. For this reason, Chapters 5 and 6 of this PhD thesis aimed to merge the potentiality of METs with already existing ammonium removal technologies, such as biotrickling filters (Jokela et al., 2002; Zhao et al., 2020). Bioelectrochemical denitrification has been largely studied either alone or in combination with aerobic nitrification (Clauwaert et al., 2007; Virdis et al., 2008). The electrification of biotrickling filters could provide a controllable denitrification activity to the already good nitrification performances achieved in the biofilters by passive oxygen diffusion (Jokela et al., 2002; Zhao et al., 2020). Initial trials performed in Chapter 5 showed that non-electrified biofilters filled with PVC granules reached higher NH_4^+ removal rates than electrified biofilters filled with granular graphite. Therefore, the upper part of the e-biofilter was filled with PVC granules to enhance aerobic conditions for nitrification while the bottom section was committed to inducing bioelectrochemical denitrification.

Two different ammonium-polluted and organic carbon-deficient wastewaters were treated using the e-biofilters: synthetic aquaculture effluent (Chapter 5) and the secondary effluent of an urban wastewater treatment plant (Chapter 6). In both cases, different water levels (WL, percentage of the reactor filled with water) and hydraulic retention times were applied (WL 50 % and 75 %, HRT between 0.3 and 1.4 days). Reducing the WL from 100 % in the initial trials to 75 and 50 % was expected to favour nitrification over denitrification. The reduction of the HRT can increase ammonium and total nitrogen removal rates, but it can also increase the concentration of nitrogen in the effluent of the e-biofilter.

The objective of treating aquaculture effluent (Chapter 5, (Pous et al., 2021)) was to transform the ammonium (50 mg $N\text{-}NH_4\ L^{-1}$) into N_2 and NO_3^- to establish an aquaponics system (Figure 22). Therefore, this treatment should provide a water stream that contains less than 0.8 mg $N\text{-}NH_4^+\ L^{-1}$ and 0.3 mg $N\text{-}NO_2^-\ L^{-1}$, and a nitrate concentration between 1 and 34 mg $N\text{-}NO_3^-\ L^{-1}$ (FAO, 2014) to enable the growth of a hydroponic culture This objective was achieved by operating the system at an HRT of 1.2 d and a WL of 75 %, producing an effluent containing 0.5 mg $N\text{-}NH_4^+\ L^{-1}$, 0.2 mg $N\text{-}NO_2^-\ L^{-1}$ and 9.8 mg $N\text{-}NO_3^-\ L^{-1}$, with an NH_4^+ removal rate of 38 g $N\text{-}NH_4^+\ m^{-3}\ d^{-1}$, a nitrogen removal rate of 31 g N $m^{-3}\ d^{-1}$ and energy consumption of 8.3 x 10^{-2} kWh g^{-1} N. On the other hand, the highest ammonium removal rate (94 g $N\text{-}NH_4^+\ m^{-3}\ d^{-1}$) was obtained working at an HRT of 0.3 d and a WL of 50 %, and the highest total nitrogen removal rate (43 g N $m^{-3}\ d^{-1}$) at HRT 0.7 d and WL 75 %. However, the effluents produced under these configurations contained excessive concentrations of ammonium and nitrite to be used for hydroponics cultivation (12.3 mg $N\text{-}NH_4^+\ L^{-1}$ and 1.7 mg $N\text{-}NO_2^-\ L^{-1}$ with HRT 0.3 d and WL 50 % and 6.0 mg $N\text{-}NH_4^+\ L^{-1}$ and 0.5 mg $N\text{-}NO_2^-\ L^{-1}$ with HRT 0.7 d and WL 75 %).

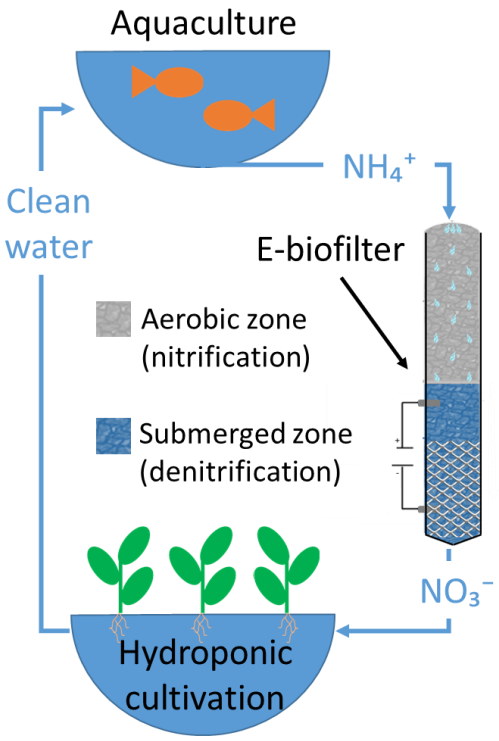

Figure 22. Scheme representing the use of an e-biofilter to remove the NH_4^+ from aquaculture wastewater with partial transformation into NO_3^-, enabling the establishment of an aquaponics system.

In Chapter 6 (Osset-Álvarez et al., 2021), the e-biofilter was used as the polishing step of a WWTP secondary effluent. The WWTP effluent contained 46.6 g N L^{-1} (mostly in the form of NH_4^+, 44.9 mg N-NH_4^+ L^{-1}), a chemical oxygen demand of 102 mg COD L^{-1} (65 mg BOD_5 L^{-1}) and a total suspended solid content of 105 mg TSS L^{-1}. The lowest nitrogen effluent concentration (16.4 mg N L^{-1} composed of 5.8 mg N-NH_4^+ L^{-1} and 10.6 mg N-NO_3^- L^{-1}) was achieved working at an HRT of 1.4 d and a WL of 75 %. This configuration yielded NH_4^+ and total nitrogen removal rates of 26 g N-NH_4^+ m^{-3} d^{-1} and 18 g N m^{-3} d^{-1}. In contrast, the highest NH_4^+ and total nitrogen removal rates, 65 g N-NH_4^+ m^{-3} d^{-1} and 42 g N m^{-3} d^{-1}, respectively, were achieved operating the e-biofilter at an HRT of 0.3 d and a WL of 75 %, which produced an effluent with 18.8 mg N-NH_4^+ L^{-1}, 0.4 mg N-NO_2^- L^{-1} and 8.2 mg N-NO_3^- L^{-1}. Moreover, the minimum energy consumption, 1.0 x 10^{-2} kWh g^{-1} N, was reached using an HRT 0.4 d and WL 50 % configuration. On top of that, most of the

organic matter and solids present in the wastewater were removed (63.1 % of the COD (79.9 % of the BOD_5) and 82.4 % of the TSS), showing the ability of e-biofilters to perform complete wastewater treatment beyond nitrogen removal. The e-biofilters consumed 2.7 x 10^{-1} kWh g^{-1} N during the treatment of WWTP secondary effluent

The main difference between synthetic aquaculture wastewater and WWTP effluent was the presence of organic matter. Organic matter could have hampered aerobic nitrification by competing with NH_4^+ for oxygen, even though it could also potentially act as the electron donor for denitrification, as shown in Figure 23. The effect of organic matter could explain why synthetic aquaculture wastewater yielded a maximum NH_4^+ removal rate (94 g N-NH_4^+ m^{-3} d^{-1}) higher than real WWTP effluent treatment (65 g N-NH_4^+ m^{-3} d^{-1}). However, the organic matter concentration in the WWTP effluent (102 mg COD L^{-1}) was low (< 300 mg COD L^{-1} (Lei et al., 2018)), so it is plausible that the organic carbon removal took place during the aerobic phase, simultaneously with the formation of NO_3^- (Farazaki & Gikas, 2019). Thus, COD was no longer available when nitrate started to be present, reducing the occurrence of heterotrophic denitrification processes (He et al., 2016). This would explain why both wastewaters presented similar maximum total nitrogen removal rates (43 g N m^{-3} d^{-1} for synthetic aquaculture wastewater and 42 g N m^{-3} d^{-1} for real WWTP effluent).

Oxygen diffusion from the air was not the only source of electron acceptors involved in ammonium oxidation in e-biofilters. Open circuit potential experiments performed during synthetic aquaculture wastewater showed that interrupting the electric current between the anode and the cathode caused a decrease of 74 % in total nitrogen removal but also a 41 % reduction in the NH_4^+ removal rate. Therefore, the electrification of the system promoted bioelectrochemical denitrification and anodic NH_4^+ oxidation. The anodic potential was higher than +2.0 V vs Ag/AgCl throughout the entire e-biofilters operation, which can promote anodic water oxidation ($H_2O \rightarrow 2H^+ + 2e^- + ½\ O_2$). Therefore, anodic O_2 could have promoted ammonium

oxidation as well. Moreover, ammonium bioelectrochemical oxidation could have also occurred at the anode

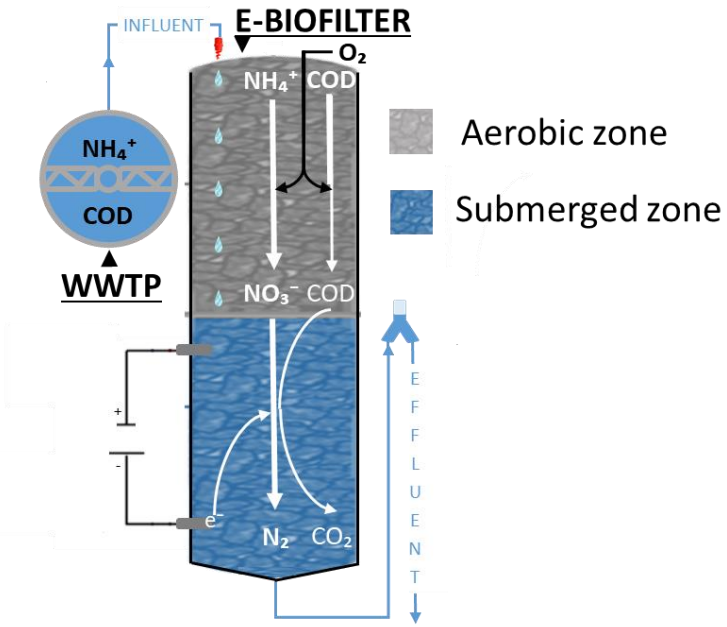

Figure 23. Schematic representation of WWTP effluent treatment by an e-biofilter.

To contextualize the e-biofilter removal activity, the best results in terms of NH_4^+ and total nitrogen removal rates obtained in this PhD thesis were compared with other biofilter-based technologies and other combinations of aerobic nitrification with METs (Table 10).

The removal rates obtained in this Ph.D. thesis (94 g N-NH_4^+ m^{-3} d^{-1} and 43 g N m^{-3} d^{-1}) were higher than the ones achieved by Aguirre-Sierra et al. (2020) (15 g N-NH_4^+ m^{-3} d^{-1} and 7 g N m^{-3} d^{-1}) with a biofilter filled with electroconductive material (to promote electron transfer reactions) but without any electrical input. These results were also better than the ones obtained by Tao et al. (2012) with a biofilter performing simultaneous partial nitrification-anammox (8 g N-NH_4^+ m^{-3} d^{-1} and 8 g N m^{-3} d^{-1}). E-biofilters performances were similar to the values reported by Zhao et al. (2020) (78 g N-NH_4^+ m^{-3} d^{-1} and 49 g N m^{-3} d^{-1}) for a biofilter treating

wastewater with a much higher organic matter (509 mg COD L^{-1}) and nitrogen concentration (807 mg N L^{-1}). However, they still fall behind in terms of ammonium and total nitrogen removal rates with other biofilter-based technologies that rely on a two-step process. For example, the two-biofilters system (a partial nitrification biofilter and an anammox biofilter) described by Jiang et al. (2018) (130 g $N\text{-}NH_4^+$ m^{-3} d^{-1} and 110 g N m^{-3} d^{-1}), or combinations of aerobic nitrification with bioelectrochemical denitrification, as the one reported by Ryu et al. (2013) (194 g $N\text{-}NH_4^+$ m^{-3} d^{-1} and 194 g N m^{-3} d^{-1}). The maximum nitrogen removal achieved with the e-biofilters (43 g N m^{-3} d^{-1}) was lower than half of the maximum ammonium removal rate (94 g N m^{-3} d^{-1}) obtained with this technology. However, e-biofilters have been used to treat wastewater containing no organic matter or a low COD (102 mg COD L^{-1}). Treating wastewaters with a higher organic carbon concentration should enhance heterotrophic denitrification and therefore improve overall nitrogen removal.

The results presented in this Ph.D. thesis demonstrate that e-biofilters can become a suitable technology for the removal of nitrogen present in wastewater. The capacity to modulate the ammonium and total nitrogen removal by changing different operational parameters such as the water flow, the water level and the electricity input, widens the possibilities to test this technology under different kinds of wastewaters. For example, hydroponic cultivation requires extremely low ammonium concentrations (< 0.8 mg $N\text{-}NH_4^+$ L^{-1}) (FAO, 2014), so the treatment of aquaculture wastewater should prioritize nitrification over denitrification. In addition, aquaponic systems are usually working in a loop mode, thus not only effluent concentrations are important, but also high removal rates. On the other hand, the goal of the WWTP effluent treatment was to minimise the overall nitrogen content in the water to reach the legal requirement set by the Spanish law for urban WWTPs designed for 10,000 and 100,000 equivalent inhabitants (15 mg N L^{-1}) (RD 509/1996, 1996).

Table 10. Influent composition and ammonium and nitrogen removal rates of e-biofilters and related technologies.

Waste-water	Operation mode	Influent NH_4^+ (mg N L^{-1})	Influent TN (mg N L^{-1})	Influent COD (mg L^{-1})	NH_4^+ removal rate (g N m^{-3} d^{-1})	TN removal rate (g N m^{-3} d^{-1})	Technology	Reference
Real	Continuous	45	55	360	15	7	Electroconductive biofilter	(Aguirre-Sierra et al., 2020)
Synthetic	Batch	310	322	-	8	8	Partial nitrification-anammox (single biofilter)	(Tao et al., 2012)
Real	Continuous	3210	3228	12980	194	194	Aerobic nitrification + bioelectrochemical denitrification	(Ryu et al., 2013)
Real	Continuous	65	67	300	130	110	Partial nitrification biofilter + anammox biofilter	(Jiang et al., 2018)
Real	Continuous	802	807	509	78	49	Tricking biofilter with soil layer (aerobic to anoxic conditions)	(Zhao et al., 2020)
Synthetic	Continuous	50	50	-	94	43	E-biofilter	Chapter 5
Real	Continuous	45	47	102	65	42	E-biofilter	Chapter 6

Chapter 8. Conclusions

This Ph.D. thesis aimed at achieving two main objectives. The first one was to unveil the mechanisms for ammonium electrochemical removal. This was accomplished by analysing the removal of nitrogen in nitrifying bioelectrochemical systems. The second goal of this PhD thesis was the electrification of conventional nitrogen treatment technologies to boost their performance. The electrification of biotrickling filters (a current NH_4^+ removal technology) led to the development of e-biofilters. These e-biofilters were operated using different configurations to adapt the system for the treatment of different ammonium-polluted wastewaters. The main conclusions extracted from this Ph.D. thesis are the following:

- NH_4^+ was removed in the niBES under anoxic conditions with an ammonium removal rate of 4.8 g N m^{-3} d^{-1} and without intermediates accumulation, being NH_4^+ oxidised to nitric oxide with the anodic electrode (potential set at +0.8 V vs SHE) serving as electron acceptor and then reduced to N_2. It was hypothesised that *Achromobacter* sp. carried out nitrification, while *Denitratisoma* sp. was responsible for NO reduction to N_2. The removal of the immediate product of NH_4^+ oxidation, hydroxylamine, was much faster (1083 g N m^{-3} d^{-1}) showing that the starting step of the process, the oxidation of NH_4^+ to NH_2OH was the bottleneck of the whole ammonium removal process. Apart from the main pathway (NH_4^+ oxidation to NO followed by reduction to N_2), other minor pathways could have contributed to ammonium removal, such as oxidation to NO followed by anammox and electro-anammox (anammox bacteria accounted for less than 2 % of the microbiota in the reactors) or direct oxidation to N_2, even though they could only have played a minor role in the process.
- The electrification of biotrickling filters (e-biofilters) successfully combined aerobic nitrification with bioelectrochemical denitrification. Moreover, it boosted ammonium oxidation by proving extra oxygen through electrochemical water oxidation. The proposed configuration was a combination of PVC granules at the top of the reactor and electrified graphite granules at the bottom. Two different wastewaters (aquaculture and secondary

wastewater) targeting two different removal goals were tested (partial nitrogen removal and full nitrogen removal).

- Aquaculture wastewater treatment was successfully achieved reaching an effluent with almost no NH_4^+ (< 0.8 mg N-NH_4^+ L^{-1}) or NO_2^- (< 0.3 mg N-NO_2^- L^{-1}) and with a certain degree of NO_3^- (> 1 and < 34 mg N-NO_3^- L^{-1}) useful to promote plant growth in hydroponic culture. Such requirements were achieved by operating the e-biofilter at an HRT of 1.2 d and a WL of 75 %, yielding an effluent containing 0.5 mg N-NH_4^+ L^{-1}, 0.2 mg N-NO_2^- L^{-1} and 9.8 mg N-NO_3^- L^{-1}. Moreover, the best ammonium removal rate, 94 g N-NH_4^+ m^{-3} d^{-1}, was achieved working at an HRT of 0.3 d and a WL of 50 %, and the best nitrogen removal rate, 43 g N m^{-3} d^{-1}, at an HRT of 0.7 d and a WL of 50 %.
- The treatment of the WWTP secondary effluent is aimed at the removal of the nitrogen and organic matter content. The lowest nitrogen concentration, 16.4 mg N L^{-1}, was obtained at an HRT of 1.4 and a WL of 75 %, and it was only slightly above the target 15 mg N L^{-1}. The best ammonium and total nitrogen removal rates (65 g N-NH_4^+ m^{-3} d^{-1} and 42 g N m^{-3} d^{-1}) were achieved with the e-biofilter being used under an HRT of 0.3 and a WL of 75 % conditions. Moreover, most of the COD (63 %) and TSS (82 %) were removed, enabling the reuse of this wastewater, which was the main objective of the treatment.

Regarding bioelectrochemical nitrification, future works should be linked to unveiling the knowledge about NH_4^+ bioelectrochemical oxidation, more specifically, about the first step of the route, the oxidation of NH_4^+ into NH_2OH. This reaction is catalysed by ammonium oxygenase, so an in-depth study of this enzyme could help to understand the process. The ammonium removal rate could be improved by either improving the design of the reactors (e.g. optimising hydrodynamics) or using selected microorganisms to enhance nitrification. Moreover, further research should also be done to clarify which are electron donors involved in the reduction of NO to N_2

On the other hand, e-biofilters showed how the electrification of conventional biotrickling filters can upgrade the nitrogen removal ability of conventional biofilters. In the future e-biofilters may be considered for the treatment of the wastewater of isolated buildings (decentralised systems), enabling the removal of multiple pollutants from the wastewater of remote facilities that are not connected to a WWTP.

Chapter 9. References

Aguirre-Sierra, A., Bacchetti-De Gregoris, T., Salas, J. J., de Deus, A., & Esteve-Núñez, A. (2020). A new concept in constructed wetlands: assessment of aerobic electroconductive biofilters. *Environmental Science: Water Research & Technology*, *6*(5), 1312–1323.

Ahn, Y. H. (2006). Sustainable nitrogen elimination biotechnologies: A review. *Process Biochemistry*, *41*(8), 1709–1721.

Akaboci, T. R. V, Gich, F., Ruscalleda, M., Balaguer, M. D., & Colprim, J. (2018). Assessment of operational conditions towards mainstream partial nitritation-anammox stability at moderate to low temperature: reactor performance and bacterial community. *Chemical Engineering Journal*, *350*, 192–200.

APHA. (2005). Standard methods for the examination of water and wastewater. In *American Public Health Association (APHA): Washington, DC, USA*.

Arends, J. B. A., & Verstraete, W. (2012). 100 Years of Microbial Electricity Production: Three Concepts for the Future. *Microbial Biotechnology*, *5*(3), 333–346.

Basha, K. A., Joseph, T. C., Lalitha, K. V, Vineetha, D., Rathore, G., Tripati, G., & Pani Prasad, K. (2018). Nitrification Potential of *Achromobacter xylosoxidans* Isolated from Fresh Water Finfish Farms of Kerala, India. *International Journal of Current Microbiology and Applied Sciences*, *7*(8), 2645–2654.

Brown, R. K., Harnisch, F., Dockhorn, T., & Schröder, U. (2015). Examining sludge production in bioelectrochemical systems treating domestic wastewater. *Bioresource Technology*, *198*, 913–917.

Buzby, K. M., & Lin, L. S. (2014). Scaling aquaponic systems: Balancing plant uptake with fish output. *Aquacultural Engineering*, *63*, 39–44.

Callahan, B. J., McMurdie, P. J., Rosen, M. J., Han, A. W., Johnson, A. J. A., & Holmes, S. P. (2016). DADA2: High-resolution sample inference from Illumina amplicon data. *Nature*

Methods, *13*(7), 581–583.

Caranto, J. D., & Lancaster, K. M. (2017). Nitric oxide is an obligate bacterial nitrification intermediate produced by hydroxylamine oxidoreductase. *Proceedings of the National Academy of Sciences*, *114*(31), 8217–8222.

Ceballos-Escalera, A., Pous, N., Chiluiza-Ramos, P., Korth, B., Harnisch, F., Bañeras, L., Balaguer, M. D., & Puig, S. (2021). Electro-bioremediation of nitrate and arsenite polluted groundwater. *Water Research*, *190*, 116748.

Chatterjee, P., Ghangrekar, M. M., & Rao, S. (2016). Development of anammox process for removal of nitrogen from wastewater in a novel self-sustainable biofilm reactor. *Bioresource Technology*, *218*, 723–730.

Clauwaert, P., Desloover, J., Shea, C., Nerenberg, R., Boon, N., & Verstraete, W. (2009). Enhanced nitrogen removal in bio-electrochemical systems by pH control. *Biotechnology Letters*, *31*(10), 1537–1543.

Clauwaert, P., Rabaey, K., Aelterman, P., De Schamphelaire, L., Pham, T. H., Boeckx, P., Boon, N., & Verstraete, W. (2007). Biological denitrification in microbial fuel cells. *Environmental Science & Technology*, *41*(9), 3354–3360.

Cohen, B. (1931). The bacterial culture as an electrical half-cell. *J. Bacteriol*, *21*(1), 18–19.

Colt, J. (2006). Water quality requirements for reuse systems. *Aquacultural Engineering*, *34*(3), 143–156.

Crab, R., Avnimelech, Y., Defoirdt, T., Bossier, P., & Verstraete, W. (2007). Nitrogen removal techniques in aquaculture for a sustainable production. *Aquaculture*, *270*(1–4), 1–14.

Cruz Viggi, C., Presta, E., Bellagamba, M., Kaciulis, S., Balijepalli, S. K., Zanaroli, G., Petrangeli Papini, M., Rossetti, S., & Aulenta, F. (2015). The “Oil-Spill Snorkel”: An innovative

bioelectrochemical approach to accelerate hydrocarbons biodegradation in marine sediments. *Frontiers in Microbiology*, *6*, 881.

Davis, J. B., & Yarbrough, H. F. (1962). Preliminary experiments on a microbial fuel cell. *Science*, *137*(3530), 615–616.

Delaide, B., Monsees, H., Gross, A., & Goddek, S. (2019). Aerobic and anaerobic treatments for aquaponic sludge reduction and mineralisation. *Aquaponics Food Production Systems*, 247.

Deng, S., Li, D., Yang, X., Xing, W., Li, J., & Zhang, Q. (2016). Biological denitrification process based on the Fe(0)-carbon micro-electrolysis for simultaneous ammonia and nitrate removal from low organic carbon water under a microaerobic condition. *Bioresource Technology*, *219*, 677–686.

Ekman, M., Björlenius, B., & Andersson, M. (2006). Control of the aeration volume in an activated sludge process using supervisory control strategies. *Water Research*, *40*(8), 1668–1676.

Endut, A., Jusoh, A., Ali, N., Wan Nik, W. B., & Hassan, A. (2010). A study on the optimal hydraulic loading rate and plant ratios in recirculation aquaponic system. *Bioresource Technology*, *101*(5), 1511–1517.

Farazaki, M., & Gikas, P. (2019). Nitrification-denitrification of municipal wastewater without recirculation, using encapsulated microorganisms. *Journal of Environmental Management*, *242*, 258–265.

FAO. (2014). *Small-scale aquaponic food production - Integrated fish and plant farming.* FAO fisheries and aquaculture technical paper. Rome.

FAO. (2018). *The state of world fisheries and aquaculture 2018 - Meeting the sustainable development goals.* Rome.

Gabarró, J., Ganigué, R., Gich, F., Ruscalleda, M., & Colprim, J. (2012). Effect of temperature on AOB activity of a partial nitritation SBR treating landfill leachate with extremely high nitrogen concentration. *Bioresource Technology*, *126*, 283–289.

Garrido-Baserba, M., Vinardell, S., Molinos-Senante, M., Rosso, D., & Poch, M. (2018). The economics of wastewater treatment decentralization: A techno-economic evaluation. *Environmental Science & Technology*, *52*(15), 8965–8976.

Godfray, H. C. J., Beddington, J. R., Crute, I. R., Haddad, L., Lawrence, D., Muir, J. F., Pretty, J., Robinson, S., Thomas, S. M., & Toulmin, C. (2010). Food security: The challenge of feeding 9 billion people. *Science*, *327*(5967), 812–818.

Gregory, K. B., Bond, D. R., & Lovley, D. R. (2004). Graphite electrodes as electron donors for anaerobic respiration. *Environmental Microbiology*, *6*(6), 596–604.

Gwynn-Jones, D., Dunne, H., Donnison, I., Robson, P., Sanfratello, G. M., Schlarb-Ridley, B., Hughes, K., & Convey, P. (2018). Can the optimisation of pop-up agriculture in remote communities help feed the world? *Global Food Security*, *18*, 35–43.

Hakeem, K. R., Sabir, M., Ozturk, M., Akhtar, M. S., & Ibrahim, F. H. (2017). Nitrate and nitrogen oxides: sources, health effects and their remediation. *Reviews of Environmental Contamination and Toxicology*, *242*, 183–217.

He, Y., Wang, Y., & Song, X. (2016). High-effective denitrification of low C/N wastewater by combined constructed wetland and biofilm-electrode reactor (CW–BER). *Bioresource Technology*, *203*, 245–251.

Hoareau, M., Erable, B., & Bergel, A. (2019). Microbial electrochemical snorkels (MESs): A budding technology for multiple applications. A mini review. *Electrochemistry Communications*, *104*, 106473.

Holmes, D. E., Dang, Y., & Smith, J. A. (2019). Nitrogen cycling during wastewater treatment.

Advances in Applied Microbiology, *106*, 113–192.

Hu, Z., Lee, J. W., Chandran, K., Kim, S., Brotto, A. C., & Khanal, S. K. (2015). Effect of plant species on nitrogen recovery in aquaponics. *Bioresource Technology*, *188*, 92–98.

Hu, Z., Lotti, T., van Loosdrecht, M., & Kartal, B. (2013). Nitrogen removal with the anaerobic ammonium oxidation process. *Biotechnology Letters*, *35*(8), 1145–1154.

Hu, Z., Wessels, H. J. C. T., Van Alen, T., Jetten, M. S. M., & Kartal, B. (2019). Nitric oxide-dependent anaerobic ammonium oxidation. *Nature Communications*, *10*(1), 1–7.

Jetten, M. S. M., Schmid, M., Schmidt, I., Wubben, M., van Dongen, U., Abma, W., Sliekers, O., Revsbech, N. P., Beaumont, H. J. E., Ottosen, L., Volcke, E., Laanbroek, H. J., Campos-Gomez, J. L., Cole, J., van Loosdrecht, M., Mulder, J. W., Fuerst, J., Richardson, D., van De Pas, K., … Kuenen, J. G. (2002). Improved nitrogen removal by application of new nitrogen-cycle bacteria. *Reviews in Environmental Science & Biotechnology*, *1*(1), 51–63.

Jiang, H., Liu, G., Ma, Y., Xu, X., Chen, J., Yang, Y., Liu, X., & Wang, H. (2018). A pilot-scale study on start-up and stable operation of mainstream partial nitrification-anammox biofilter process based on online pH-DO linkage control. *Chemical Engineering Journal*, *350*, 1035–1042.

Jokela, J. P. Y., Kettunen, R. H., Sormunen, K. M., & Rintala, J. A. (2002). Biological nitrogen removal from municipal landfill leachate: low-cost nitrification in biofilters and laboratory scale in-situ denitrification. *Water Research*, *36*(16), 4079–4087.

Kartal, B., De Almeida, N. M., Maalcke, W. J., Op Den Camp, H. J. M., Jetten, M. S. M., & Keltjens, J. T. (2013). How to make a living from anaerobic ammonium oxidation. *FEMS Microbiology Reviews*, *37*(3), 428–461.

Kartal, B., Maalcke, W. J., De Almeida, N. M., Cirpus, I., Gloerich, J., Geerts, W., Op Den Camp, H. J. M., Harhangi, H. R., Janssen-Megens, E. M., Francoijs, K. J., Stunnenberg, H. G.,

Keltjens, J. T., Jetten, M. S. M., & Strous, M. (2011). Molecular mechanism of anaerobic ammonium oxidation. *Nature*, *479*, 127–130.

Khin, T., & Annachhatre, A. P. (2004). Novel microbial nitrogen removal processes. *Biotechnology Advances*, *22*(7), 519–532.

Kim, J. R., Zuo, Y., Regan, J. M., & Logan, B. E. (2008). Analysis of ammonia loss mechanisms in microbial fuel cells treating animal wastewater. *Biotechnology and Bioengineering*, *99*(5), 1120–1127.

Kissil, G. W., & Lupatsch, I. (2004). Successful replacement of fishmeal by plant proteins in diets for the gilthead seabream, *Sparus aurata* L. *Israeli Journal of Aquaculture-Bamidgeh*, *56*(3), 188–199.

Koch, C., Korth, B., & Harnisch, F. (2018). Microbial ecology-based engineering of Microbial Electrochemical Technologies. *Microbial Biotechnology*, *11*(1), 22–38.

Koffi, N. J., & Okabe, S. (2021). Bioelectrochemical anoxic ammonium nitrogen removal by an MFC driven single chamber microbial electrolysis cell. *Chemosphere*, *274*, 129715.

Kozich, J. J., Westcott, S. L., Baxter, N. T., Highlander, S. K., & Schloss, P. D. (2013). Development of a dual-index sequencing strategy and curation pipeline for analyzing amplicon sequence data on the MiSeq Illumina sequencing platform. *Applied and Environmental Microbiology*, *79*(17), 5112–5120.

Kuypers, M. M. M., Marchant, H. K., & Kartal, B. (2018). The microbial nitrogen-cycling network. *Nature Reviews Microbiology*, *16*(5), 263–276.

Lai, A., Aulenta, F., Mingazzini, M., Palumbo, M. T., Papini, M. P., Verdini, R., & Majone, M. (2017). Bioelectrochemical approach for reductive and oxidative dechlorination of chlorinated aliphatic hydrocarbons (CAHs). *Chemosphere*, *169*, 351–360.

Lei, Z., Yang, S., Li, Y. Y., Wen, W., Wang, X. C., & Chen, R. (2018). Application of anaerobic membrane bioreactors to municipal wastewater treatment at ambient temperature: A review of achievements, challenges, and perspectives. *Bioresource Technology*, *267*, 756–768.

Leigh, N. G., & Lee, H. (2019). Sustainable and resilient urban water systems: The role of decentralization and planning. *Sustainability*, *11*(3), 918.

Losordo, T. M., Masser, M. P., & Rakocy, J. E. (1999). Recirculating aquaculture tank production systems: a review of component options. *Southern Regional Aquaculture Center*, *453*.

Lovley, D. R. (2008). The microbe electric: conversion of organic matter to electricity. *Current Opinion in Biotechnology*, *19*(6), 564–571.

Lu, Z., Mo, W., Dilkina, B., Gardner, K., Stang, S., Huang, J. C., & Foreman, M. C. (2019). Decentralized water collection systems for households and communities: Household preferences in Atlanta and Boston. *Water Research*, *167*, 115134.

Ma, J., Wang, Z., He, D., Li, Y., & Wu, Z. (2015). Long-term investigation of a novel electrochemical membrane bioreactor for low-strength municipal wastewater treatment. *Water Research*, *78*, 98–110.

Marx Sander, E., Virdis, B., & Freguia, S. (2018). Bioelectrochemical denitrification for the treatment of saltwater recirculating aquaculture streams. *ACS Omega*, *3*(4), 4252–4261.

MAT-RAS. (2020). Trickle filters for aquaculture. URL: https://mat-ras.com/equipment/trickle-filters-aquaculture/ (accessed on 10th August 2020)

McMurdie, P. J., & Holmes, S. (2012). Phyloseq: a bioconductor package for handling and analysis of high-throughput phylogenetic sequence data. In *Pacific Symposium on Biocomputing* (pp. 235–246).

Mook, W. T., Chakrabarti, M. H., Aroua, M. K., Khan, G. M. A., Ali, B. S., Islam, M. S., & Abu Hassan, M. A. (2012). Removal of total ammonia nitrogen (TAN), nitrate and total organic carbon (TOC) from aquaculture wastewater using electrochemical technology: A review. *Desalination*, *285*, 1–13.

Nutrient Reduction Technology Cost Task Force. (2002). *Nutrient reduction technology cost estimations for point sources in the Chesapeake bay watershed. Annapolis, MD: Chesapeake Bay Program*.

Oksuz, S. T., & Beyenal, H. (2021). Enhanced bioelectrochemical nitrogen removal in flow through electrodes. *Sustainable Energy Technologies and Assessments*, *47*, 101507.

Oshiki, M., Ali, M., Shinyako-Hata, K., Satoh, H., & Okabe, S. (2016). Hydroxylamine-dependent anaerobic ammonium oxidation (anammox) by "*Candidatus* Brocadia sinica." *Environmental Microbiology*, *18*(9), 3133–3143.

Osset-Álvarez, M., Pous, N., Chiluiza-Ramos, P., Bañeras, L., Balaguer, M. D., & Puig, S. (2022). Unveiling microbial electricity driven anoxic ammonium removal. *Bioresource Technology Reports*, *17*, 100975.

Osset-Álvarez, M., Pous, N., Hasan, S. W., Naddeo, V., Balaguer, M. D., & Puig, S. (2021). Electrified biotrickling filters as tertiary urban wastewater treatment. *Case Studies in Chemical and Environmental Engineering*, *4*, 100143.

Osset-Álvarez, M., Rovira-Alsina, L., Pous, N., Blasco-Gómez, R., Colprim, J., Balaguer, M. D., & Puig, S. (2019). Niches for bioelectrochemical systems on the recovery of water, carbon and nitrogen in wastewater treatment plants. *Biomass and Bioenergy*, *130*, 105380.

Padhi, S. K., & Maiti, N. K. (2017). Molecular insight into the dynamic central metabolic pathways of *Achromobacter xylosoxidans* CF-S36 during heterotrophic nitrogen removal processes. *Journal of Bioscience and Bioengineering*, *123*(1), 46–55.

Park, H. I., Kim, D. K., Choi, Y. J., & Pak, D. (2005). Nitrate reduction using an electrode as direct electron donor in a biofilm-electrode reactor. *Process Biochemistry*, *40*(10), 3383–3388.

Park, J., Lee, B., Tian, D., & Jun, H. (2018). Bioelectrochemical enhancement of methane production from highly concentrated food waste in a combined anaerobic digester and microbial electrolysis cell. *Bioresource Technology*, *247*, 226–233.

Penuelas, J., Janssens, I. A., Ciais, P., Obersteiner, M., & Sardans, J. (2020). Anthropogenic global shifts in biospheric N and P concentrations and ratios and their impacts on biodiversity, ecosystem productivity, food security, and human health. *Global Change Biology*, *26*(4), 1962–1985.

Potter, M. C. (1911). Electrical effects accompanying the decomposition of organic compounds. *Proceedings of the Royal Society of London. Serie B*, *84*, 260–276.

Pous, N., Koch, C., Vilà-Rovira, A., Balaguer, M. D., Colprim, J., Mühlenberg, J., Müller, S., Harnisch, F., & Puig, S. (2015b). Monitoring and engineering reactor microbiomes of denitrifying bioelectrochemical systems. *RSC Advances Advances*, *5*(84), 68326–68333.

Pous, N., Korth, B., Osset-Álvarez, M., Balaguer, M. D., Harnisch, F., & Puig, S. (2021). Electrifying biotrickling filters for the treatment of aquaponics wastewater. *Bioresource Technology*, *319*, 124221.

Pous, N., Puig, S., Balaguer, M. D., & Colprim, J. (2015a). Cathode potential and anode electron donor evaluation for a suitable treatment of nitrate-contaminated groundwater in bioelectrochemical systems. *Chemical Engineering Journal*, *263*, 151–159.

Pous, N., Puig, S., Balaguer, M. D., & Colprim, J. (2017). Effect of hydraulic retention time and substrate availability in denitrifying bioelectrochemical systems. *Environmental Science: Water Research and Technology*, *3*(5), 922–929.

Prado, A., Ramírez-Vargas, C. A., Arias, C. A., & Esteve-Núñez, A. (2020). Novel

bioelectrochemical strategies for domesticating the electron flow in constructed wetlands. *Science of The Total Environment*, *735*, 139522.

Puig, S., van Loosdrecht, M. C. M., Flameling, A. G., Colprim, J., & Meijer, S. C. F. (2010). The effect of primary sedimentation on full-scale WWTP nutrient removal performance. *Water Research*, *44*(11), 3375–3384.

Qu, B., Fan, B., Zhu, S., & Zheng, Y. (2014). Anaerobic ammonium oxidation with an anode as the electron acceptor. *Environmental Microbiology Reports*, *6*(1), 100–105.

Rabaey, K., Ossieur, W., Verhaege, M., & Verstraete, W. (2005). Continuous microbial fuel cells convert carbohydrates to electricity. *Water Science and Technology*, *52*(1–2), 515–523.

Rabaey, K., Vandekerckhove, T., Van de Walle, A., & Sedlak, D. L. (2020). The third route: Using extreme decentralization to create resilient urban water systems. *Water Research*, *185*, 116276.

Ramírez-Vargas, C. A., Arias, C. A., Carvalho, P., Zhang, L., Esteve-Núñez, A., & Brix, H. (2019). Electroactive biofilm-based constructed wetland (EABB-CW): A mesocosm-scale test of an innovative setup for wastewater treatment. *Science of the Total Environment*, *659*, 796–806.

RD 1620/2007. (2007). Royal Decree of December 7th, 2007, which establishes the legal regime for the reuse of treated water. *BOE*, *294*, 50639–50661.

RD 509/1996. (1996). Royal Decree of March 15th, 1996, which establishes the standards applicable to the treatment of urban wastewater. *BOE*, *77*, 12038–12041.

Read, P., & Fernandes, T. (2003). Management of environmental impacts of marine aquaculture in Europe. *Aquaculture*, *226*(1–4), 139–163.

Ruiz-Urigüen, M., Steingart, D., & Jaffé, P. R. (2019). Oxidation of ammonium by Feammox

Acidimicrobiaceae sp. A6 in anaerobic microbial electrolysis cells. *Environmental Science: Water Research & Technology*, *5*, 1582–1592.

Ryu, J. H., Lee, H. L., Lee, Y. P., Kim, T. S., Kim, M. K., Anh, D. T. N., Tran, H. T., & Ahn, D. H. (2013). Simultaneous carbon and nitrogen removal from piggery wastewater using loop configuration microbial fuel cell. *Process Biochemistry*, *48*(7), 1080–1085.

Sakakibara, Y., & Nakayama, T. (2001). A novel multi-electrode system for electrolytic and biological water treatments: electric charge transfer and application to denitrification. *Water Research*, *35*(3), 768–778.

Sander, E. M., Virdis, B., & Freguia, S. (2017). Bioelectrochemical nitrogen removal as a polishing mechanism for domestic wastewater treated effluents. *Water Science and Technology*, *76*(11), 3150–3159.

Schröder, U. (2011). Discover the possibilities: microbial bioelectrochemical systems and the revival of a 100-year–old discovery. *Journal of Solid State Electrochemistry*, *15*, 1481–1486.

Schröder, U., Harnisch, F., & Angenent, L. T. (2015). Microbial electrochemistry and technology: terminology and classification. *Energy & Environmental Science*, *8*(2), 513–519.

Shaw, D. R., Ali, M., Katuri, K. P., Gralnick, J. A., Reimann, J., Mesman, R., van Niftrik, L., Jetten, M. S. M., & Saikaly, P. E. (2020). Extracellular electron transfer-dependent anaerobic oxidation of ammonium by anammox bacteria. *Nature Communications*, *11*(1), 2058.

Siegert, M., & Tan, A. (2019). Electric Stimulation of Ammonotrophic Methanogenesis. *Frontiers in Energy Research*, *7*, 17.

Sleutels, T. H. J. A., Ter Heijne, A., Buisman, C. J. N., & Hamelers, H. V. M. (2012). Bioelectrochemical systems: An outlook for practical applications. *ChemSusChem*, *5*(6),

1012–1019.

Su, J., Liang, D., & Lian, T. (2018). Comparison of denitrification performance by bacterium Achromobacter sp. A14 under different electron donor conditions. *Chemical Engineering Journal*, *333*, 320–326.

Tao, W., He, Y., Wang, Z., Smith, R., Shayya, W., & Pei, Y. (2012). Effects of pH and temperature on coupling nitritation and anammox in biofilters treating dairy wastewater. *Ecological Engineering*, *47*, 76–82.

Tejedor-Sanz, S., de Gregoris, T. B., Salas, J. J., Pastor, L., & Esteve-Núñez, A. (2016). Integrating a microbial electrochemical system into a classical wastewater treatment configuration for removing nitrogen from low COD effluents. *Environmental Science: Water Research and Technology*, *2*(5), 884–893.

Thauer, R. K., Jungermann, K., & Decker, K. (1977). Energy conservation in chemotrophic anaerobic bacteria. *Bacteriological Reviews*, *41*(1), 100–180.

Tilman, D., Fargione, J., Wolff, B., D'Antonio, C., Dobson, A., Howarth, R., Schindler, D., Schlesinger, W. H., Simberloff, D., & Swackhamer, D. (2001). Forecasting agriculturally driven global environmental change. *Science*, *292*(5515), 281–284.

Tiquia-Arashiro, S. M., & Pant, D. (2020). *Microbial Electrochemical Technologies*. CRC Press.

Torre, A., Vázquez-Rowe, I., Parodi, E., & Kahhat, R. (2021). Wastewater treatment decentralization: Is this the right direction for megacities in the Global South? *Science of the Total Environment*, *778*, 146227.

Tsujino, S., Uematsu, C., Dohra, H., & Fujiwara, T. (2017). Pyruvic oxime dioxygenase from heterotrophic nitrifier *Alcaligenes faecalis* is a nonheme Fe (II)-dependent enzyme homologous to class II aldolase. *Scientific Reports*, *7*, 39991.

Tutar Oksuz, S., & Beyenal, H. (2021). Enhanced bioelectrochemical nitrogen removal in flow through electrodes. *Sustainable Energy Technologies and Assessments*, *47*, 101507.

Tyson, R. V, Simonne, E. H., Treadwell, D. D., White, J. M., & Simonne, A. (2008). Reconciling pH for ammonia biofiltration and cucumber yield in a recirculating aquaponic system with perlite biofilters. *HortScience*, *43*(3), 719–724.

Tyson, R. V, Treadwell, D. D., & Simonne, E. H. (2011). Opportunities and challenges to sustainability in aquaponic systems. *HortTechnology*, *21*(1), 6–13.

van Rijn, J., Tal, Y., & Schreier, H. J. (2006). Denitrification in recirculating systems: Theory and applications. *Aquacultural Engineering*, *34*(3), 364–376.

van Teeseling, M. C. F., Neumann, S., & van Niftrik, L. (2013). The anammoxosome organelle is crucial for the energy metabolism of anaerobic ammonium oxidizing bacteria. *Journal of Molecular Microbiology and Biotechnology*, *23*(1–2), 104–117.

Vegas Niño, O. T., Martínez Alzamora, F., & Tzatchkov, V. G. (2021). A decision support tool forwater supply system decentralization via distribution network sectorization. *Processes*, *9*(4), 642.

Venkata Mohan, S., Amulya, K., & Modestra, J. A. (2020). Urban biocycles – Closing metabolic loops for resilient and regenerative ecosystem: A perspective. *Bioresource Technology*, *306*, 123098.

Vilajeliu-Pons, A., Bañeras, L., Puig, S., Molognoni, D., Vilà-Rovira, A., Hernandez-del Amo, E., Balaguer, M. D., & Colprim, J. (2016). External resistances applied to MFC affect core microbiome and swine manure treatment efficiencies. *PLoS ONE*, *11*(10), e0164044.

Vilajeliu-Pons, A., Koch, C., Balaguer, M. D., Colprim, J., Harnisch, F., & Puig, S. (2018). Microbial electricity driven anoxic ammonium removal. *Water Research*, *130*, 168–175.

Vineyard, D., Hicks, A., Karthikeyan, K. G., & Barak, P. (2020). Economic analysis of electrodialysis, denitrification, and anammox for nitrogen removal in municipal wastewater treatment. *Journal of Cleaner Production*, *262*, 121145.

Virdis, B., Rabaey, K., Rozendal, R. A., Yuan, Z., & Keller, J. (2010). Simultaneous nitrification, denitrification and carbon removal in microbial fuel cells. *Water Research*, *44*(9), 2970–2980.

Virdis, B., Rabaey, K., Yuan, Z., & Keller, J. (2008). Microbial fuel cells for simultaneous carbon and nitrogen removal. *Water Research*, *42*(12), 3013–3024.

Virdis, B., Rabaey, K., Yuan, Z., Rozendal, R. A., & Keller, J. (2009). Electron fluxes in a microbial fuel cell performing carbon and nitrogen removal. *Environmental Science & Technology*, *43*(13), 5144–5149.

Wongkiew, S., Hu, Z., Chandran, K., Lee, J. W., & Khanal, S. K. (2017). Nitrogen transformations in aquaponic systems: A review. *Aquacultural Engineering*, *76*, 9–19.

Wu, M. R., Hou, T. T., Liu, Y., Miao, L. L., Ai, G. M., Ma, L., Zhu, H. Z., Zhu, Y. X., Gao, X. Y., Herbold, C. W., Wagner, M., Li, D. F., Liu, Z. P., & Liu, S. J. (2021). Novel *Alcaligenes ammonioxydans* sp. nov. from wastewater treatment sludge oxidizes ammonia to N2 with a previously unknown pathway. *Environmental Microbiology*, *23*(11), 6965–6980.

Xie, S., Liang, P., Chen, Y., Xia, X., & Huang, X. (2011). Simultaneous carbon and nitrogen removal using an oxic/anoxic-biocathode microbial fuel cells coupled system. *Bioresource Technology*, *102*(1), 348–354.

Xu, D., Xiao, E., Xu, P., Zhou, Y., He, F., Zhou, Q., Xu, D., & Wu, Z. (2017). Performance and microbial communities of completely autotrophic denitrification in a bioelectrochemically-assisted constructed wetland system for nitrate removal. *Bioresource Technology*, *228*, 39–46.

Yang, W. H., Weber, K. A., & Silver, W. L. (2012). Nitrogen loss from soil through anaerobic ammonium oxidation coupled to iron reduction. *Nature Geoscience*, *5*(8), 538–541.

Yin, H., Yang, C., Jia, Y., Chen, H., & Gu, X. (2018). Dual removal of phosphate and ammonium from high concentrations of aquaculture wastewaters using an efficient two-stage infiltration system. *Science of the Total Environment*, *635*, 936–946.

Zhan, G., Zhang, L., Tao, Y., Wang, Y., Zhu, X., & Li, D. (2014). Anodic ammonia oxidation to nitrogen gas catalyzed by mixed biofilms in bioelectrochemical systems. *Electrochimica Acta*, *135*, 345–350.

Zhang, F., & He, Z. (2012). Simultaneous nitrification and denitrification with electricity generation in dual-cathode microbial fuel cells. *Journal of Chemical Technology & Biotechnology*, *87*(1), 153–159.

Zhang, G. D., Zhao, Q. L., Jiao, Y., Zhang, J. N., Jiang, J. Q., Ren, N., & Kim, B. H. (2011b). Improved performance of microbial fuel cell using combination biocathode of graphite fiber brush and graphite granules. *Journal of Power Sources*, *196*(15), 6036–6041.

Zhang, Y., & Angelidaki, I. (2013). A new method for in situ nitrate removal from groundwater using submerged microbial desalination–denitrification cell (SMDDC). *Water Research*, *47*(5), 1827–1836.

Zhang, Y., Noori, J. S., & Angelidaki, I. (2011a). Simultaneous organic carbon, nutrients removal and energy production in a photomicrobial fuel cell (PFC). *Energy & Environmental Science*, *4*(10), 4340–4346. https://doi.org/10.1039/c1ee02089g

Zhao, B., Xie, F., Zhang, X., & Yue, X. (2020). Enhancing the nitrogen removal from swine wastewater digested liquid in a trickling biofilter with a soil layer. *RSC Advances*, *10*(40), 23782–23791.

Zhao, H., Yuan, M., Strokal, M., Wu, H. C., Liu, X., Murk, A., Kroeze, C., & Osinga, R. (2021).

Impacts of nitrogen pollution on corals in the context of global climate change and potential strategies to conserve coral reefs. *Science of the Total Environment*, *774*, 145017.

Zhou, G. W., Yang, X. R., Li, H., Marshall, C. W., Zheng, B. X., Yan, Y., Su, J. Q., & Zhu, Y. G. (2016). Electron Shuttles Enhance Anaerobic Ammonium Oxidation Coupled to Iron(III) Reduction. *Environmental Science & Technology*, *50*(17), 9298–9307.

Zhou, Q., Yang, N., Zheng, D., Zhang, L., Tian, C., Yang, Q., & Li, D. (2021). Electrode-dependent ammonium oxidation with different low C/N ratios in single-chambered microbial electrolysis cells. *Bioelectrochemistry*, *142*, 107889.

Zhu, T., Zhang, Y., Bu, G., Quan, X., & Liu, Y. (2016). Producing nitrite from anodic ammonia oxidation to accelerate anammox in a bioelectrochemical system with a given anode potential. *Chemical Engineering Journal*, *291*, 184–191.

Zhu, T., Zhang, Y., Liu, Y., & Zhao, Z. (2021). Electrostimulation enhanced ammonium removal during Fe(III) reduction coupled with anaerobic ammonium oxidation (Feammox) process. *Science of The Total Environment*, *751*, 141703.

Chapter 10. Supplementary information

10.1 Supplementary information for Chapter 4

Summary:

- 10.1.1: Experimental set-up and granular graphite composition.

- 10.1.2: Set of data of reactors A and B.

- 10.1.3: Abiotic tests on nitrite and hydroxylamine abiotic oxidation on granular graphite.

- 10.1.4: Relative abundance of main orders with Planctomycetes.

10.1.1 Experimental set-up and granular graphite composition.

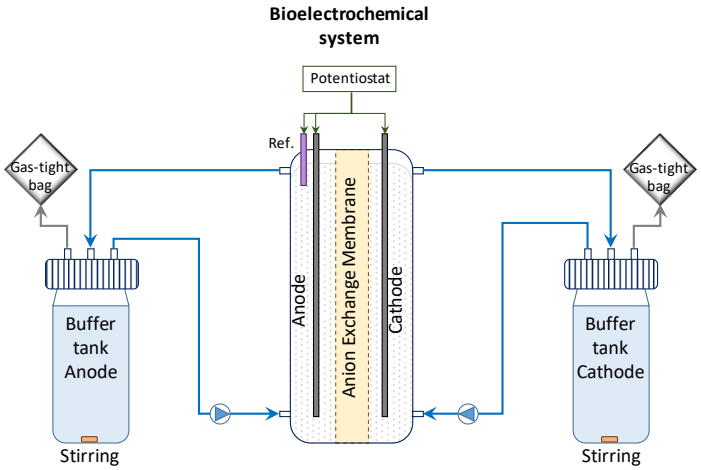

Figure S4.1. Scheme of the experimental set-up used in Chapter 4.

Table S4.1. Concentrations of major impurities (> 1 mg $Kg_{graphite}^{-1}$) detected in the granular graphite used in Chapter 4.

Component	Concentration (mg Kg $_{granular\ graphite}^{-1}$)	Component	Concentration (mg Kg $_{granular\ graphite}^{-1}$)
Silicon	235.1 ± 4.8	Aluminum	8.0 ± 1.3
Boron	72.8 ± 10.9	Sodium	5.8 ± 0.6
Sulfur	58.1 ± 2.2	Iron	5.7 ±0.2
Calcium	46.1 ± 2.6	Magnesium	2.0 ±0.0
Lithium	33.5 ± 0.8	Titanium	1.4 ± 0.3
Potassium	11.7 ± 1.0	Arsenic	1.5 ± 0.0
Phosphorous	11.6 ± 1.5	Barium	1.3 ± 1.5
Bromine	10.3 ±0.6	Strontium	1.1 ± 0.0

10.1.2 Set of data of reactors A and B.

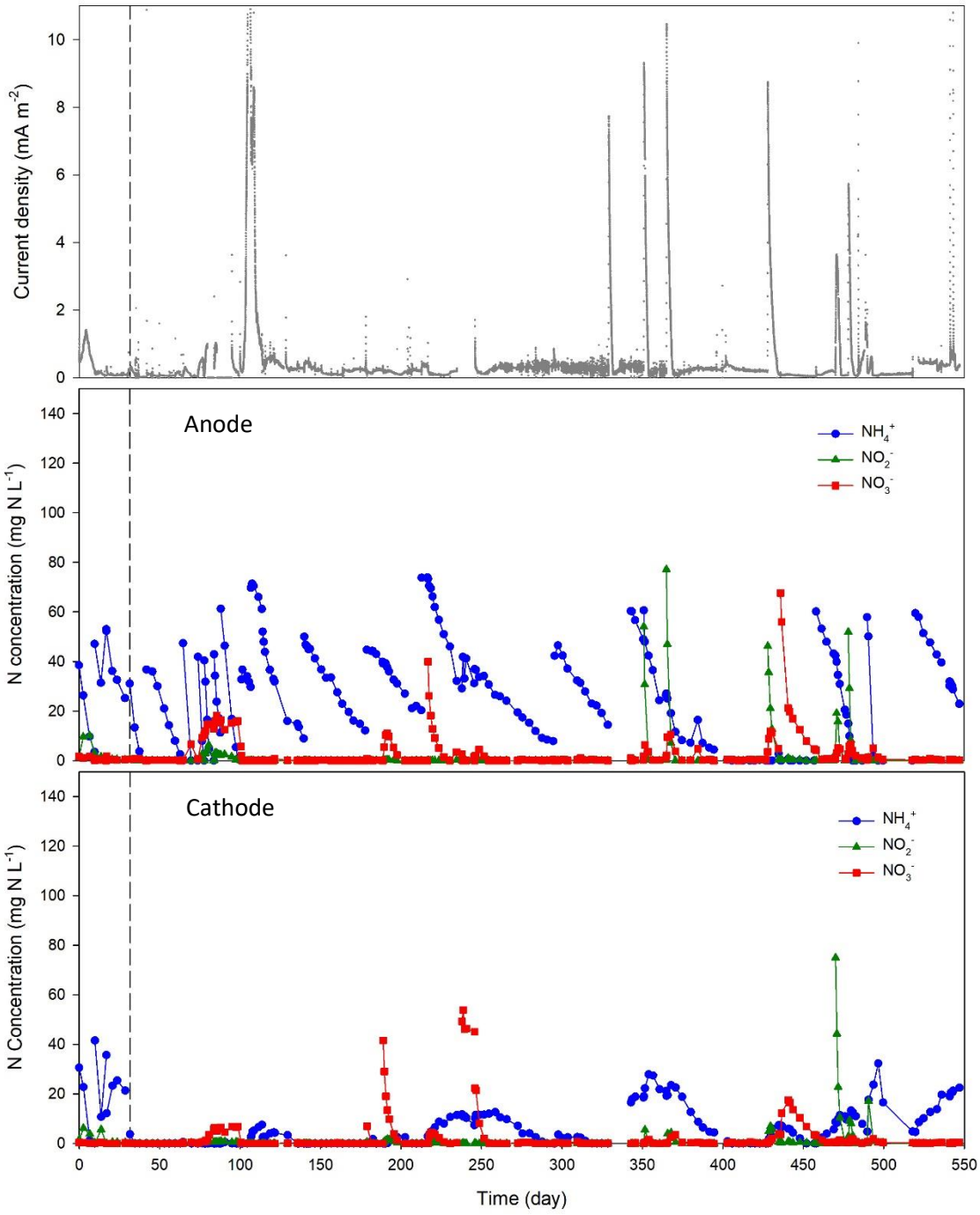

Figure S4.2. Evolution of nitrogen species concentration and current density (top), nitrogen species concentration at the anode (middle) and nitrogen species at the cathode (bottom) in reactor A during the complete duration of Chapter 4. The grey dashed line marks the end of the inoculation phase.

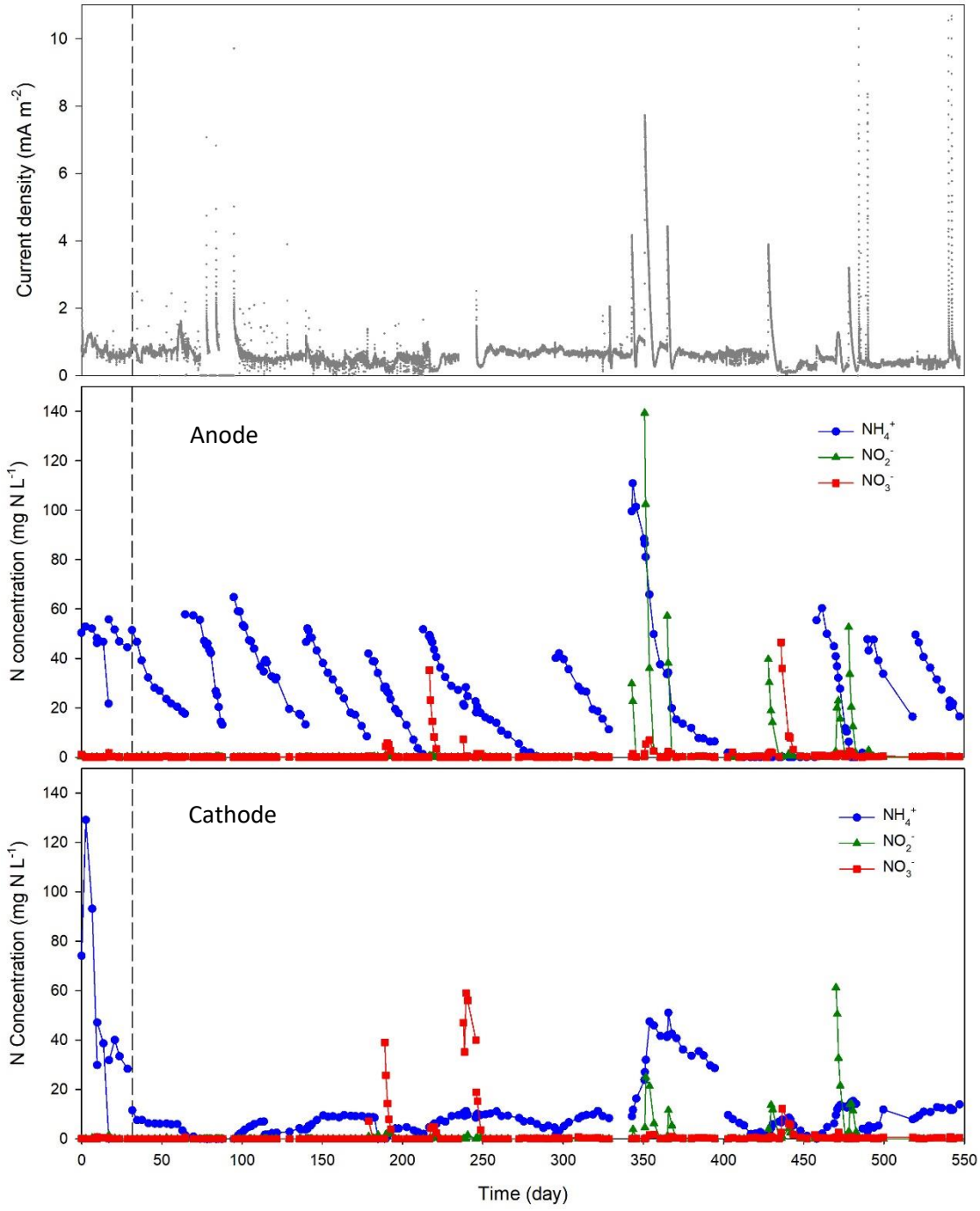

Figure S4.3. Evolution of nitrogen species concentration and current density (top), nitrogen species concentration at the anode (middle) and nitrogen species at the cathode (bottom) in reactor B during the complete duration of Chapter 4. The grey dashed line marks the end of the inoculation phase.

10.1.3 Abiotic tests on nitrite and hydroxylamine abiotic oxidation on granular graphite.

Abiotic tests were carried out to evaluate the abiotic electrochemical oxidation of two intermediate nitrogen species: NO_2^- and hydroxylamine (NH_2OH). For these tests, 400 mL glass bottles were filled with 200 mL of buffer solution containing NO_2^- or NH_2OH, and 100 mL granular graphite (same class as in the biotic tests, but without inoculation). This granular graphite was connected with a potentiostat by a graphite rod, acting all together as the anodic electrode. A Ti-MMO rod, placed inside the reactor contacting the liquid but not the graphite, served as the cathodic electrode, and an Ag/AgCl reference electrode (+0.197 V vs SHE) was also introduced in the reactor. Nitrogen gas was continuously flushed to remove oxygen from the reactor. The anodic potential was set at +0.8 V vs SHE as in the biotic experiments.

To assess nitrite electrochemical oxidation, a buffer solution containing 285 mg $N\text{-}NO_2^-$ L^{-1} was introduced into the reactor (Figure S4.4). All this NO_2^- was oxidised to nitrate within one day, generating a current intensity peak with a maximum of 10.7 mA. Additional 22 mg $N\text{-}NO_2^-$ L^{-1} was spiked after 8 days, being completely oxidised to NO_3^- in one day, generating a current peak with a maximum of 6.0 mA.

Hydroxylamine electrochemical oxidation was studied by introducing a buffer solution containing 45.0 mg $N\text{-}NH_2OH$. This NH_2OH was electrochemically oxidised to NO_2^- (3.4 mg $N\text{-}NO_2^-$ L^{-1}) and NO_3^- (40.3 mg $N\text{-}NO_3^-$ L^{-1}) in 24 hours, generating an electrochemical peak reaching 11.3 mA (Figure S4.5). The solution in the reactor was substituted by fresh buffer containing 45.0 mg $N\text{-}NH_2OH$, which was again completely oxidised in one day (generating 5.8 mg $N\text{-}NO_2^-$ L^{-1}, 40.3 mg $N\text{-}NO_3^-$ L^{-1} and an electric current peak with a maximum of 8.6 mA). These results suggest that there are electrochemical pathways for the NH_2OH and NO_2^- oxidation in the niBES that may not require microbial activity, but the accumulation of NO_3^- in the abiotic tests indicates that the microbiota in the niBES was responsible for the denitrification observed in the biotic test

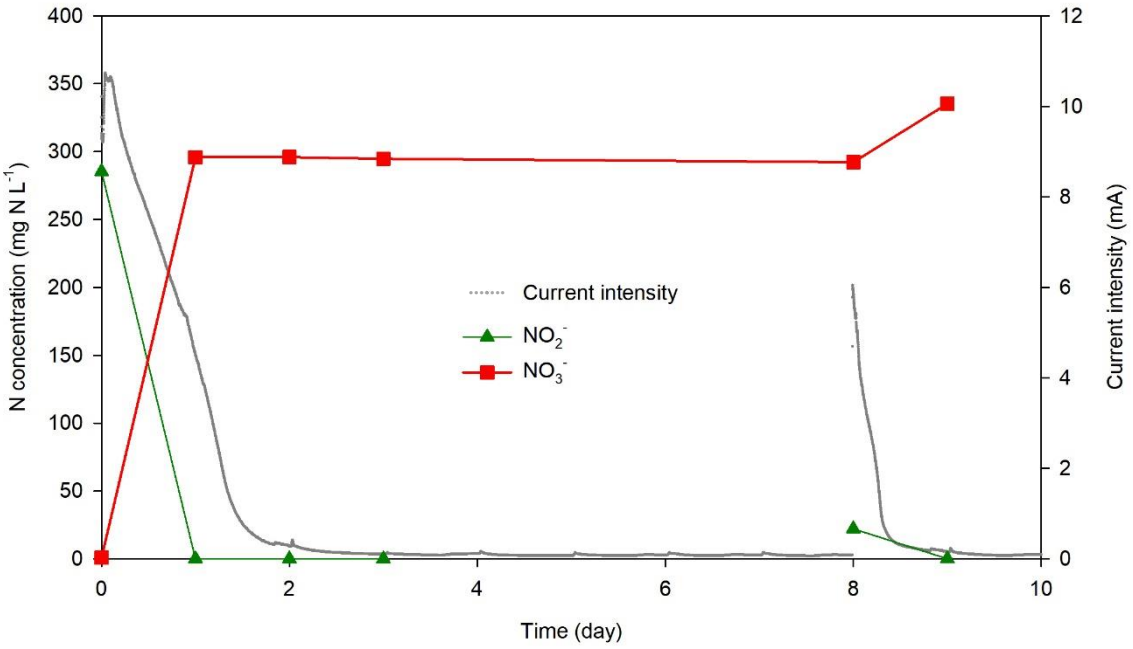

Figure S4.4. Evolution of nitrogen species concentration and current intensity during the abiotic nitrite electrochemical oxidation test in Chapter 4.

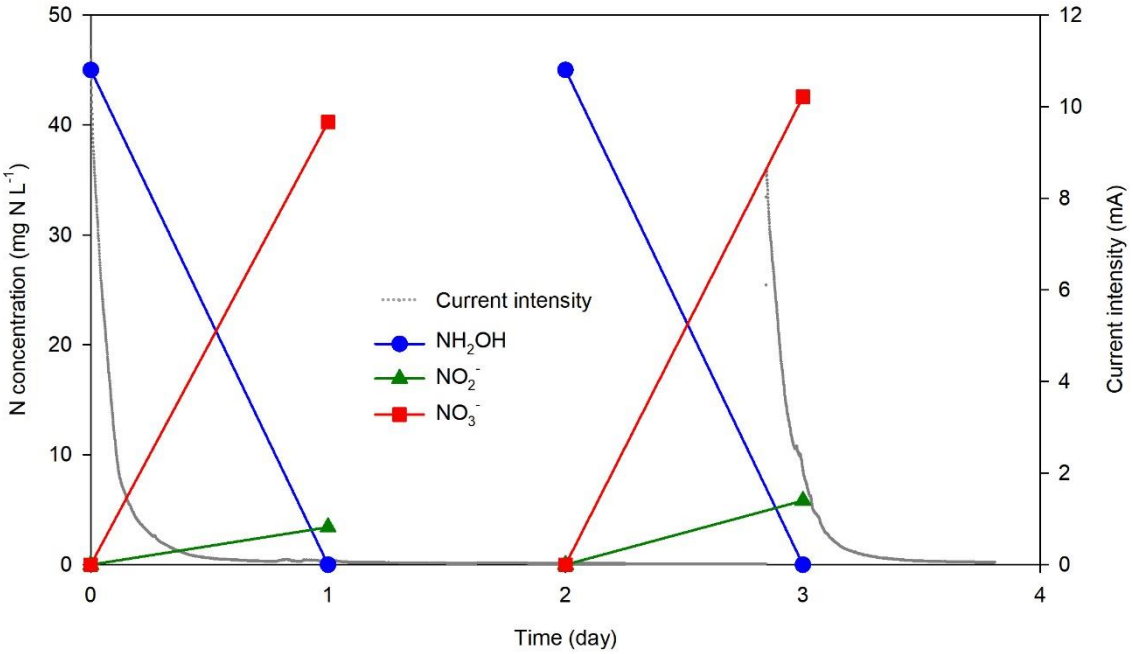

Figure S4.5. Evolution of nitrogen species concentration and current intensity during the abiotic hydroxylamine electrochemical oxidation test in Chapter 4.

10.1.4 Relative abundance of main orders with Planctomycetes.

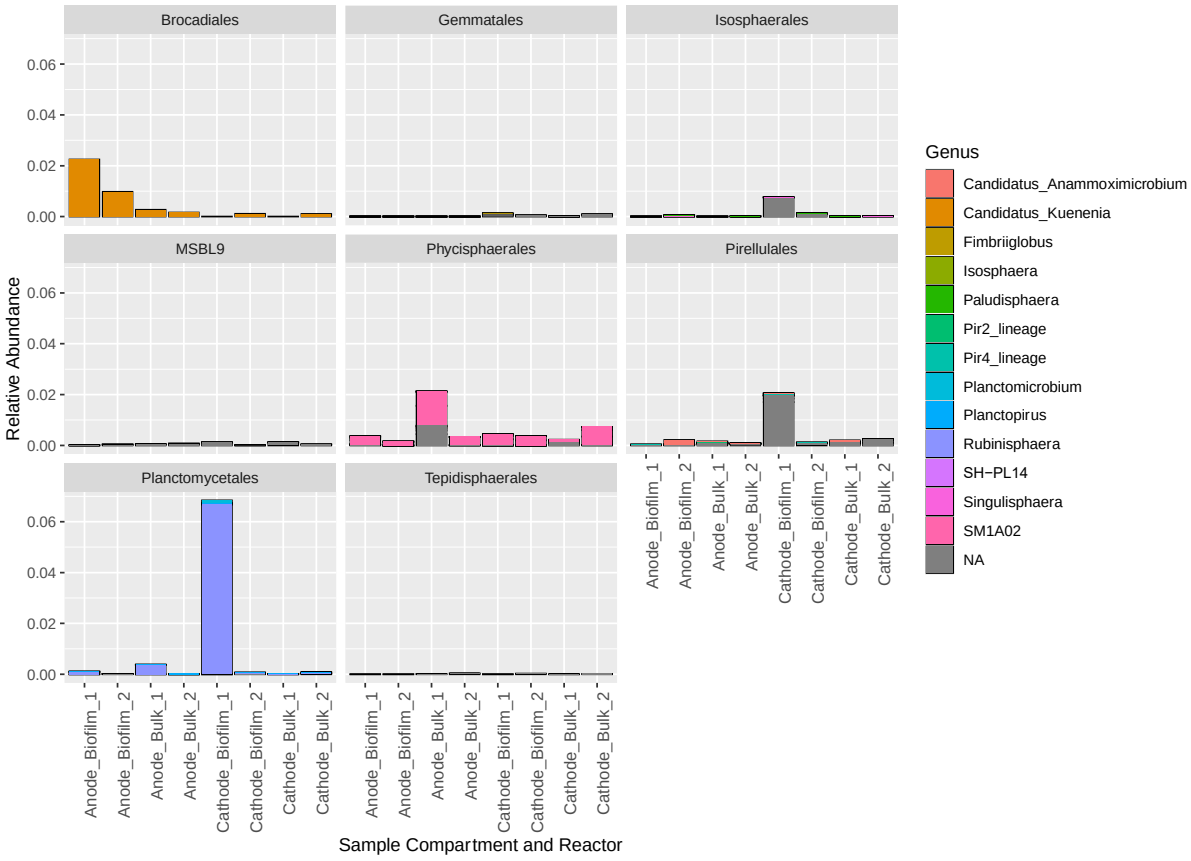

Figure S4.6. Relative abundance (total number of sequences) of main orders within Planctomycetes in the reactors studied in Chapter 4. Samples are organized as per reactor and compartments (Anode-Cathode, bulk-biofilm) inside the reactor. Colours inside bars indicate differences according to the classification of sequences at the Genus level. Faint lines within bars indicate ASVs abundance. NA- ASVs not assigned to Genus level

10.2 Supplementary information for Chapter 5

Summary:

- 10.2.1: Pictures of the reactors used in this study

- 10.2.2: Evolution of reactors performances during the start-up period

- 10.2.3: Evolution of the potential at the current collectors of reactor designs A, B and C

- 10.2.4: Evolution of the potential at the current collectors of reactors design D

- 10.2.5: Dissolved oxygen, N_2O concentration and reactor D performance after COVID-19 lockdown

10.2.1 Pictures of the reactors used in this study

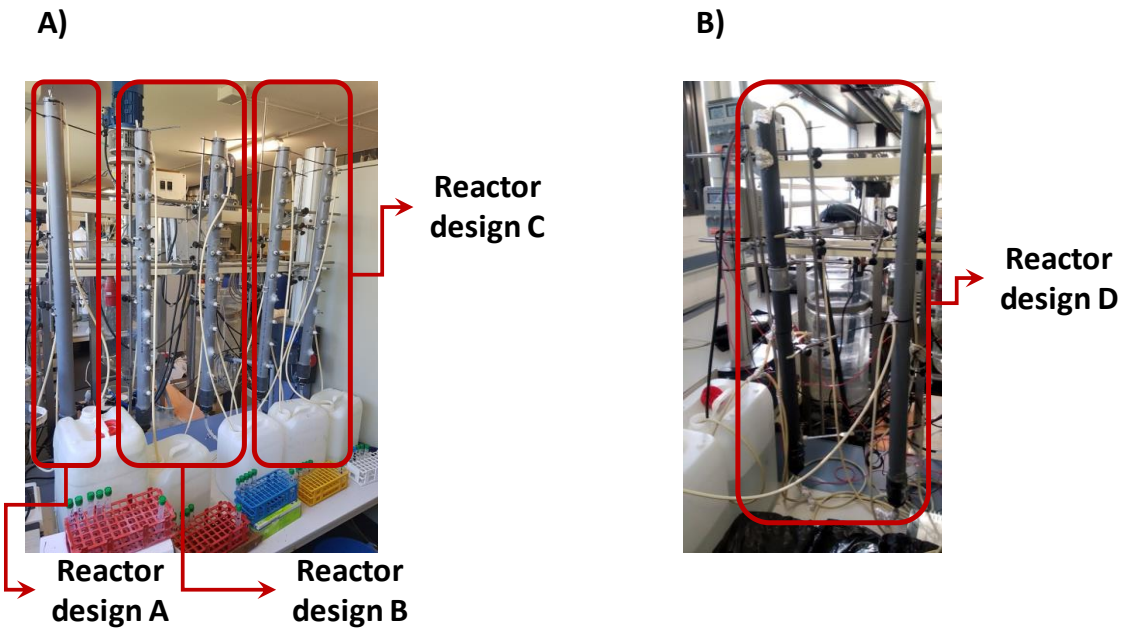

Figure S5.1. Reactors used in Chapter 5. A) Picture of the experimental set-up for reactor designs A, B and C. B) Picture of the experimental set-up for reactor design D.

10.2.2 Evolution of reactors performances during the start-up period

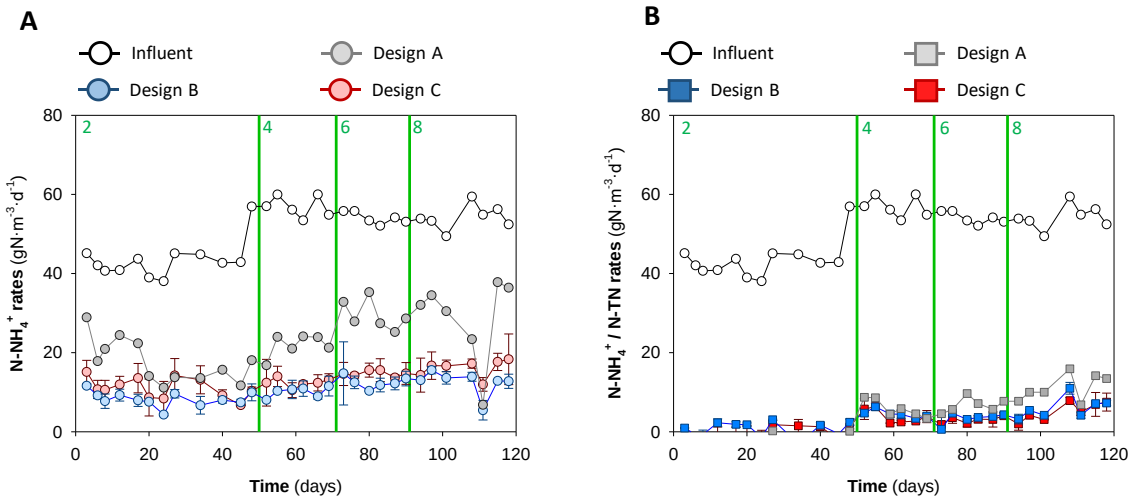

Figure S5.2. Performances of reactor designs A, B, and C during the first 118 days of Chapter 5. Different number of current collectors located at different heights (2, 4, 6, or 8; indicated by green vertical lines) were connected to the electrical circuit in case of reactor design C. A) Influent N-NH_4^+ loading rate and removal rates for reactor designs A, B, and C. B) Influent N-NH_4^+ loading rate and N-TN removal rates for reactor designs A, B, and C.

10.2.3 Evolution of the potential at the current collectors of reactor designs A, B and C

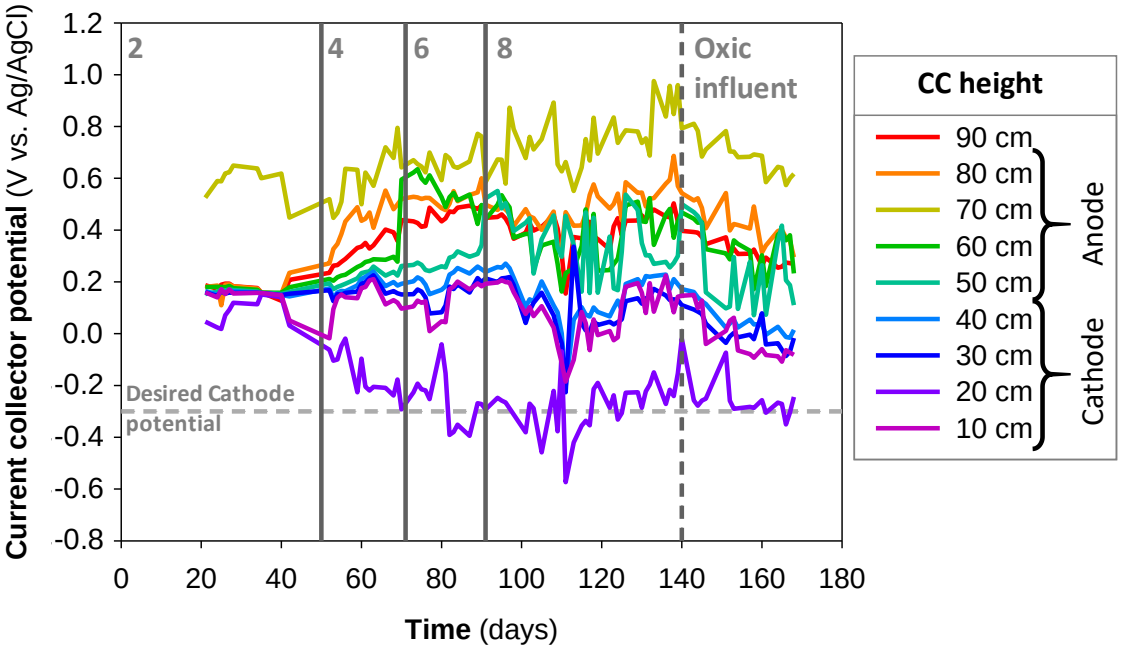

Figure S5.3. Evolution of CCs redox potentials in reactor design C (mean value of both replicates used in Chapter 5 is plotted). The dark grey vertical lines indicate the number of electrically connected CCs (2, 4, 6, or 8). The dark grey vertical dashed line indicates the change from N_2-flushed to not-flushed influent. The grey horizontal dashed line indicates the desired cathode potential (-0.3 V).

10.2.4 Evolution of the potential at the current collectors of reactors design D

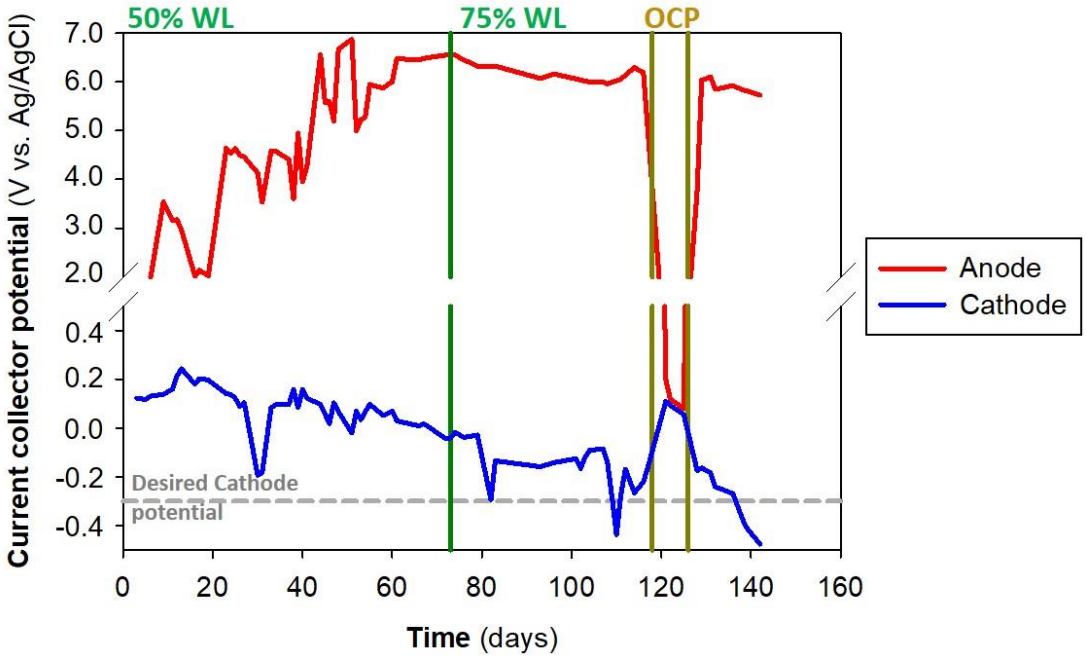

Figure S5.4. Evolution of CCs potentials in reactor design D (mean value of both replicates used in Chapter 5). Vertical lines indicate changing of WL from 50 % to 75 % and the time frame at OCP. The grey horizontal dashed line indicates the desired cathode potential (-0.3 V).

10.2.5 Dissolved oxygen, N_2O concentration and reactor D performance after COVID-19 lockdown

Table S5.1. Effluent characteristics and removal rates of reactor design D after COVID-19 lockdown in Chapter 5.

HRT (h)	$N\text{-}NH_4^+$ Inf (mg N L^{-1})	$N\text{-}NH_4^+$ eff (mg N L^{-1})	$N\text{-}NH_4^+{}_{RR}$ (mg N L^{-1} d^{-1})	$N\text{-}NH_4^+$ rem (%)	$N\text{-}NO_2^-$ eff (mg N L^{-1})	$N\text{-}NO_3^-$ eff (mg N L^{-1})	$N\text{-}N_2O$ eff (mg N L^{-1})	N_2O/TN_{rem} (%)	$N\text{-}TN_{RR}$ (mg N L^{-1} d^{-1})	N-TN rem (%)	DO (mg O_2 L^{-1})
1.2 ± 0.1	45.7 ± 0.3	0.2 ± 0.3	37 ± 3	100 ± 1	0.0 ± 0.0	4.1 ± 7.4	0.0 ± 0.0	0.0 ± 0.0	33 ± 6	91 ± 16	< LOD
0.7 ± 0.0	43.7 ± 4.1	13.5 ± 12.1	45 ± 18	69 ± 28	0.4 ± 0.3	10.3 ± 2.6	1.2 ± 1.6	3.1 ± 3.6	45 ± 17	55 ± 20	< LOD
0.4 ± 0.0	47.8 ± 4.8	20.3 ± 10.5	78 ± 33	57 ± 24	1.1 ± 1.0	14.3 ± 8.7	0.0 ± 0.0	0.0 ± 0.0	42 ± 13	29 ± 6	< LOD